Preclinical Study of PI3K and BRAF Inhibitors in Malignant Melanoma

(Estudio preclínico de inhibidores de PI3K y BRAF en melanoma maligno)

Marta López Fauqued

PhD Thesis

PRECLINICAL STUDY OF PI3K AND BRAF INHIBITORS IN MALIGNANT MELANOMA

ESTUDIO PRECLÍNICO DE INHIBIDORES DE PI3K y BRAF EN MELANOMA MALIGNO

Marta López Fauqued

Barcelona, 2010

Universidad de Barcelona
Facultad de Biología
Departamento de Bioquímica y Biología Molecular
Programa de doctorado de Biomedicina
Bienio 2005-2007

PRECLINICAL STUDY OF PI3K AND BRAF INHIBITORS IN MALIGNANT MELANOMA

ESTUDIO PRECLÍNICO DE INHIBIDORES DE PI3K y BRAF EN MELANOMA MALIGNO

Memoria presentada por

Marta López Fauqued

para optar al grado de **Doctora en Biología** por la Universidad de Barcelona.

Esta tesis doctoral ha sido realizada en el Programa de Investigación en Oncología Médica en el Instituto de Investigación del Hospital Universitario de la Vall d'Hebron bajo la dirección del **Dr. Juan Ángel Recio Conde** y la tutoría de la **Dra. Monique Robert Gates**.

El director,	La tutora,	La doctoranda,
Dr. Juan Ángel Recio Conde	Dra. Monique Robert Gates	Marta López Fauqued

Barcelona, marzo del 2010

To my family,

A mi familia,

ACKNOWLEDGMENTS / AGRADECIMIENTOS

Siempre he dicho que los agradecimientos de mi tesis tenían que empezar dando las gracias a Sir Alexander Fleming. Mi interés por la biología y la investigación en general se despertó gracias a un trabajo que realicé en el instituto sobre el descubrimiento de la penicilina. Y ahora, diez años más tarde, tengo aquí delante el resultado del trabajo duro en el laboratorio durante estos últimos cuatro años y ha llegado el momento de escribir los agradecimientos.

Gracias a Kelle por admitirme en su laboratorio y confiar en mi para realizar este proyecto. Gracias por dirigirme, enseñarme, animarme en los momentos de bajón y permitir que nos sintiéramos en el laboratorio como en casa.

A Monique Robert, por aceptar ser mi tutora sin conocerme y haber estado siempre tan atenta y disponible cuando la he necesitado.

Gracias a todas y cada una de las personas que durante estos cuatro años han pasado por el laboratorio (¡que no son pocas!) y con las que he compartido tantas horas de trabajo, risas y también enfados, por qué negarlo. Pero eso pasa hasta en las mejores familias, ¡¡¡a nadie le gusta limpiar!!!. A pesar de todo, también nos hemos ayudado cuando ha sido necesario. Empezando por los que ya estaban cuando llegué, Carlos, Rosaura y Nohe y los que llegaron después por mucho o poco tiempo: Jessica, William, Pedro, Anna, Rosa Gil y Judit Grueso.

A Nohe, Isa, Anna y Rosa Gil por enseñarme y ayudarme siempre que lo he necesitado con los ratones. A los cuidadores y veterinarios del estabulario del Institut de Recerca por encargarse que todos los animales estuvieran siempre en las mejores condiciones posibles. A Judit Grueso por sus inmunofluorescencias y a Javier Hernández Losa y Teresa Moliné del departamento de Anatomía Patológica por ayudarnos con las inmunohistoquímcas. Gracias a Sergi Ruiz por su tiempo y ayuda en el diseño de la portada de esta tesis.

A todas las personas del programa de oncología que no nombro, pero han contribuido de una forma u otra al avance de este trabajo, ya sea mediante sugerencias en los seminarios del programa, palabras de ánimo o pequeños favores rutinarios que ayudan a llevarlo mejor.

De esta tesis, además de experiencia profesional, me llevo unos cuántos amigos.. Podría hacer una larga lista de nombres, pero no lo haré. Toda esa gente a la que tengo que agradecer tantos momentos, comidas, cenas, viajes y fiestas varias lo saben y no hace falta nombrarlas.

Gracias también a los amigos de fuera del laboratorio que han seguido el proceso de esta tesis desde el principio y me han ayudado a desconectar tanto.

Y por último, gracias a mis padres por haberme permitido estudiar lo que más me ha gustado y apoyarme pese a los horarios locos que he tenido que hacer para conseguir estar aquí. Gracias también al resto de mi familia, abuela, tíos y primos por su apoyo e interés en el desarrollo de esta tesis.

A todos,

GRACIAS

Marta

CONTENTS

LIST OF FIGURES

I. INTRODUCTION

III. MATERIAL AND METHODS

IV. RESULTS

V. DISCUSSION

LIST OF TABLES

III. MATERIAL AND METHODS

IV. RESULTS

ABBREVIATIONS

A, B, C, D

AKT	Thymoma viral proto-oncogene
APS	Ammonium Persulfate
ATP	Adenosine triphosphate
BCL-2	B-cell lymphoma 2
BRAF	v-raf nurine sarcoma viral oncogene homolog B1
BSA	Bovine Serum Albumine
c-MET	Mesenchymal-epithelial transition factor
CDK1	Cyclin dependent kinase 1
CDK4	Cyclin dependent kinase 4
CDKN2A	Cyclin dependent kinase inhibitor 2a
DAB	Diaminobenziamide
Dct	Dopachrome tautomerase
DMBA	7,12-dimethylbenz[α]anthracene
DMEM	Dullbeco's Modified Eagle's Medium
DMSO	Dymethyl sulfoxide
DNA	Deoxyribonucleic acid
DTIC	Dacarbazine

E, F, G, H

E1a	Adenovirus small early region 1a
FAS	Apoptosis stimulating fragment
EGF	Epidermal Growth Factor
EGFR	Epidermal Growth Factor Receptor
ERK	Extracellular Related Kinase
FACS	Fluorescence activated cell sorting
FBS	Fetal Bovine Serum
FOXO	Forkhead box family of transcrpition factors
FVB	Friend-virus B subtype
GAPDH	Glyceraldehyde 3-phosphate dehydrogenase
GI50	Growth inhibition concentration to 50%
GSK-3	Glycogen synthase kinase-3
GFP	Green fluorescence protein

GRB2	Growth factor receptor-bound protein 2
GAP	GTPase activating proteins
GDP	Guanosine diphosphate
GEF	Guanidine exchange factor
GTP	Guanosine 5' triphosphate
HGF	Hepatocyte Growth Factor
HER2	Human Epidermal Growth Factor Receptor 2

I, J, K, L

IC50	Inhibition concentration to 50%
IF	Immunofluorescence
IFN-α	Interferon α
Ig	Immunoglobuline
IGFR1	Insuline-lke growth factor receptor 1
IHQ	Immunohistochemistry
IL-10	Interleukine 10
IL-2	Interleukine 2
IL-6	Interleukine 6
ILK	Integrin-linked kinase
ip	Intraperitoneal
IRS1	Insulin Receptor Substrate 1
JAK	Janus Kinase

M, N, O, P, Q

MAPK	Mitogen activated pathway Kinase
MC1R	Melanocortin-1 receptor
Mcl-1	Myeloid cell leukemia sequence
MEK	MAPK/Extracellular signal-regulated kinase
MTIF	Microphtialmia-associated transcription factor
mTOR	Mammalyan target of Rapamycin
n.a.	Not avaliable
NK	Natural killer
NOD	Non obsese-diabetic
O/N	Overnight

p/s	Peniciline-streptomycin
p70S6K	Ribosomal protein S6 kinase
PBS	Phosphate Buffered saline 3
PCR	Polymerase chain reaction
PDGFRβ	Platelet-derived growth factor receptor β
PDK1	Phosphoinositol dependent kinase 1
PH	Pleckstrin homology
PI3K	Phosphoionositide 3-kinase
PIP3	Phosphoionositol 3 phosphate
PKA	Protein Kinase A
PKB	Protein kinase B
PKCα	Protein Kinase C α
PKCγ	Protein Kinase C γ
PRAS40	Proline-rich AKT Substrate of 40 KDa
PTEN	Phosphate and tensin homologue
PVDF	Polyvinylidene fluoride
qRT-PCR	Quantitative reverse transcriptase PCR

R, S, T, U

RAPTOR	Regulatory associated protein of mTOR
RCC	Renal cell carcinoma
RGP	Radial growth phase
RICTOR	Rapamycin-insensitve companion of mTOR
RNA	Ribonucleic acid
RT	Room temperature
RTK	Receptor tyrosin kinase
SCC	Squamous cell carcinoma
SCID	Severe combined immunodeficiency
SDS	Sodium Dodecyl Sulfate
SOS	Son of sevenless
Src	Sarcoma
SSM	Superficial spreading melanoma
STAT3	Signal transducer and activator of transcription 3
TBS	Tris Buffered saline
TEMED	N, N, N', N'. Tetramethylethylenediamine

TLP2	Tumor progression locus 2
TNF	Tumor necrosis factor
TPA	12-O-tetradecanoyl-phorbol-13-acetate
TRAIL	TNF-related apoptosis inducing ligand
Treg	Regulatory T cells
Trp1	Tyrosinase related protein 1
TSC1	Tuberous sclerosis 1 protein
TSC2	Tuberous sclerosis 2 protein
TUNEL	Terminal Transferase dUTP Nick End Labelling
UTP	Uridine-5' triphosphate
UV	Ultraviolet

V, W, X, Y, Z

V_f	Final volume
VEGF	Vascular Endothelial Growth Factor
VEGFR1	Vascular Endothelial Growth Factor Receptor 1
VEGFR2	Vascular Endothelial Growth Factor Receptor 2
VGP	Vertical growth phase
v/v	volume/volume
W/V	weight/volume
WB	Western blot
WT	Wild type
WHO	World Health Organization

α, β…

1, 2, 3, 4…

αMSH	Melanocyte-stimulating hormone
4EBP1	4 Elongation binding protein 1
7AAD	7 Aminoactinomicine D

I. INTRODUCTION

1. Cancer overview

Cellular homeostasis requires equilibrium between four basic processes for cell life: cell proliferation, cell growth, differentiation and apoptosis [1].

Any alteration in any of these processes can lead to an uncontrolled cell growth that ends in benign or malign tumor formation. Malignant tumors are able to invade other tissues, metastasize and grow in other organs whereas benign tumors are well localized.

Cancer is the disease caused by cells that have escaped from this cellular homeostasis and are able to grow in other organs.

Malignant cells differ from benign cells in some characteristics:

- Growth requirements. Normal cells have a limited proliferation rate, which means that they are sensitive to antiproliferative signals, and importantly, they are growth factor and anchorage dependent. On the contrary, tumor cells have an uncontrolled proliferation rate; they are able to grow in a growth factor and anchorage independent manner as well as they are able to evade apoptosis.
- Size and morphology.
- Metabolic rate. Malignant cells have a higher metabolic rate, as their ATP requirements are elevated.
- Metastasis and angiogenesis dependence. Tumor cells acquire new abilities for surviving. These cells are able to metastasize and grow in other organs. Malignant cells are also very dependent on blood vessels formation because of its nutrients and oxygen supplier function.

This malignant phenotype is a consequence of a group of genetic lesions in molecules involved in regulation of cell physiology. Those genes affected have been classified in two big groups:

- **Proto-oncogenes**: a proto-oncogene is a gene that codificates for a protein whose function is the promotion of cell growth and division in a controlled mode. An **oncogene** is a proto-oncogene that carries a gain of function mutation. Hence, an oncogene is producing a protein that activates constitutively cell growth and division. Gain of function mutations includes point-activating mutations (for instance, $BRAF^{V600E}$ in

melanoma), genetic amplifications (c-myc in neuroblastoma) and chromosome rearrangements that produce deregulated proteins (c-myc in Burkit Lymphoma).

- **Tumor suppressor genes:** a tumor suppressor gene is a gene that codifies for a protein whose function is the inhibition of cell cycle. They need two genetic alterations in order to promote tumor growth. Tumor suppressor genes are characterized by loss of function mutations, which can be given because of an inactivating point mutation or a genetic deletion.

1.1 Incidence

According to World Health Organization (WHO) data, cancer accounts for 13% of all deaths worldwide, which means that it is the second cause of death behind cardiovascular diseases. It is thought that this death percentage will increase up to 45% in 2030 because of population growth and ageing.

1.2 Cancer types

Cancer can affect to both genders in any part of the body. The most frequent cancer types are lung cancer, stomach cancer, colorectal cancer, liver cancer and breast cancer.

Skin cancer is not the most frequent one, but its incidence is increasing considerably in the last two decades.

2. Skin cancer

2.1 Incidence

Skin cancer incidence has increased considerably in the last decades in accordance with the ozone layer depletion. It is thought that every 10% depletion in the ozone layer causes around 300000 skin cancer cases and 4500 melanomas. Nowadays, it is estimated that there are around 2 and 3 millions skin cancer cases and 132000 melanoma worldwide every year. Skin cancer is the cancer type which incidence is increasing faster (data obtained from the WHO).

2.2 Skin biology

The skin is the biggest organ in the body. Its main functions are physical protection against external agents and body temperature regulation.

The anatomy of the skin distinguishes three different layers: epidermis, dermis and hypodermis. The epidermis is separated from the dermis through the basal layer (Figure 1).

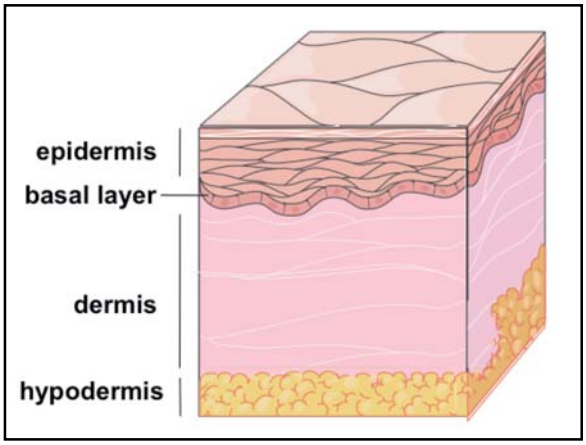

Figure 1. Skin layers.

Scheme showing the main layers of the skin.

- The outer layer of the skin is the **epidermis**. The epidermis is a stratified layer with a high rate of renewal that lacks a blood vessel network. Its thickness depends on the body localization.

  Mainly three different cell types compose the epidermis:

  - **Keratinocytes.** Keratinocytes are the most frequent cell type; they constitute the 95% of the epidermis. They are epithelial cells that originate in the basal layer. When they divide, they migrate slowly towards the outer layers while going through a

morphological and biochemical differentiation process during which they express keratin filaments. The main function of keratinocytes is protection against external agents.

- **Melanocytes** are neural crest derived cells that have migrated to the epidermis. They reside in the **basal layer** surrounded by keratinocytes and proliferate very slowly. The proportion of melanocytes varies between human races and body localization. Melanocytes contain in its cytoplasm melanosomes, which are vesicles that accumulate melanin. Melanin is a natural skin pigment derived from tyrosine. Melanocytes release melanin in response to ultraviolet radiation protecting keratinocytes from UV-induced damage.

- There are other cell types present in the epidermis, although in a very low proportion: **Langerhan cells** and **Merkel cells.** Langerhan cells play a role in skin immunologic responses while Merkel cells are thought to act as mechanic sensory receptors.

- The epidermis and dermis are connected through a **basal layer**, which is synthesized by keratinocytes from epidermis and fibroblasts from the dermis. It gives physical support to the epidermis as well as it regulates metabolite exchange between the two layers.

- The **dermis** is the thicker layer in the epidermis. It contains a huge amount of elastic and collagen fibers as well as a big variety of structural appendixes such as blood and lymph vessels, hair follicles, sweat glands or nerve endings. It helps to the epidermis sustaining.

- The deepest layer in the skin is named **hypodermis.** It is composed of a huge amount of fat tissue; therefore, its main functions are temperature and energetic regulation as well as protection against mechanic injuries.

2.3 Skin cancer types

Skin cancer types are divided in two big categories:

- ***Non-melanoma skin cancers***

  As it is named, this cancer type is derived from uncontrolled proliferation of non-melanocyte skin cancer cells. Around 90% of non-melanoma skin cancer has been related to UV radiation, as it is detected mainly at body sites that have been exposed severely to the sun (face, neck, extremities…). This cancer type can be easily treated.

  Two types of non-melanoma skin cancers can be distinguished:

  - Basal cell carcinoma (BCC). It affects keratinocytes located in the basal layer of the epidermis. It is the most frequent form of skin cancer, about one million cases are diagnosed every year.

  - Squamous cell carcinoma (SCC). This cancer type affects keratinocytes of the outer layers. It is the second most common form of skin cancer, around 250.000 cases are diagnosed every year.

- **Melanoma skin cancer**

  Melanoma is the skin cancer type that affects melanocytes. It is the less frequent skin cancer type, but in the last decades its incidence has increased at a faster rate than that of any other cancer types. Moreover, melanoma is the most dangerous skin cancer form, as it accounts for 75% of skin cancer deaths and the prognosis is a 5-year survival.

  Melanoma can be easily treated by surgery when it is detected in an early stage. However, when detected in its advanced stages it becomes resistant to therapies and has no cure.

3. Melanoma biology

3.1 Melanoma classification

Melanoma can be classified according to its behavior and anatomic localization in two categories: non-invasive melanomas and invasive melanomas.

- Non-invasive melanomas:

Non-invasive melanomas are those that spread horizontally without dermal invasion. They can be easily treated by surgery. Three different subtypes can be distinguished according to its localization and sun exposure.

- **Superficial spreading melanoma (SSM).** SSM is the most common melanoma subtype since it accounts for the 70% of melanomas cases. It is very common in young people. They are easily palpable melanomas that appear in localizations that have been intermittently exposed to the sun, as trunk and legs.

- **Lentigo maligna**. Lentigo melanomas are flat dark tumors that appear in sun-exposed body localizations and frequently surrounding hair follicles: face, neck, ears…etc. This is a common skin cancer in the elderly.

- **Acral lentiginous melanoma.** Acral melanomas are located under the nails or in the palms and soles. This is the most prevalent melanoma in dark-skinned in African, American and Asiatic population.

- Invasive melanomas:

Invasive melanomas are those that proliferate vertically and are able to invade the dermis. These melanomas are more aggressive than the non-invasive melanomas because they are able to reach the blood vessels and metastasize to any distant organ. Nowadays, this type of melanoma has no efficient therapy.

- **Nodular melanomas** are the most aggressive form of melanoma. It accounts for 10-15% of the cases diagnosed. It is characterized for growing very fast in deepness. Its prognosis is poor because it doesn't always appear from pre-existing lesions and it is often detected in an advanced stage. It can occur at any age, but is more common in the old people.

3.2 Melanoma risk factors

The risk factors to develop a melanoma can be divided into environmental and genetic factors, although the interaction between both can be important to the disease development.

3.2.1 Environmental risk factors

- UV-exposure

The most suggested environmental risk factor for melanoma development is UV exposure. UV exposure is epidemiologically related to melanoma risk. Experiments in UV-induced melanoma mouse models have revealed that is UV-B the responsible of melanoma development [2] In addition, it is known that UV exposure causes genetic changes in the skin, impairs the cutaneous immune function, increases the production of growth factors and induces the formation of DNA-damaging reactive oxygen species that affects keratinocytes and melanocytes. All together contributes to melanoma development [3].

- Immunosuppression

It has been reported that patients immunosuppressed after a renal transplantation are prone to develop melanomas. In accordance, UV-B radiation is known to cause local immunosuppression in the skin [4].

- Other factors

There are other environmental factors, which have been related to be a melanoma risk factor although they are yet not well known and further studies are needed.

One of them is the increase of melanoma cases in people who had been previously exposed to pesticides. There are three case-control studies performed in Australia, UK and Italia that support this fact.

There is also an occupational risk to develop melanoma. It has been detected that airline crews have a higher incidence of melanoma, which could be caused because of an increased sun exposure in locations where there is a higher UV irradiation.

3.2.2 Genetic risk factors

Melanoma has a genetic component, since 5% of malignant cutaneous melanoma occurs in families with two or more close relatives affected. The usual melanoma patient is characterized by having a pale-skinned complexion, red or blonde hair, blue eyes and a high number of large and irregular benign nevus. The presence of high number of nevus is directly correlated with UV exposure.

Genetic-screening in melanoma-prone families history has provided information about genes that could be responsible of an increased susceptibility to develop melanoma [3].

- CDKN2A

CDKN2A is a gene involved directly in cell cycle entry. It encodes two tumor suppressor proteins named $p16^{INK4A}$ and $p14^{ARF}$.

$P16^{INK4A}$ acts after DNA damage and it blocks cell cycle at the G1-S checkpoint inhibiting CDK4, a cyclin dependent Kinase. $P14^{ARF}$ is a product of the alternative reading frame of the locus CDKN2A that increases p53 stability. Hence, increased p53 levels arrests cells at the G2-M phase allowing DNA-damaged repair or inducing apoptosis.

About one third of melanoma patients around the world carry CDKN2A inactivating mutations or deletions, which indicates that CDKN2A might be a susceptibility gene.

♦ CDK4

Punctual mutations in CDK4 have been identified in a few cases of melanoma. These mutations impede the binding of CDK4 with INK4A, thus activating constitutively cell cycle progression.

♦ MC1R

Melanocortin-1 receptor (MC1R) encodes the melanocyte-stimulating hormone (αMSH) membrane receptor. Sun exposure induces αMSH synthesis, which signals through MC1R to produce eumelanin, a sun-protective pigment.

There are genetic variants in MC1R that are the responsible of the synthesis of non-sun-protective pigments, such as pheomelanin, the responsible of the red-haired and freckles phenotype. These melanin intermediate products contribute to malignancy by increasing the oxidative stress.

3.3 Melanoma progression

Normal melanocytes can progress toward malignant melanoma through different stages. During transformation, melanocytes accumulate molecular and histopathological changes that are all considered in Clarck's Model [5,6].

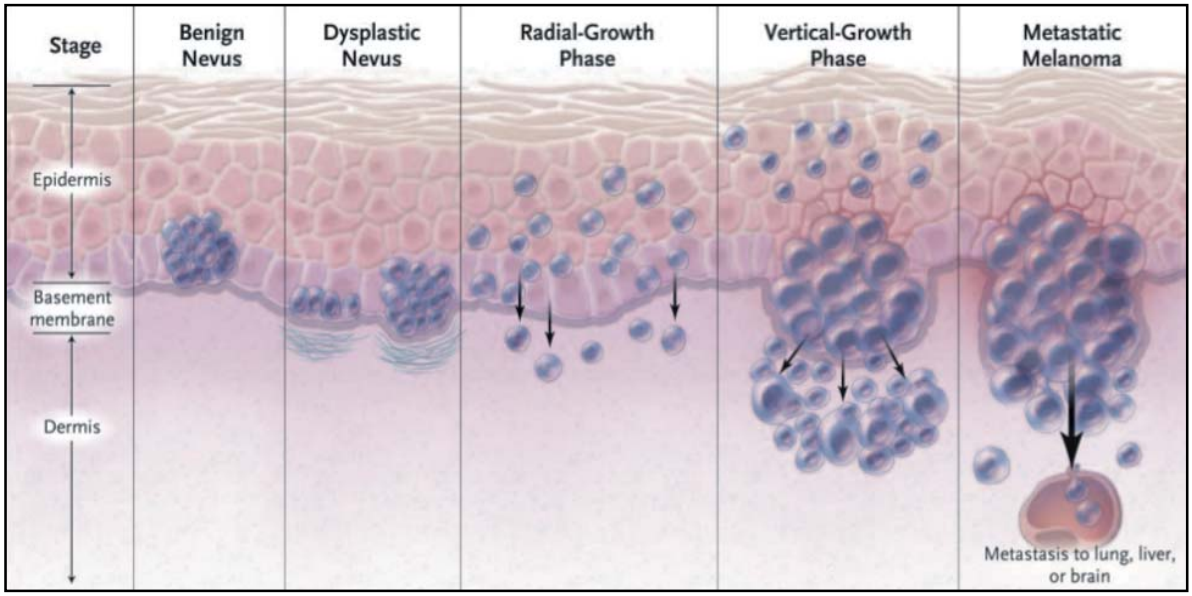

Figure 2. Histological stages in melanoma progression.

Adapted from [6].

The first stage in melanoma formation describes the development of **melanocytic nevus.** Nevi are clonal benign clusters of melanocytes which have lose their contact with keratinocytes and have a limited growth due to oncogene-induced cell senescence [7]. They can be localized in the dermis (*daermal nevus*), in the epidermis (*junctional naevus*) or in both (*compound naevus*). Nevi are frequently senescent for decades and they rarely progress into malignancy.

The next step into melanoma progression involves the aberrant growth of melanocytes within a preexisting nevus or in a new localization. These growth leads to the development of dysphasic **nevus** or irregular lesions in the skin.

This nevus can accumulate certain mutations that lead to the uncontrolled growth of melanocytes in a stage named **radial growth phase** (**RGP**). This phase is characterized by the presence of pagetoid spreads, which are melanocytes microinvasions to the epidermis that remains *in situ*. Melanomas in this stage can be totally treated by surgery, as they are not able to invade the dermis neither to metastasize. Non-invasive melanomas (lentginous melanoma, acral lentiginous melanoma and SSM) are melanomas that remain in this phase.

Contrary, malignant melanocytes in **vertical growth phase** (**VGP**) are able to invade the dermis and proliferate in this new localization. As the dermis is the most vascularized layer in the skin, malignant melanocytes are able to enter the bloodstream or lymphatic vessels and migrate to distant organs in a new stage called **metastatic melanoma.** Metastatic melanoma is the most aggressive melanoma and has a high rate of mortality, as there is no effective treatment available.

3.4 Molecular mechanisms involved in melanoma development and progression

The big increase in melanoma incidence and its high mortality rate has encouraged the scientific community around the world to study the molecular mechanisms involved in melanoma progression. It has been possible thanks to the availability of human melanoma samples and the study of melanoma-prone families.

The main molecular alterations in melanoma have been identified in molecules involved in cell cycle and signal transduction pathways. A signal transduction pathway is the mechanism by which cells are able to transduce external signals into a cell response in the nucleus through a protein phosphorilation cascade.

The main pathways that are involved in melanoma development and progression are the MAPK (mitogenic activating pathway kinase) and PI3K (phosphoinositol 3 phosphate kinase) pathways.

3.4.1 Receptor tyrosine Kinase activation

Signaling pathways can be activated by the binding of a growth factor to a tyrosine kinase receptor in the cell membrane. This binding leads to a phosphorilation cascade that activates a group of adaptor proteins, among them GRB2. GRB2 interacts with other proteins involved in the activation of RAS, which is a key mediator of various signaling pathways as well as an oncogene frequently mutated in various cancer types.

RAS belongs to the G small proteins subfamily. It plays a role in different biological functions such as survival, apoptosis or senescence. There are three different RAS isoforms in mammals: N-RAS, H-RAS and K-RAS.

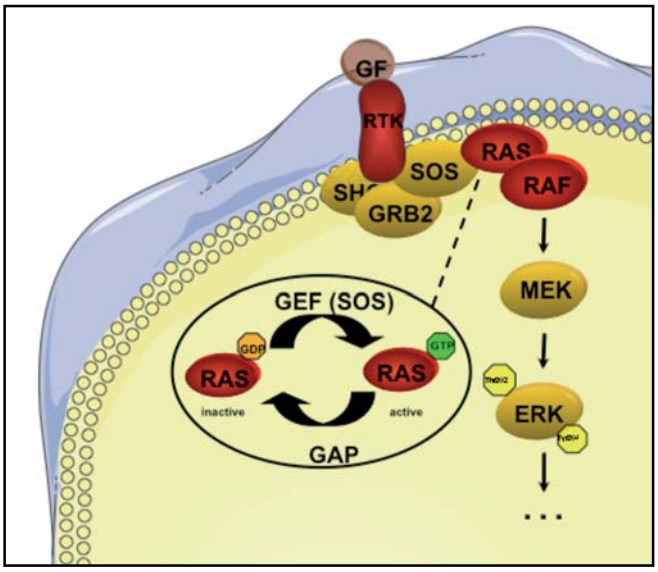

Figure 3. RAS/RAF/ERK1/2 activation pathway.

Small G proteins are GTPases that cycle between inactive and active status depending on the phospho-nucleotide to which it is bound. Inactive forms are bound to GDP while the active forms are bound to GTP.

The proteins that mediate G-protein activation are called guanidine exchange factors (GEF). SOS1, SOS2 and RASGFR are three examples of GEF in mammals. GEFs, in particular SOS1, represent an important connection link between GRB2 and RAS.

There are also proteins responsible for the inactivation of the G-proteins. Those are called GTPases activating proteins (GAP).

Activated RAS is translocated to the plasma membrane where it can bind and activate its multiple effectors, among them RAF [8 9] and PI3K [10].

3.4.2 RAF/MEK/ERK pathway

RAF is a serine-threonine kinase that has a mayor function in melanoma development and progression. There are three RAF isoforms: A-RAF, B-RAF and C-RAF. RAF activity is regulated through a complex process that involves the participation of phosphatases, kinases, GTPases…etc.

Inactivated RAF is located in the cell cytoplasm but it is translocated to the cell membrane by GTP-RAS. There, RAF goes through a serial of conformational changes that favors the phosphorilation of activating residues within the catalytic domain.

The best characterized pathway downstream RAF is the RAF/MEK/ERK pathway. RAF phosphorilates MEK in two serine residues (Ser 217 and Ser 221) and MEK activates ERK through the phosphorilation of Tyr 202 and Thr 204.

ERK's substrates are located in the cytoplasm and in the nucleus. ERK needs to be accurately regulated as it is involved in a wide range of processes such as proliferation, invasion, metastasis, angiogenesis and apoptosis evasion.

3.4.3 PI3K pathway

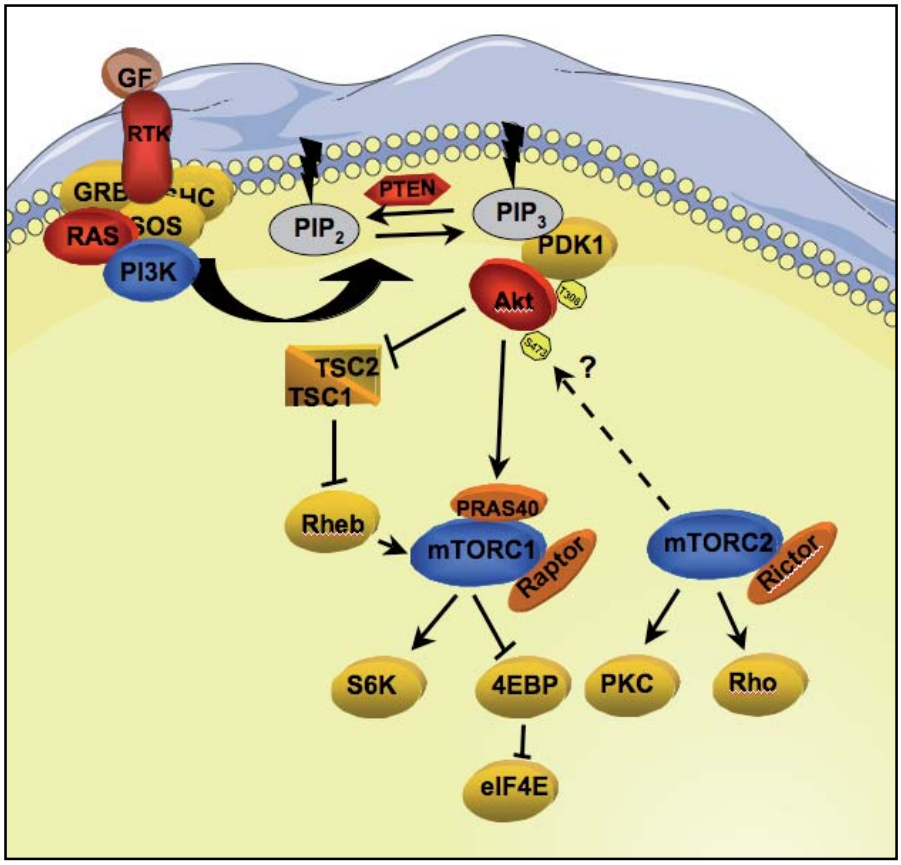

Figure 4. PI3K pathway scheme.

PI3K pathway is involved in biological processes such as cell proliferation, cell survival, differentiation, angiogenesis, motility and metabolism regulation.

PI3K is a lipid kinase. These kinases have been classified into three classes according to their structure and mechanism of action. The most important and best-characterized class in eukaryotes is **PI3K class Ia**, which are activated by tyrosine kinases receptors, G-coupled receptors and the small G-protein RAS. PI3K is a heterodimer protein containing a catalitcal subunit (p110) and a regulatory subunit (p85). P85 maintains p110 inactivated in basal conditions. Upon signaling, p85 binds to phospho-tyrosine residues in membrane receptors or adaptor proteins, for instance the insulin receptor substrate (IRS). In this way, p85 translocates p110 to the membrane and then PI3K will be activated by RAS-GTP.

PI3K phosphorilates a membrane lipid called phosphoinositol-4.5-biphosphate ($PI(4,5)P_2$) to phosphoinositol-3,4,5-triphosphate ($PI(3,4,5)P_3$). Levels of $PI(3,4,5)P_3$ (PIP_3) are accurately regulated by phosphatase and tensin homologue (**PTEN**), which reverses PI3K reaction. PTEN is an important tumor suppressor in many cancers.

PIP_3 levels are recognized by some proteins that have a PH (pleckstrin homology) domain. Among them, **AKT** (also named PKB) or **PDK1 (**phosphoinositide dependent kinase 1) are the most important ones. Both proteins are recruited to the plasma membrane and this new localization allows their interaction and the phosphorilation of AKT by PDK1 in threonine 308 [11,12]. To be fully activated, AKT needs also the phosphorilation in serine 473. It's not clear which is the kinase responsible for serine 473 phosphorilation. It has been suggested that it can be mediated by PDK1, AKT itself [13], DNA-dependent protein kinase [14], ILK [15] or mTOR (mammalian target of rapamycin)/RICTOR complex [16].

AKT is a serine-treonine kinase that phosphorilates a wide range of substrates according to its biological function. Thus, the pathway can promote survival, proliferation or regulates the metabolism by phosphorilation of the antiapoptotic protein BCL-2, GSK-3-kinase or FOXO transcription factor. Within this big substrate list, stands mTOR out.

mTOR is a serine-treonine kinase that belongs to family IV of PI3K and it is involved in cell growth and proliferation regulation and acts as an energy level sensor. There are two mTOR complexes: **mTORC1,** which is rapamycin sensitive, and **mTORC2**, which is rapamycin insensitive. **mTORC1** complex is composed of a catalytical subunit mTOR, a regulatory subunit RAPTOR, and PRAS40, which is at the same time an AKT substrate. **mTORC2** is composed of mTOR and the regulatory subunit RICTOR.

mTORC1 can be activated directly trough the phosphorilation of PRAS40, or indirectly, by the inactivation of TSC2 (tuberous sclerosis 2 protein), a tumor suppressor that inhibits mTORC1. Two well-known mTORC1 targets are 4EBP1 (4E binding protein1) and p70S6K (ribosomal protein S6 Kinase), both involved in protein synthesis

The most important function of **mTORC2** is AKT activation by serine 473 phosphorilation [16], although it is also involved in other small GTPases activation such as Rho.

3.5 Molecular mechanisms altered in melanoma

Tumor cell growth may be dependent on a particular pathway because of the presence of mutations that have been positively selected during its development. In case of melanoma, genetic alterations of key members of the signaling pathways as well as autocrine loops that activate these pathways seem to be accountable for melanoma progression [17].

3.5.1 Receptor Tyrosin Kinases

Receptor tyrosine kinases (RTK) are frequently mutated in many cancer types. Mutations in different RTK have been described in melanoma although so far very little is known about them [18].

Among them, a receptor involved in melanoma progression is **c-MET**, which is a proto-oncogene frequently mutated in many cancer types and works as the Hepatocyte Growth Factor (HGF) receptor. In melanoma, it has been shown that c-MET expression correlates directly with the progression of the disease. Thus, c-MET is more expressed in metastatic melanoma samples rather than in nevi [19,20]. Additionally, it has been described that in metastatic melanoma samples, c-MET expression could be regulated by αMSH (melanocyte stimulating hormone) [20], and MITF (Microphtalmia-associated transcription factor) [21]. αMSH and MITF are molecules involved in melanoma progression.

HGF is a multifunctional cytokine that acts as a mitogenic, motogenic and morphogenic agent in epithelial cells. It is secreted by mesenchymal cells and activates melanocyte proliferation through the activation of c-MET. It has been reported that both c-MET and HGF are highly expressed in melanoma cells, thus enabling an autocrine stimulation of the receptor. HGF is implicated in a wide range of functions in melanoma such as proliferation [22] and motility, cell adhesion [23] and invasion through MMP2 [24]. In accordance, there is an HGF transgenic malignant melanoma mouse model, which presents a hyperpigmentation of the skin [25]. Moreover, this model in response to neonatal UV irradiation develops cutaneous malignant melanoma highly reminiscent to human melanoma [26].

3.5.2 RAS/ERK1/2 pathway

In regard to the RAS/ERK1/2 pathway, the finding that more than 90% melanomas have a hiperactivation of ERK [17,27], suggested that it could have an essential function in melanoma development and progression. In fact, it has been reported that the constitutive activation of the RAS/ERK1/2 pathway is related with the progression of the disease [28], cell metabolism control and resistance to apoptosis [29-31].

Several studies in melanoma samples revealed that 15-30% of melanomas harbored activating mutations in **N-RAS** [32,33]. The most common mutation is the substitution of a leucine for a glutamine at position 61 (Q61L)[34,35]. Moreover, animal model studies supported the oncogenic role of RAS in melanoma [36].

In addition, **B-RAF** is mutated in 60-70% of melanomas [34]. The most common mutation is a glutamic acid for valine substitution at position 600 (B-RAF^{V600E}). B-RAF^{V600E} mutation represents an 80% among all BRAF mutations.

On the other hand, no mutations have been found in A-RAF neither C-RAF in melanoma probably because these proteins require two hits to be mutated while B-RAF requires only one [37].

Interestingly, genetic alterations in NRAS and BRAF rarely coexist in melanoma [38], suggesting that mutant BRAF or NRAS alone are able to activate the pathway.

3.5.3 PI3K pathway

PI3K pathway also plays an important role in melanoma progression due to high levels of p-AKT detected in melanoma patient samples [39-41]. These analyses revealed that 12% of the nevi, 53% of primary melanomas and 67% of malignant melanoma are positive for p-AKT [40], suggesting a pathway deregulation acquired during melanoma progression. It has been proved that 43-60% of malignant melanomas overexpress one of the three AKT isoforms, **AKT3,** and also that high levels of p-AKT reduce melanoma apoptosis *in vivo* [40]. Besides, some studies disclose that 30% of melanomas have a deletion in the tumor suppressor **PTEN.** The PTEN genetic deficiency resulted to be relevant in melanoma tumor development in mice [42]. To a lesser extent, inactivating point mutations in PTEN [43-46] or activating mutations in PI3K [47] have also been identified. All these data support the significant role of the PI3K pathway in melanoma development.

3.6 Molecular targets and therapeutics in malignant melanoma

Melanoma is a very aggressive disease with a very poor prognosis. Around 80% of primary melanomas are treated by surgery when detected in an early stage of development. However, when diagnosed in an advanced stage it becomes resistant to standard therapies and has a prognosis of only five years.

Melanoma cells have a very low basal rate of apoptosis comparing with other tumor types and they have resulted to be *in vitro* resistant to apoptosis-inducing drugs [48]. A good number of chemotherapeutical agents induce apoptosis in other type of malignant cells, so this resistance to drug-induced apoptosis could be an explanation for melanoma resistance to therapies and new therapeutics approaches should be addressed.

Traditional melanoma therapies include the modulation of the immune system with interferon-α (IFN-α) or interleukin-2 (IL-2) but a very low response and some toxicity have been observed. Other classical chemotherapeutical drugs used in melanoma without much success include dacarbazine (DTIC) (citotoxic agent), carmusin, paclitaxel (taxol), cisplatin and temoxolamide.

The recently identification of the signaling pathways involved in melanoma development and progression underscore multiple attractive new targets that could be targeted with the development of new specific compounds. This hypothesis relies on the fact that cancer cells are more dependent on these affected pathways than do normal cells. Hence, malignant cells carrying mutations in these pathways are expected to be more sensitive to the pathway inhibition than do normal cells. Targeted therapies may suppose a step-forward to personal therapies according to the individual genetic lesions.

In the last years, many specific drugs have been developed and they are currently being tested alone or in combination in preclinical and clinical studies.

3.6.1 Therapeutical potential of targeting the RAS/ERK1/2 pathway in malignant melanoma

The finding that 60% of melanomas carries the V600E mutation in BRAF [34] and that 40% carries activating mutations in NRAS [32,33] has suggested that RAS/ERK1/2 pathway could be an attractive pathway to target. The inhibition of the RAS/ERK1/2 pathway could stop the progression of malignant tumors by slowing the tumor growth or inducing tumor cell death.

Since this find, several studies have supported this idea showing that melanoma cell proliferation is dependent on the RAS/ERK1/2 pathway, particularly in those which are $BRAF^{V600E}$ mutated [49,50]. Others have suggested that BRAF could be an attractive target in melanoma since its suppression disrupts human melanocyte transformation and induces apoptosis [49]. Moreover, $BRAF^{V600E}$ is reported to be necessary for tumor growth in melanoma xenografts as its silencing abrogates tumor formation [51].

In addition, NRAS silencing has also been shown to promote apoptosis in NRAS-mutant melanoma cells [52].

All these data support the development of new compounds targeting specifically the members of this pathway.

3.6.1.1 Inhibitors

Taking into account the high importance of the MAPK pathway in different tumor types, several small kinase inhibitors targeting key molecules in this pathway have been developed.

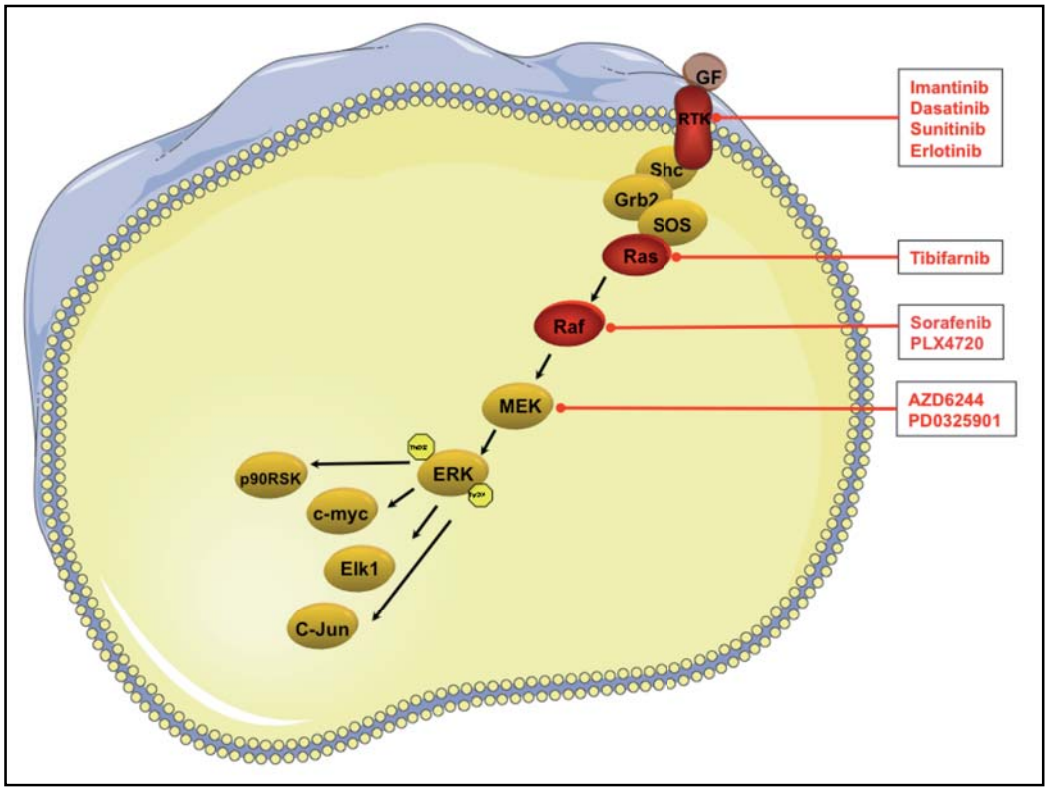

Figure 5. RAS/ERK1/2 pathway inhibitors.

Representative scheme showing some of the inhibitors that target RAS/ERK1/2 pathway in melanoma. In red are the proteins that have been found to be mutated in melanoma.

3.6.1.1.1 RAS inhibitors

The first drug targeting RAS is a farnesyl-transferase inhibitor called **Tibifarnib** (R115777), which impedes RAS membrane-translocation, thus inactivating the pathway [53]. This drug has been proved to have some positive effect when combined with cisplatin but its effects are not very specific [54].

3.6.1.1.2 RAF inhibitors

The first small kinase inhibitor targeting the RAS/ERK1/2 pathway that has entered clinical trials is the bis-aryl urea **BAY43-9006 (sorafenib).** Sorafenib is a multi-kinase inhibitor that blocks both, wild type and V600E mutant BRAF kinases as well as other kinases such as C-RAF, VEGFR-2 and 3, PDGFR and c-KIT [55].

Its effectiveness has already been tested in melanoma cell lines. Sorafenib is able to block $BRAF^{V600E}$ kinase activity in melanoma cells at the micromolar range, induces apoptosis in melanoma cells [56] [57] and it is able to attenuate tumor growth in xenograft models.

Despite these encouraging results, sorafenib has not been effective in clinical trials as a single agent with advanced melanoma patients [58]. However, it has been effective in patients with refractory renal cell carcinoma (RCC) [59]. RCC is an angiogenesis dependent malignancy where any BRAF mutation has been identified. Thus, it seems that sorafenib efficacy may derive from its antiangiogenic activity rather than BRAF blockage.

Nevertheless, sorafenib has shown partial responses in advanced melanoma patients when combined with other chemotherapeutical agents such as carboplatin and paclitaxel [60,61], dacarbazine [62] or temozolomide [63].

PLX4720 (Plexicon) is a new specific $BRAF^{V600E}$ inhibitor that has recently come out. PLX4720 has been reported to be effective in $BRAF^{V600E}$ melanoma cells *in vitro* and *in vivo* [64]. This drug is currently undergoing Phase I clinical trials with advanced melanoma patients showing promising responses in those harboring the $BRAF^{V600E}$ mutation (data not published). Currently, phase II and III clinical trials with this inhibitor are being planned.

3.6.1.1.3 MEK inhibitors

MEK is another candidate to target in melanoma since it is the downstream-effector of BRAF. Several MEK inhibitors have been developed given that it has been described that melanomas harboring the $BRAF^{V600E}$ mutation are more sensitive to MEK inhibition than those without this mutation [65]. **PD032509** (Pfizer Oncology) and **AZD6244** (AstraZeneca) are MEK inhibitors that are involved in phase II clinical trials with patients with advanced melanoma. It has been observed that only patients bearing $B\text{-}RAF^{V600E}$ mutations had a partial response to AZD6244 [66]. However, it has been recently identified in melanoma patients a MEK1 mutation that confers resistance to AZD6244 treatment [67]. Moreover, MEK can also be activated by TLP2, a kinase

involved in the regulation of innate immunity indicating that chronic treatment with MEK inhibitors could have undesired effects regarding the innate immunity.

3.6.2 Therapeutical potential of targeting the PI3K pathway in malignant melanoma

The PI3K pathway regulates many important processes of tumorigenesis, including cell proliferation, survival, motility and angiogenesis. Moreover, it is well established that the PI3K pathway has a strong importance in malignant melanoma. High levels of p-AKT have been found in human melanoma samples [39,40,41.] The most common genetic alterations in the PI3K pathway in melanoma are the loss of PTEN and the overexpression of AKT3. Point mutations in specific components of this pathway have also been identified although at a very low frequency [47].

Interestingly, it has been shown that AKT3 silencing or PTEN expression in melanoma cells significantly abolishes melanoma tumor development *in vivo* promoting apoptosis [40,68]. In addition to this, it has been observed that targeting the PI3K pathway increases the sensitivity to other chemotherapeutical agents (for review [69])

All together, these data suggest that the PI3K pathway is a good candidate to target malignant melanoma and small kinase inhibitors targeting this pathway have been developed.

3.6.2.1 *Inhibitors*

There is a broad collection of small kinase inhibitors targeting the PI3K/AKT/mTOR pathway, some of which are currently being used in clinical trials (for review [70]).

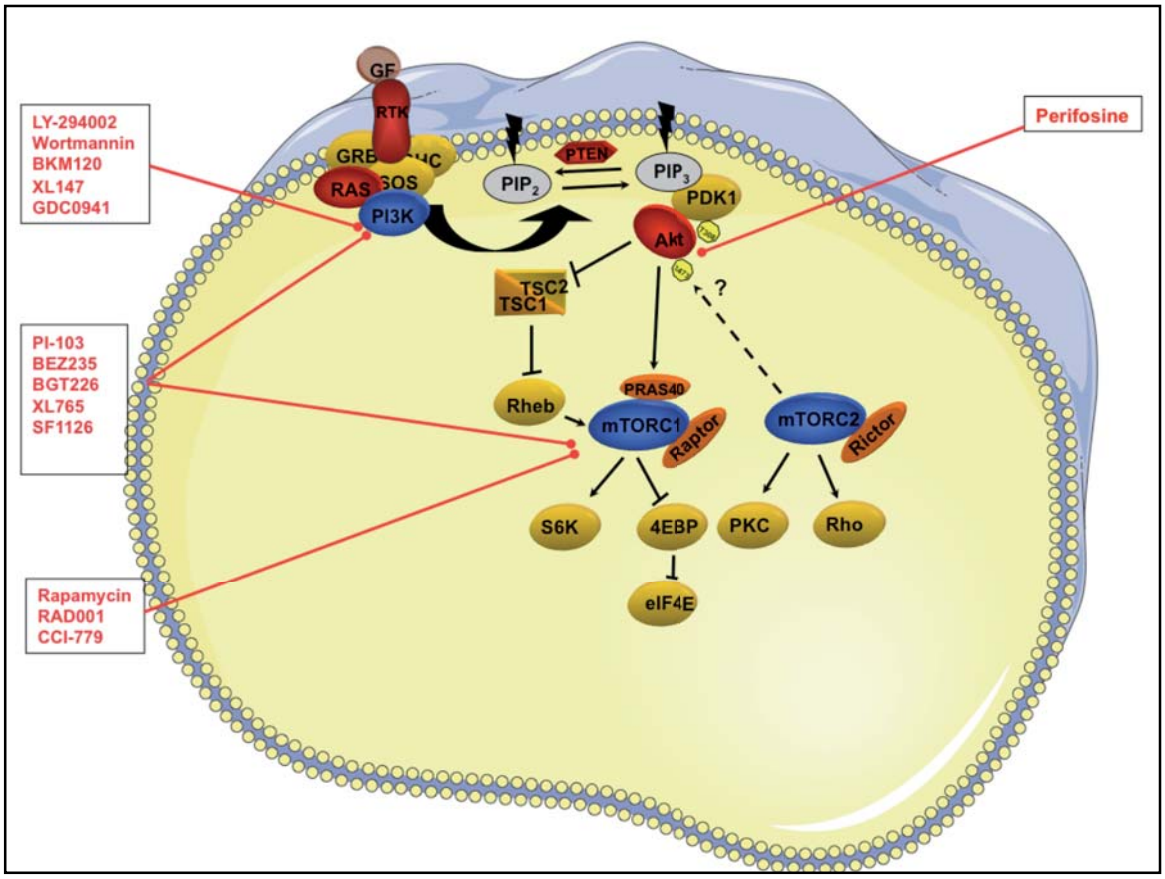

Figure 6. PI3K/mTOR pathway inhibitors.

Representative scheme of some of the inhibitors targeting the PI3K/mTOR pathway in melanoma. In red are the proteins that have been found to be mutated in melanoma.

3.6.2.1.1 PI3K inhibitors

LY294002 (Eli Lilly) and **wortmannin** are two of the first generation of PI3K inhibitors. Several preclinical studies with these inhibitors have contributed to the PI3K pathway knowledge in melanoma but, unfortunately, they are not used in clinical trials because of their poor pharmacokinetics characteristics.

Many other pure PI3K inhibitors with better pharmacokinetical characteristics (**BKM120** (Novartis), **XL147** (Exelixis), **GDC0941** (Genentech)) have been developed and have been recently included y in phase I-II clinical trials.

3.6.2.1.2 AKT inhibitors

AKT is another attractive candidate to target within the RTK/PI3K pathway. The inhibitors targeting AKT include lipid-bases-phosphatydilinositol analogues, ATP-competitive inhibitors and allosterics inhibitors. Among them, **Perifosine** (Kenyx) is the most clinically advanced AKT inhibitor. It prevents the AKT translocation to the membrane and it inhibits melanoma cell proliferation *in vitro* successfully [71]. Perifosine is currently being used in phase I-II clinical trials in patients with advanced solid tumors, including melanoma.

3.6.2.1.3 mTOR inhibitors

Rapamycin (Sirolimus, Rapamune, Wyeth) is the most well known mTOR inhibitor but it has been described to be an immunosuppressant [72,73]. Several analogues of rapamycin (also called rapalogues) with improved pharmacological properties have been developed. These include **RAD001** (Everolimus, Novartis) or **CCI-779** (Temsirolimus, Wyeth). Rapalogues are approved for treatment of advanced renal cell carcinoma. However, clinical trials in other tumor types, including melanoma, showed a low response rate [74].

3.6.2.1.4 Dual PI3K/mTOR inhibitors

It has been observed that the mTOR pathway has a feedback loop that leads to the inactivation of AKT. Then, specific inhibition of mTOR could activate AKT [75,76]. Hence, dual PI3K and mTOR inhibitors could have an improved antitumor activity preventing this feedback loop. The most part of dual PI3K/mTOR inhibitors have provided encouraging preclinical data and are currently in phase I clinical trials in patients with advanced solid tumors (**BEZ235** (Novartis), **BGT226** (Novartis), **XL765** (Exelixis), **SF1126** (Semafor)).

3.6.3 Therapeutical potential of targeting RTK in malignant melanoma

As mentioned above, RTK are involved in melanoma progression, particularly c-MET, PDGFR, c-Kit, EGFR or Src. Moreover, the signaling cascade of these RTK is propagated to the PI3K and RAS/ERK1/2 pathway. Thus, the inhibition of the RTK may be another therapeutical approach.

3.6.3.1 *Inhibitors*

RTK inhibitors

Imantinib (c-Kit and PDGFR inhibitors), **dasatinib**, **sunitinib** (multiple RTK inhibitor) and **erlotinib** (EGFR inhibitor) are some of the RTK's inhibitors that are currently undergoing clinical trials in patients with melanoma. It has been shown that c-kit mutant melanomas are sensitive to imantinib [77].

3.6.4 Therapeutical potential of targeting apoptosis in malignant melanoma

Cytotoxic chemotherapy induces cancer cell death through the mitochondria-dependent apoptosis. The mitochondria-mediated apoptosis is initiated by the release of the cytocrom C and consequent activation of caspase-9. There are some antiapoptotic proteins that prevent the release of the cytocrom C from the mitochondria. Bcl-2 is one of them, and importantly, it has been described to be involved in drug resistance mechanisms in melanoma [48]. Interestingly, it has been described that the overexpression of Bcl-2 in tumoral cells confers resistance to drugs treatment [78]. In the same way, depletion of Bcl-2 with antisense oligonucleotids results in tumor growth reduction in melanoma *in vivo* models [79].

These data suggested that Bcl-2 is an attractive target to consider in melanoma treatment.

3.6.4.1 Bcl-2 antisense olignonucleotides

Oblimersen sodium (Genasense) is a Bcl-2 antisense olignoculeotide, which has been used in phase III clinical trials in combination with dacarbazine in patients with advanced melanoma [80]. The treatment did not demostrate significance although patients treated with oblimersen had a slightly better and longer response.

There are many others inhibitors targeting these antiapoptotic family proteins but further investigation is needed.

3.6.5 Rational combined treatments

Some genomic studies in melanoma have revealed that mutations in PI3K or PTEN loss can coexist with mutations in NRAS or BRAF [35]. That indicates that the PI3K and RAF pathways cooperate in melanoma progression and it has been corroborated in an animal model [81]. In addition, the tumor sensitivity to monotherapy targeting one of the pathways could be affected by the presence of these mutations. Thus, combinations of drugs targeting both pathways may have further benefits. In fact, there are some preclinical studies in melanoma mouse models where the combination of MEK and PI3K inhibitors were effective blocking tumor growth [81,82], suggesting that targeting RAS and PI3K pathways simultaneously might be an effective therapeutic approach in melanoma.

3.7 Melanoma mouse models

Animals' models are widely used in research in order to characterize the role of particular genes in a disease progression or to test new therapeutical approaches in a physiological context. The most common animal model used in research is the mouse. As mice are also mammals, they have an anatomy and a physiology quite similar to the humans. Moreover, the recently identification of the mouse genome has revealed that humans and mice have a quite similar genome with some non-coding sequences well conserved. Thus, the genome of the mice can be easily manipulated, a large collection of mutations can be generated and that helps to create transgenic mice that could reproduce tumors in a similar way to that in humans.

In case of melanoma, it is difficult to get a good melanoma mouse model. It should be noticed that the skin of mice is different than the skin of humans. In humans, melanocytes reside in the epidermal-dermal junction of the skin whereas in mice, melanocytes are located mainly in the hair follicles and sometimes in the dermis, but rarely in the epidermal-dermal junction.

There are different types of melanoma mouse models, which include the non-transgenic mouse models and the transgenic ones.

3.7.1 Non-transgenic melanoma mouse models

The non-transgenic mouse models include the generation of orthotopic xenografts models by subcutaneous or intravenous injection of melanoma cells in the mice.

Since the most part of the scientific community works with human melanoma cells, the most frequent mice model used are **immunocompromised mice** so as to evade the rejection response driven by the immune system of the mouse. There are different models of immunocompromised mice with different degree of immunosuppression. For instance, **balb/c nude** mice are athymic and are unable to develop T cells, but they still have B cells, natural killer cells and a response to the complement. Other mice have a more severe immunodeficient phenotype, such as **NOD/SCID** mice, which are unable to produce T cells, B cells, and natural killer cells and have an impaired complement function.

Others work with mouse cell lines that have been isolated from spontaneous tumors raised in melanoma mouse models. Those cell lines are particularly interesting in order to do preclinical studies. Since these cells are syngenic with the mouse, they

can be injected in immunocompetent mice and its effects are going to be tested in a more physiological model. Moreover, they permit the study of tumor–host interactions using different genetically engineered animals.

3.7.2 Transgenic melanoma mouse models

Thanks to the great advance in genetic engineering technologies, several transgenic melanoma mouse models have been developed in order to obtain a proper tool to better understand the melanomagenesis or to test new drugs (for review [83]).

The most common melanoma mouse models include the overexpression of relevant genes under the regulation of melanocyte-specific promoter sequences, such as tyrosinase related protein 1 (Trp1) or dopachrome tautomerase (Dct) promoters. Melanomas can be spontaneously induced in transgenic mice with chemical or environmental carcinogens, such as DMBA, TPA or UV radiation. However, the majority of models generated up to date have a low penetrance, long tumor latencies, a limited metastatic potential or most important, a low similarity with the human melanoma histology (for review [83,84]).

Interestingly, the UV-induced HGF-transgenic mice resulted to be an appropriate melanoma mouse model.

3.7.2.1 UV-induced HGF transgenic melanoma mouse model

HGF is a multifunctional cytokine that regulates cell growth, invasiveness and motility. Notably, HGF activates both RAS and PI3K pathway through the binding to its receptor c-MET. As mentioned before, those pathways play an important role in melanoma development and progression. Moreover, C-MET is a tyrosine kinase receptor, which is expressed in several cancer types [85,86] and its expression is directly correlated with melanoma progression [19].

HGF transgenic mice express the HGF gene in several organs under the metallothiotienin-1 promoter [25]. As mentioned above, the melanocytes of normal mice are situated at the base of hair follicle. Nevertheless, HGF transgenic mice are characterized because their melanocytes are located in the dermis, epidermis and basal layer of the epidermis, thus resembling better the human skin [87]. HGF transgenic mice are able to develop spontaneous dermal melanomas at an approximate age of 21 months. Interestingly, a single dose of erythremal UV irradiation in neonatal HGF mice, but not in adults nor in wild type mice, was sufficient to induce melanomas with high penetrance in these animals. Moreover, those tumors recapitulate chronologically and

histopathologically all the stages of human melanoma, including metastasis [26]. On the other hand, the chronic exposure of adult HGF mice to suberythremal UV irradiation resulted in the development of non-melanocytic tumors, mainly SCC [88]. These observations in the HGF mouse correlate consistently with the epidemiological data that suggests that childhood sunburn supposes a high risk for developing melanoma [89,90].

Thus, the HGF melanoma mouse model supposes a relevant mouse model since it recapitulates molecular, histopathological and epidemiological features of the human melanoma. The availability of this melanoma mouse model provides a good opportunity to describe new molecular mechanisms involved in melanomagenesis upon a significant environmental agent such as the UV radiation as well as an interesting tool to perform preclinical studies of new drugs.

II. OBJECTIVES

The scientific community agrees that PI3K and MAPK pathways are two good candidate pathways to target in melanoma [82,91]. We obtained two small kinase inhibitors targeting these pathways: the dual PI3K/mTOR inhibitor PI-103 and the RAF kinase inhibitor sorafenib.

The availability of the HGF transgenic melanoma mouse model and melanoma cell lines syngenic with these mice supposes a great opportunity to test these drugs' effectiveness in a relevant melanoma mouse model.

The main objectives of this report are:

1. To test PI-103 and sorafenib effectiveness *in vitro* alone or in combination in melanoma cell lines obtained from spontaneous tumors raised in the UV-induced melanoma mouse model.

2. To test PI-103 and sorafenib effectiveness *in vivo* alone or in combination in orthotopic xenografts in immunocompetent mice.

III. MATERIAL AND METHODS

1. *In vitro* assays

1.1 Cell culture

1.1.1 Cell lines description

In this study we used the following mouse and human primary melanoma cell lines.

37-31E are melanoma cells obtained from melanomas raised in the Hepatocyte Growth Factor / Scatter Factor (HGF/SF) transgenic mouse melanoma model induced by ultraviolet irradiation [26] (Figure 7A). 37-31E-F0 cells were labeled in our laboratory by stable retroviral infection with pRetroSuper-GFP vector [92]. 37-31E-F3 is the third generation of a cell line after several passages through mice. To this purpose, 10^6 37-31E-F0 cells were injected subcutaneously in the back of the animals. When tumors were big enough, animals were sacrificed with CO_2 inhalation and tumors were dissected and processed to obtain a primary cell line 37-31 E-F1 as described later. Once the primary cell line is established, 10^6 of 37-31E-F1 cells were re-injected in another mice and the same procedure as above was performed to obtain the next cell generation (Figure 7B).

MGPM-3 and MLNM-10 are two primary human melanoma cell lines isolated from metastatic lesions from patients from the Vall d'Hebron Hospital.

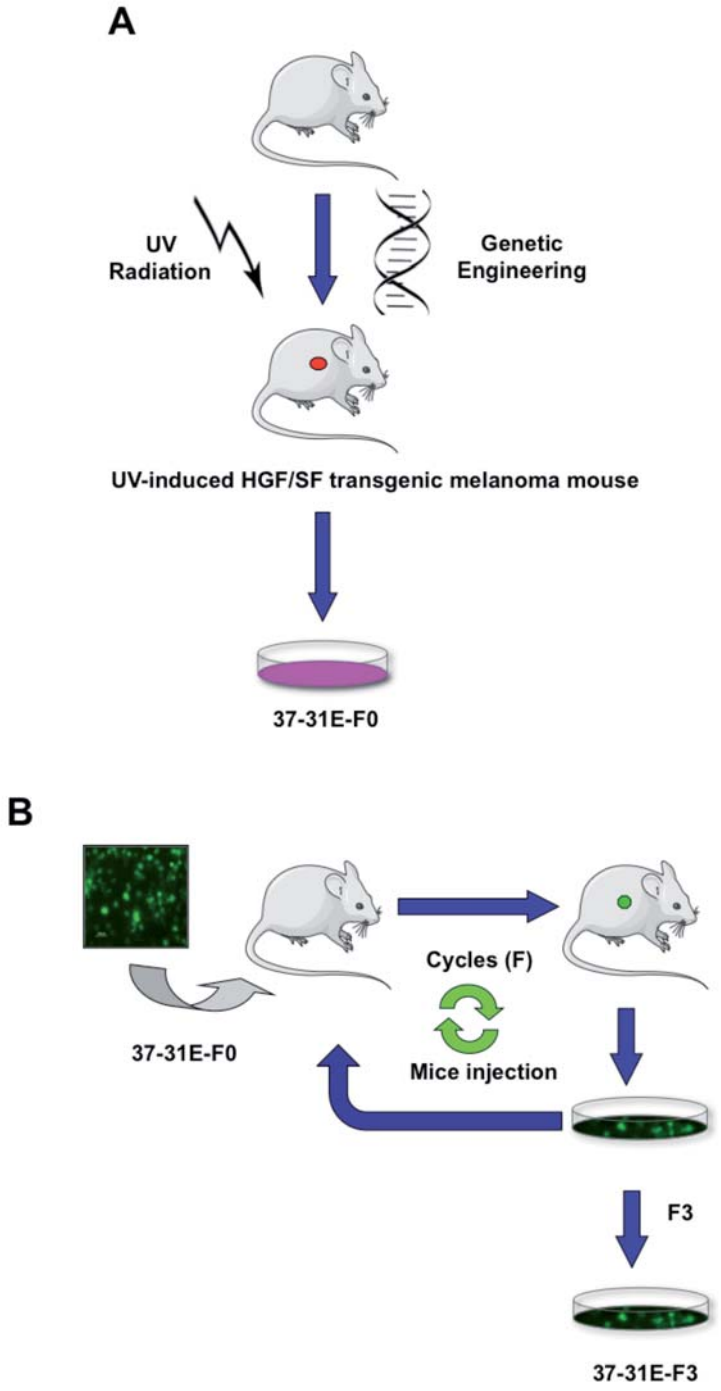

Figure 7. Mouse melanoma cell lines isolation.

*Generation of 37-31E-F0 (**A**) and 37-31E-F3 (**B**) cells.*

1.1.2 Cell lines maintenance and storage

For long term storage, cells were diluted in FBS (Invitrogen, Carlsbad, CA, USA) plus 10% DMSO (Sigma-Aldrich, Inc., Saint Louis, MO, USA). Freezing process was done gradually in a recipient with isopropanol at -80ºC. Next day, cells were stored in Nitrogen liquid containers.

To recover the cell lines, cells were thawed at 37ºC and resuspended in culture media. Then, cells were spinned down, resuspended in medium to remove DMSO and seeded into plates.

	CELL LINE	MEDIA
MICE	37-31E-F0	DMEM, 10%FBS, P/S (100 µg/ml), EGF (50 ng/ml), Insulin (100 µg/ml)
	37-31E-F3	DMEM, 10%FBS, P/S (100 µg/ml), EGF (50 ng/ml), Insulin (100 µg/ml)
	37-31E-F3K61	DMEM, 10%FBS, P/S (100 µg/ml), EGF (50 ng/ml), Insulin (100 µg/ml)
	37-31E-F3K63	DMEM, 10%FBS, P/S (100 µg/ml), EGF (50 ng/ml), Insulin (100 µg/ml)
HUMAN	MGPM-3	DMEM, 20% FBS, P/S (100 µg/ml)
	MLNM-10	DMEM, 20% FBS, P/S (100 µg/ml)

Table 1. Cell lines and growing conditions.

DMEM was obtained from Labclinics (Barcelona, Spain), FBS, EGF and insuline from Invitrogen (Carlsbad, CA, USA) and Penicilin/Streptomycin (P/S) from Cultek (Madrid, Spain).

1.1.3 Drugs

Cells were treated with different doses of PI-103 and sorafenib. **PI-103** was obtained from PIramed (Slough, Berkshire, UK), Genentech (South San Francisco, CA, USA) and Calibochem (San Diego, CA, USA). **Sorafenib (BAY-43-9006)** was obtained from Bayer (Leverkusen, Germany). PI-103 and sorafenib were diluted in DMSO and used at the concentrations indicated. Both drugs were stored at -20ºC. **BEZ-235** was purchased from LC Laboratories (Woburn, MA, USA).

1.1.4 Dose-response assays

To perform the different dose-response experiments, an appropriate number of cells according to the type of experiment were seeded in culture plates: 600.000 cells in p60 wells (Sarstedt, Nümbrecht, Germany) for 2 hours treatment experiments or 150.000 cells in p6 wells (Sarstedt, Nümbrecht, Germany) for treatments up to 72 hours. Next day, cells were monitorized to check their confluence and initial conditions. Then, plates were washed with sterile PBS and drugs were added to the media at the concentrations and time points indicated in each experiment. All experiments were performed at 37ºC and 5% CO_2.

1.1.5 Proliferation and viability assays

1.1.5.1 Cell counting

Cell counting has been performed using Guava ViaCount (Millipore Corp., Bedford, MA, USA) cell counter. $25 \cdot 10^3$ cells of each cell line were seeded in triplicates in 6 wells plates (Sarstedt, Nümbrecht, Germany) 12 h before adding treatment. Next day, treatments were added at the concentrations indicated in complete media and time point 0 h was measured. Cells were recovered from the plate, spinned down and diluted in 1 ml media. Then, a serial dilution was incubated in Guava reagent (Millipore Corp., Bedford, MA, USA) for 15 minutes at room temperature protected from light. This assay allows the identification of live cells and dead cells in culture by flow cytometry using the Guava cell analyzer (Millipore Corp., Bedford, MA, USA).

This process was repeated for different time points (24, 48, 72 and 96 h). All treatments and media were replaced every 48 h. The data was statistically analyzed using Microsoft Excel (Microsoft Corp., Redmond, OR, USA), Prism4 (Graphpad Software Inc., La Jolla, CA, USA) and/or VASTAT (University of Virginia, freeware software).

1.1.5.2 Viability assays

Colony formation is an easy and useful test as it allows us to check viability and proliferation in response to a stimulus by analyzing the number and intensity of stained colonies.

Three hundred cells per condition in triplicates were seeded in 6 wells plate (Sarstedt, Nümbrecht, Germany). Next day, corresponding treatments in complete media were added to each well. Every two days, treatments and media were replaced. Plates were maintained at 37ºC and 5% CO_2 until clones were identified in control plates (usually, from one to two weeks). Next, plates were washed with PBS and fixed with 4% formaldehyde (Sigma-Aldrich, Inc., Saint Louis, MO, USA) in PBS for 10 minutes. Cells were stained with 1% crystal violet (Sigma-Aldrich, Inc., Saint Louis, MO, USA) for 10 minutes, washed with tap water and representative pictures were taken.

Colonies were counted manually or using NIH ImageJ freeware software and results were analyzed with Prism4 (Graphpad Software Inc., La Jolla, CA, USA) and/or VasStat (University of Virginia, freeware software).

1.2 Protein analysis techniques

1.2.1 Protein extracts isolation

1.2.1.1 *Total protein extracts isolation from cell lines*

Cell plates were rinsed with PBS and scrapped with RIPA buffer supplemented with phosphatase inhibitors and protease inhibitors (Sigma-Aldrich, Inc., Saint Louis, MO, USA) on ice. Protein extracts were incubated 20 minutes on ice and after that, they were spinned down at 14000 rpm for 20 minutes. Supernatants containing proteins were transferred to a new tube and pellets were discarded.

1.2.1.2 Total protein extracts isolation from tumor tissues

Fresh tumor pieces were lysed in RIPA buffer supplemented with phosphatase inhibitors and protease inhibitors (Sigma-Aldrich, Inc., Saint Louis, MO, USA). Lysis was performed on ice with a rotor-stator Labgen homogenyenyzer 125 (Cole-Parmer, Illinois, USA). Next, lysates were incubated 20 minutes on ice and processed as described for cell lines.

1.2.1.3 Buffers:

RIPA

Tris HCl 50 mM pH=7,4
NaCl (Sigma-Aldrich, Inc., Saint Louis, MO, USA) 150 mM
EGTA (Sigma-Aldrich, Inc., Saint Louis, MO, USA) 0,5 mM
Nonidet NP40 (Roche Diagnostics, Basel, Switzerland) 0,5%
H_2O (miliQ)

Phosphatase inhibitors:

Sodium ortovanadate (Na_3VO_4) (Sigma-Aldrich, Inc., Saint Louis, MO, USA):

Stock= 250 mM Working concentration: 1 mM

1. Make a 250 mM sodium ortovanadate solution in water.
2. Adjust pH to 10 with HCl 1N or NaOH 1N.
3. Boil the solution until it gets colorless. Let the solution cool down at room temperature.
4. Readjust PH to 10 and repeat steps 3 and 4 until the solution turns colorless and PH.
5. Aliquot and store at -20 ºC.

Sodium fluoride (NaF) (Sigma-Aldrich, Inc., Saint Louis, MO, USA)

Stock= 1 M Working concentration: 50 mM

Aliquots are stored at -20ºC

1.2.2 Total protein quantification

Protein extracts were quantified using BCA Protein Assay Kit (Pierce Chemical Co., Rockford, IL, USA). This method is based on the fact that proteins reduce Cu^{2+} to Cu^{1+} in an alkaline media. Bicinchoninic acid (BCA) binds to Cu^{1+} and makes a soluble compound with a maximum absorbance of 562 nm. Protein concentration was calculated comparing the absorbance results with those from a serial dilution of known BSA standard concentrations.

1.2.3 Protein samples preparation, electrophoresis and transference

The desired amount of protein (50 µg) was suspended in protein SDS-loading buffer and denatured at 100ºC for 5 minutes.

Samples were resolved in 10, 12 or 15% acrylamide gels depending on the size of proteins of interest. Electrophoresis was performed at 120 V for 60-70 minutes. Proteins were transferred at 110 V for 90 minutes to a PVDF membrane (Millipore Corp., Bedford, MA,

USA), previously activated with methanol (Panreac Química, Barcelona, Spain) and rehydrated. Electrophoresis and transfer was performed using BioRad equipment (Bio-Rad Laboratories, Inc, Hercules, CA).

Membranes were blocked with 5% Milk (Santa Cruz Biotechnology, Inc., Santa Cruz, CA, USA) in TBS-Tween (Sigma-Aldrich, Inc., Saint Louis, MO, USA) for 1 hour at room temperature and then incubated with the desired antibodies at the optimized concentrations and conditions (Table 3).

Next membranes were incubated with the appropriate secondary antibody linked to horseradish-peroxidase (GE Healthcare, Buckinghamshire, UK), developed with the peroxidase substrate ECL (GE Healthcare, Buckinghamshire, UK) and exposed to films (Fujifilm Medical System, Stamford, CT, USA). Films were scanned and quantified using NIH Image J freeware software.

Membranes were stripped and reprobed with different primary antibodies. To that purpose, membranes were incubated with stripping solution twice for 20 minutes and re-blotted again with another primary antibody.

1.2.3.1 Buffers:

Protein loading buffer 2x:

Tris HCl pH= 6,8 0,5 M
SDS 4,4% (w/v) (Sigma-Aldrich, Inc., Saint Louis, MO, USA)
Glycerol 20% (v/v) (Sigma-Aldrich, Inc., Saint Louis, MO, USA)
Bromophenol blue 0,005% (Sigma-Aldrich, Inc., Saint Louis, MO, USA)
Before boiling samples, 10% ß-Mercaptoethanol (Sigma-Aldrich, Inc., St Louis, MO, USA) is added to the loading buffer.
Aliquots are stored at -20ºC

Acrylamide gel:

To make two acrylamide gels, 15 ml from the solutions listed in table 2 are mixed with 150 µl APS (Sigma-Aldrich, Inc., St. Louis, MO, USA) 10% and 10 µl TEMED (Thermo Scientific, Waltham, MA, USA). Once polymerized, stacking solution is added.

Stacking solution is composed of 6 ml stacking solution (Table 2), 60 µl APS 10% and 6 µl TEMED.

ACRYLAMIDE GELS (V_f= 500 ml)	10%	12%	15%
H_2O	203	170	121
Acrylamide 30% (Merck)	164	197	246
TRIS 1M PH= 8,8	123	123	123
SDS 10% (Sigma)	5	5	5

STACKING	V_f=500 ml
H_2O	342
TRIS 1M PH= 6,8	83
Acrylamide 30% (Merck)	62,5
SDS 10% (Sigma)	5

Table 2. Acrylamide and stacking gels composition.

Merck & Co, Inc., Whitehouse Station, NJ, USA.

Sigma-Aldrich, Inc., Saint Louis, MO, USA.

APS 10%:

For 1 ml:

0,1 g APS (Sigma-Aldrich, Inc., Saint Louis, MO, USA)

1 ml H_2O (milliQ)

This solution can be stored for a week at 4ºC

TBS-Tween solution:

TBS 1x

Tween 0,1% (BioRad Laboratories, Inc., Hercules, CA, USA)

H_2O (miliQ)

Solutions were stored at RT.

Stripping solution:

Tris HCl 50 mM pH=2

H_2O (miliQ)

Adjust pH to 2 with HCl

Solutions were stored at RT.

Antibodies:

The following antibodies were used (Table 3).

ANTIBODY	APPLICATION	DILUTION	CONDITIONS	COMERCIAL	REFERENCE
p-p44/42 MAPK (Thr202/Tyr204)	WB	1/1000	O/N 4ºC	Cell Signaling	9101
p-Akt (Ser.473)	WB	1/1000	O/N 4ºC	Cell Signaling	9271
Akt	WB	1/1000	1 h RT	Cell Signaling	9272
p-Stat 3 (Tyr 705) (D3A7)	WB	1/1000	O/N 4ºC	Cell Signaling	9145
Stat 3	WB	1/1000	1h RT	Cell Signaling	9132
p-S6 ribosomal protein (Ser 235)	WB	1/1000	O/N 4ºC	GenScript	A00315
Erk2	WB	1/1000	1 h RT	Santa Cruz	SC-154
Mcl-1	WB	1/200	O/N 4ºC	Dako	
Bcl-XS/L	WB	1/500	O/N 4ºC	Biolegend	633901
Bcl-2	WB	1/500	O/N 4ºC	Biolegend	633501
Cyclin D1 (clone SP4)	WB	1/200	O/N 4ºC	Thermo Scientific	RM-9104-S1
Actin	WB	1/5000	1 h RT	Chemicon Inc.	
GAPDH	WB	1/5000	1 h RT	Trevigen Inc.	2275-PC-100

Table 3. Antibodies and optimized conditions used for WB.

Cell signaling (Danvers, MA, USA), GenScript Corp. (Piscataway, NJ, USA), Santa Cruz Biotechnology, Inc., (Santa Cruz, CA, USA), Dako (Glostrup, Denmarck), Biolegends (San Diego, CA, USA), Thermo Scientific (Waltham, MA, USA), Chemicon Inc./Millipore (Bedford, MA, USA), Trevigen, Inc. (Gaithersburg, MD, USA).

1.3 RNA analysis techniques

1.3.1 RNA Isolation

1.3.1.1 RNA isolation from cell lines

RNAs from cell lines were isolated using the RNeasy Kit (Quiagen, Hilden, Germany) according to the manufacturer's recommendations.

1.3.1.2 RNA isolation from tumor tissues

Fresh tumor samples were disrupted using a rotor-stator Labgen homogenizer 125 (Cole-Parmer, Illinois, USA). Tumor pieces were resuspended in liysis buffer from RNeasy Kit (Quiagen, Hilden, Germany) in polystyrene tubes (BD Biosciencies, San Jose, CA, USA). RNAs were purified using RNeasy Kit (Quiagen, Hilden, Germany) and following the manufacturer's instructions

1.3.2 Quantitative-Reverse transcriptase polymerase chain reaction (qRT-PCR)

Amount and quality of all RNAs were assessed by spectrometric measurements with Nanodrop® (Nanodrop Company, Wilmington, DE, USA) (A260/280 and A260/230 ratios).

Then, 200 ng RNA per sample were used to obtain the sample's cDNA using SuperScript™ III First-Strand Synthesis System for RT-PCR (Invitrogen, Carlsbad, CA, USA). cDNA was used to perform qRT-PCR in a SDS 7900 System according to manufacturer's recommendations (Applied BioSystem, Foster City, CA, USA). All Taqman probes used (Applied BioSystem, Foster City, CA, USA) were previously validated.

cDNA dilutions used to perform the reaction were:

IL-6 (Mm 99999064_m1): not diluted

IL-10 (Mm 99999062_m1): not diluted

VEGFα (Mm 01281447_m1): 1/10 dilution in water

GAPDH (Mm 03302249_g1): 1/10 dilution in water

Measurements were calculated applying the ΔΔCt method using SDS 2.3 software.

2. *In vivo* assays

2.1 Animal care

Animals' welfare has been assessed under the supervision of Vall d'Hebron Research Institute's Ethics Committee. These include animals' appearance and behavior observation as well as tumor growth and weights following every two days. Animals showing discomfort signs or weight loss were sacrificed by CO_2 inhalation.

2.2 Drugs for *in vivo* use

PI-103 was obtained from PIramed (Slough, Berkshire, UK), Genentech (South San Francisco, CA, USA) and Calibochem (San Diego, CA, USA).

BAY 54-9085 (sorafenib) is an improved version of **BAY 43-9006** used for *in vivo* studies and was obtained from Bayer (Leverkusen, Germany).

Rapamycin and **LY 294002** were purchased in LC Laboratories (Woburn, MA, USA).

All drugs were diluted in DMSO (Sigma-Aldrich, Inc., St. Louis, MO, USA) and were given via intraperitoneal.

2.3 Tumor-growth experiments in response to sorafenib and PI-103

Every experimental design includes five to ten male mice from three to six month old per experimental group. The mouse strains used in this study were FVB/N and Balb c/nude.

FVB/N (Charles River Laboratories International, Inc., Wilmington, MA, USA) is an inbred albino mice strain with a complete immune system which has been described to be sensitive to the B strain of Friend Leukemia Virus (FVB). It's widely used to generate transgenic mouse models and to perform immunocompetent studies.

Balb c/nude mice (Charles River Laboratories International, Inc., Wilmington, MA, USA) are immunodeficient mice since they don't have a thymus and consequently, are not able to produce T cells. These mice are commonly used to study tumors' biology performing orthotopic xenographs.

For tumor growth experiments, 10^6 cells suspended in PBS were injected subcutaneously in the back of every mouse. Cell lines used were low passages 37-31E-F0 or 37-31E-F3.

The mice's supervision was increased to three times per week and tumor size was measured with a vernier caliper. Tumor volume was calculated according to $Vt= (d^2 \times D) \times \pi/6$ where *d* stands for small diameter and *D* stands for big diameter. All drug treatments started when tumors reached 50 mm^3.

Drugs were diluted in DMSO (Sigma-Aldrich, Inc., St. Louis, MO, USA) and were given daily to the mice by intraperitoneal injection at indicated dosage (10 mg/Kg, 70 mg/Kg PI-103, 50 mg/Kg sorafenib) as previously described [93] [94] [95]. Control animals received an equal volume of DMSO.

Once the treatment was started, animals' weight and tumor size was monitored every two days until tumors reached the maximum size allowed by the Ethical Committee. Mice were sacrificed by CO_2 inhalation, representative tumor pictures were taken and samples for immunohistochemistry, RNA extraction, protein extraction and primary culture establishment were obtained.

2.3.1 Primary culture establishment

Excised tumors were incubated overnight in PBS with double concentration of penicilin-streptomycin (P/S, 200μg/ml, Cultek (Madrid, Spain). Next, tumor was cut into small pieces with a scalpel in sterile conditions. Culture media supplemented with double penicillin-streptomycin (200μg/ml, Cultek (Madrid, Spain)) was added and plates were incubated at 37ºC and 5% CO_2. When cells attached to the plate, tumor pieces were removed, remaining cells were washed with PBS and fresh media was added.

2.3.2 Immunohistochemistry and Immunofluorescence

Tumor tissue samples were fixed overnight in formalin (Sigma-Aldrich, Inc., St. Louis, MO, USA). Next day, they were changed to 70% ethanol (Merck & Co, Inc., Whitehouse Station, NJ, USA). Samples were included in paraffin-embedded blocks and cut into 4 μmicrons sections for immunohistochemistry staining.

2.3.2.1 Immunohistochemistry for p-Erk1/2, p-Akt, p-S6, p-4EBP1 and cyclin D1

p-Erk1/2, p-Akt, p-S6, p-4EBP1 and cyclin D1 immunohistochemistries were processed using BenchMark® XT System (Ventana, Tucson, AZ, USA) in collaboration with the Pathology Department from Vall d'Hebron Hospital. Antigens were unmasked for 1 h with a Tris Basic Buffer at pH=8 provided by the manufacturer. The incubation conditions for the primary antibodies are summarized in table 4. p-Erk1/2, p-S6, p-4EBP1 and cyclin D1 were revealed using Ultraview™ Universal DAB Detection Kit (Ventana, Tucson, AZ, USA) and p-AKT was revealed using EnVision™ Flex (Dako, Glostrup, Denmarck).

2.3.2.2 Immunohistochemistry for p-Stat3

p-Stat3 immunohistochemistry was performed manually as follows:

Slides were deparaffined at 65ºC overnight followed by two washes in xylene (Panreac, Barcelona, Spain) of 20 minutes each. Next, samples were rehydrated through consecutive passages of 10 minutes in serial decreasing concentrations of ethanol (Merck & Co, Inc., Whitehouse Station, NJ, USA) (absolute, 95% ethanol, 75% ethanol and water).

To unmask the antigens, slides were brought into boil in a 10 mM sodium citrate (Sigma-Aldrich, Inc., St. Louis, MO, USA) buffer pH 6. Samples were maintained at subboiling temperatures for 20 minutes and then, they were let to cool down at RT. Samples were permeabilized with 0,5% Triton X-100 (Sigma-Aldrich, Inc., St. Louis, MO, USA) at RT. Slides were incubated with 3% hydrogen peroxide (Sigma-Aldrich, Inc., St. Louis, MO, USA) to inactivate the endogenous peroxidase followed by 1 hour blocking at RT in TBS-Tween-20 0,1%, 5% goat serum (Invitrogen, Carlsbad, CA, USA) to avoid unspecific bindings. Slides were incubated with the primary antibody overnight at 4ºC according to manufacturer's recommendations.

Next day, samples were incubated with secondary antibody and were revealed with Dako REAL™ Envision ™ Detection System,

Peroxidase/DAB+, Rabbit/Mouse Kit (Dako, Glostrup, Denmarck). Diaminobenziamide reaction was stopped in water and sections were counterstained with hematoxyline.

Finally, samples were dehydrated through an ethanol serial of increasing concentrations (water, 75% ethanol, 95% ethanol, absolute ethanol) and xylene (Panreac, Barcelona, Spain). Slides were mounted with DPX (Sigma-Aldrich, Inc., St. Louis, MO, USA) and representative pictures were taken.

2.3.2.3 Immunofluorescence for Ki67 and cleaved caspase-3

Slides were deparaffined at 65ºC overnight followed by two washes in xylene (Panreac, Barcelona, Spain) of 20 minutes each. Next, samples were rehydrated through consecutive passages of 10 minutes in serial decreasing concentrations of ethanol (Merck & Co, Inc., Whitehouse Station, NJ, USA), (absolute, 95% ethanol, 75% ethanol and water).

Samples were permeabilized with TBS-Tween-20 0,5% (BioRad Laboratories, Inc., Hercules, CA, USA) for 10 minutes at RT. The antigen unmasking was performed with sodium citrate as described for p-Stat3 immunohistochemistry. The slides were blocked with 5% FBS (Invitrogen, Carlsbad, CA, USA) in TBS-0,1%Tween-20 for 30 minutes at RT. Slides were incubated with the primary antibody diluted in TBS-Tween-20 0,1% (BioRad Laboratories, Inc., Hercules, CA, USA) for 1 hour at RT at the concentrations indicated in table 4. Next, samples were incubated with Fluorescein anti Rabbit IgG (H+L) (Vector Laboratories, Burlingname, CA, USA) 1/200 and Hoebchst (10 μg/μl) (Sigma-Aldrich, St. Louis, MO, USA) for 1 hour at 37ºC. Slides were mounted using Vectashield® (Vector Laboratories, Inc., Burlingname, CA, USA) and representative pictures were taken under a fluorescence microscope (Olympus BX61) (Olympus, Hamburg, Germany).

2.3.2.4 Tunel assay

The tunel assay (Terminal Transferase dUTP Nick End Labeling) was performed in the Pathology Department of the Vall d'Hebron

Hospital using the *In situ* Cell Death Detection Kit (Roche Diagnostics, Basel, Switzerland), following the manufacturer's recommendations.

2.3.2.5 Buffers and antibodies

Alcohols

Ethanol 95%

For 100 ml:

95 ml Ethanol (Merck & Co, Inc., Whitehouse Station, NJ, USA)

5 ml H_2O (milliQ)

Ethanol 75%

For 100 ml:

75 ml Ethanol (Merck & Co, Inc., Whitehouse Station, NJ, USA)

25 ml H_2O (milliQ)

Unmasking buffer

Sodium citrate

Sodium citrate 10 mM (Sigma-Aldrich, St. Louis, MO, USA)

H_2O (milliQ)

Adjust pH to 6 with HCl

Permeabilization buffers

Triton X-100 0,5% (Sigma-Aldrich, Inc., St. Louis, MO, USA)

H_2O (milliQ)

Blocking buffers

Goat serum 5% or Fetal Bovine serum 5% (Invitrogen, Carlsbad, CA, USA)

TBS-Tween-20 0,1% (BioRad Laboratories, Inc., Hercules, CA, USA)

Antibodies

The following antibodies were used (Table 4)

ANTIBODY	APPLICATION	DILUTION	CONDITIONS	COMERCIAL	REFERENCE
p-Stat 3 (Tyr 705)	IHC	1/50	O/N 4ºC	Cell Signaling	9145
p-S6 (Ser 240/244)	IHC	1/100	32' RT	Cell Signaling	2215
p-Erk1/2	IHC	1/200	1 h RT	Cell Signaling	9101
p-Akt (Thr308)	IHC	1/50	2h RT (pH=9)	Cell Signaling	9266
Ki67 (SP6)	IF	ready to use	1 h 37ºC	Master Diagnostica	MAD00310QD
Cyclin D1	IHC	ready to use	20' RT	Biocare Medical	PP236AA
Cleaved caspase 3	IF	1/100	1 h RT	Cell Signaling	9664

Table 4. Antibodies used for immunohistochemistry and immunofluorescence.

Cell signaling (Danvers, MA, USA), Master Diagnostica (Granada, Spain), Biocare Medical (Concord, CA, USA).

2.4 Immune suppression assays

Experimental design includes five to ten male mice from three to six month aged per condition. Mice were treated for a week with indicated dosage of PI-103 (40 mg/Kg), LY 294002 (25 mg/kg) or Rapamycin (1 mg/Kg). After treatment, animals were sacrificed and thymus and spleens were isolated as described below.

2.4.1 Thymocyte and Splenocyte isolation

Thymus and spleens were removed from the animal *post-mortem* by surgery. Spleens and thymus were placed in RPMI1640 media (Gibco, Invitrogene, Carlsbad, CA, USA) at RT. The organs were squeezed between two glass slides to prepare the single cell suspension. The cell suspension was transferred to a 1,5 ml tube and thymocytes were spinned down at 1000 rpm for 5 minutes at RT. Supernatants were discarded and cells were washed with PBS at 1000 rpm for 5 minutes at RT. Cell pellets were resuspended in Guava Reagent (Millipore Corp., Bedford, MA, USA) and were counted as described for proliferation assays.

IV. RESULTS

The scientific community agrees that PI3K and MAPK pathways are two good candidate pathways to target in melanoma [35,82]. Thus, we obtained two small kinase inhibitors that target these pathways and we first tested its effectiveness *in vitro* in two mouse melanoma cell lines.

PI-103

PI-103 is a dual PI3K/mTOR inhibitor that inhibits specifically the p110α-catalytical subunit of PI3K [96]. PI-103 works as an ATP-competitive inhibitor. It has been shown that PI-103 is more potent and more specific than the pan PI3K inhibitor LY 294002 according to the *in vitro* IC50 in kinase activity (concentration needed to inhibit the kinase to a 50%) summarized in table 5.

Kinase target	PI-103 *In vitro* IC50 (μM)	LY 294002 *In vitro* IC50 (μM)
p110α	0,008	0,7
p110β	0,088	0,306
p110δ	0,048	1,33
p110γ	0,25	7,26
mTORC1	0,02	8,9
mTORC2	0,083	n.a.

Table 5. IC50 values for PI-103 in vitro kinase activity. *(Adapted from [96] and [97])*

BAY 43-9006 (sorafenib)

BAY 43-9006 (sorafenib) is an ATP-competitive multikinase inhibitor that targets wild type BRAF, $BRAF^{V600E}$, CRAF, PDGFR, C-KIT and VEGFR with the IC50s summarized at table 6.

Kinase target	Sorafenib *In vitro* IC50 (nM)
C-RAF	6
Wild type B-RAF	25
B-RAF V600E	38
VEGFR1	26
VEGFR2	90
PDGFR β	57
c-KIT	68
MEK1, ERK1, EGFR, HER2/neu, IGFR1, PKA, PKB, CDK1, cyclin B, pim-1, PKCα, PKCγ	>10000

Table 6. In vitro biochemical profile of sorafenib. *(Adapted from [98])*

1. PI-103 and sorafenib i*n vitro* characterization in melanoma cell lines

1.1 Pathways inhibition characterization

In order to study the *in vitro* effectiveness of the drugs, we performed kinase inhibition screenings using two different mice melanoma cell lines (37-31E-F0 and 37-31E-F3). These cell lines were derived form primary lesions arose in the UV-induced HGF transgenic mouse melanoma model [26]. Furthermore, these cells can be used for *in vivo* tumor formation assays in a syngeneic immunocompetent context. We investigated the dugs' efficacy inhibiting Ras/Erk1/2 and Pi3k pathways in response to hepatocyte growth factor (HGF) to avoid serum's pleiotropic effects. To that end, melanoma cell lines were treated with increased concentrations of PI-103 or sorafenib for 2 hours in serum starvation and then, cells were treated with HGF for 10 minutes. Finally, we determined by western-blot the levels of p-Erk1/2 and p-Akt as reliable indicators of the activation of Ras/Erk1/2 and Pi3k pathway respectively (Figure 8).

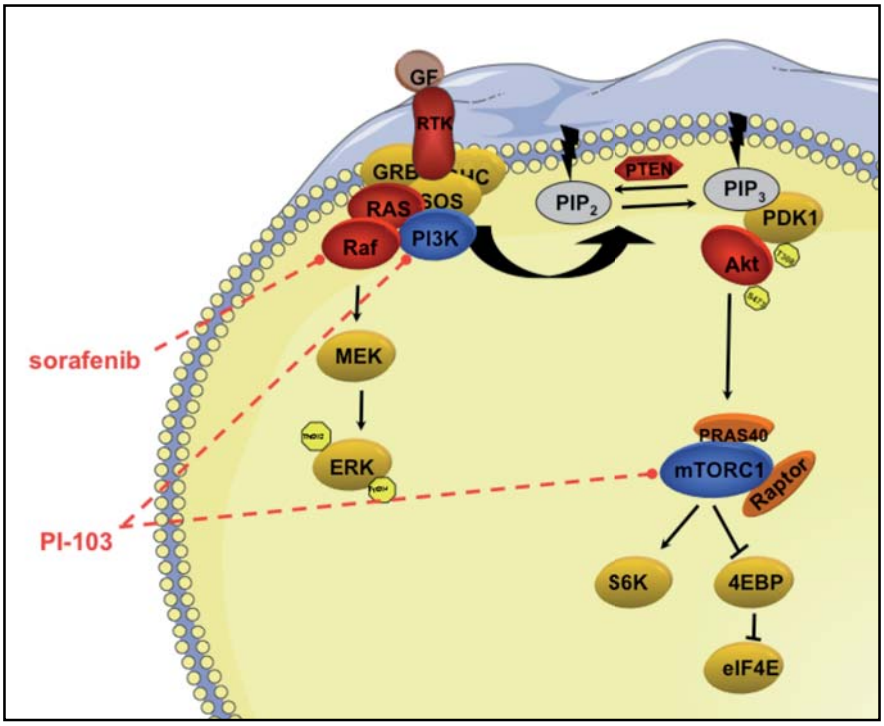

Figure 8. PI3K and RAS/ERK1/2 pathways scheme.

The scheme shows the main kinases and effectors of the PI3K and RAS signaling pathways. The targets of PI-103 and sorafenib are indicated.

1.1.1 PI-103 inhibit the Pi3k pathway in a dose-dependent manner

First, we analyzed the inhibition of the Pi3k pathway by PI-103 in response to hepatocyte growth factor.

In 37-31E-F0 cells, the addition of 15±3,2 nM PI-103 inhibited the activation of Pi3k pathway by 50% upon HGF treatment. Concentrations higher than 20 nM of PI-103 were able to block completely Akt phosphorylation. p-Erk1/2 levels were not affected except for the 50 nM PI-103 treatment where p-Erk1/2 levels were downregulated (Figure 9A).

37-31E-F3 cells appeared to be less sensitive to the Pi3k/mTOR inhibitor. Inhibition of Akt phosphorylation by 50% was reached at 20±1,2 nM of PI-103. According to the p-Erk1/2 levels, PI-103 treatment only interfered with Ras/Erk1/2 pathway activation at 50 nM (Figure 9B).

These results suggested that PI-103 inhibited *in vitro* Pi3k/mTOR pathway of the melanoma cell lines tested albeit with slight different sensitivities.

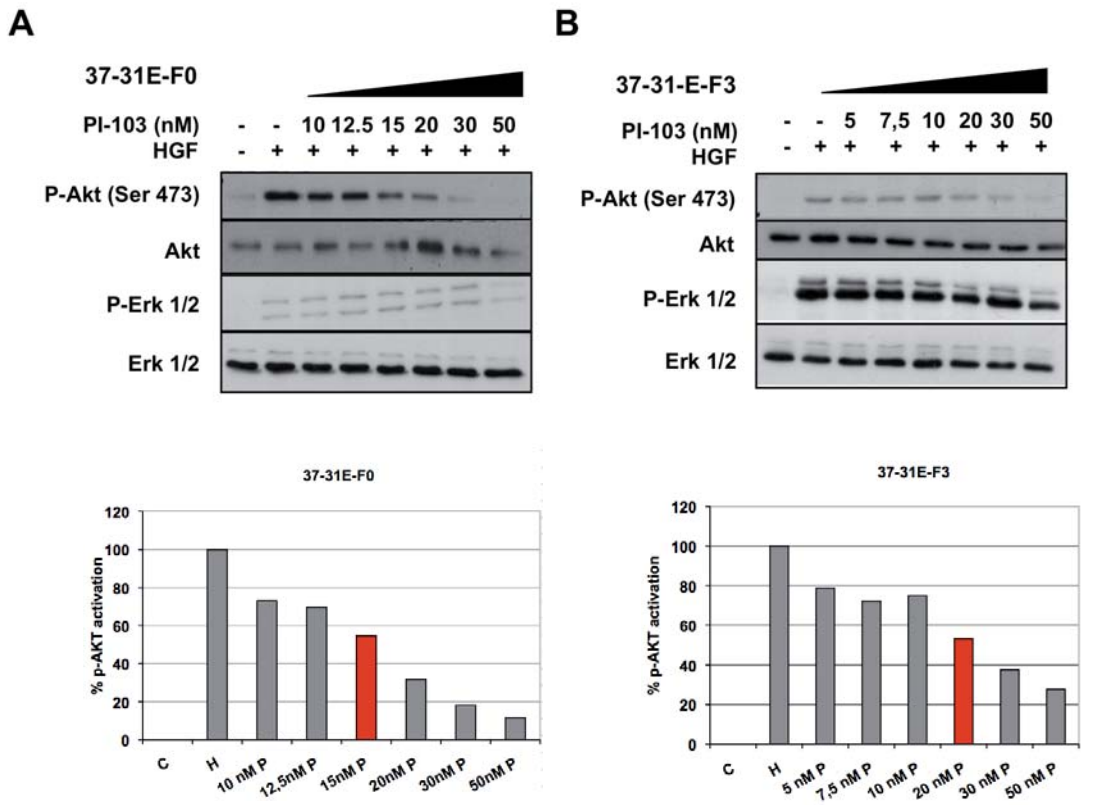

Figure 9. IC50 determination in pathway inhibition in 37-31E-F0 and 37-31E-F3 cells.

*37-31E-F0 (**A**) and 37-31E-F3 (**B**) cells were treated with the increasing concentrations of PI-103 indicated in the figures. Then, pathway inhibition status was assessed by western blot with the indicated antibodies. Graphs represent the % of pathway activation. Red bars are the PI-103 concentrations that inhibit by 50% the activation of the pathway.*

1.1.2 Sorafenib targets Ras/Erk1/2 pathway in a dose-dependent manner

We also analyzed the inhibition of the Ras/Erk1/2 pathway mediated by sorafenib in response to hepatocyte growth factor.

In 37-31E-F0 cells, 5±2,1 μM sorafenib was enough to inhibit Erk1/2 phosphorylation by 50% in response to HGF (Figure 10A). 37-31E-F3 cells were more sensitive to sorafenib, where the addition of 1±2,1 μM of sorafenib was enough to inhibit the Ras/Erk1/2 pathway activation by 50% upon HGF treatment (Figure 10B). Moreover, p-Akt levels indicated that Pi3k pathway activation upon HGF treatment was not affected by sorafenib treatment.

These data suggested that sorafenib inhibited *in vitro* the Ras/Erk1/2 pathway of 37-31E-F0 and 37-31E-F3 melanoma cell lines in a dose-dependent manner.

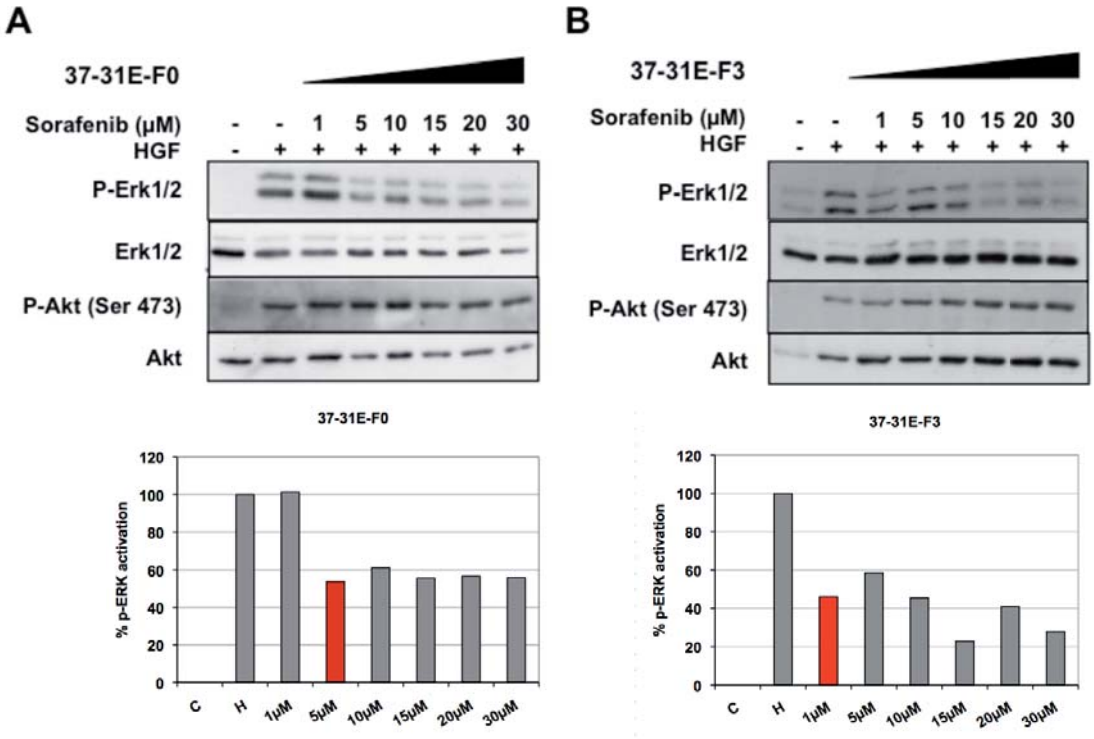

Figure 10. Sorafenib inhibits Ras/Erk1/2 pathway in a dose dependent manner.

*37-31E-F0 (**A**) and 37-31E-F3 cells (**B**) were treated with the indicated concentrations of sorafenib in serum starvation conditions for 2 hours. Then, cells were triggered with HGF for 10 minutes and protein samples were analyzed by western blot. Graphs represent the % of pathway activation according to sorafenib concentration. Red bars represent the sorafenib concentrations inhibiting the activation of the pathway by 50%.*

1.2 Biological effect of PI-103 and sorafenib as single agents in melanoma cell lines

To further characterize the *in vitro* effects of PI-103 and sorafenib, we performed cell proliferation and clonogenic assays in complete media plus the addition of the growth factor. To that end, we tested increasing concentrations of the drug in each cell line measuring cell proliferation by cell counting and cell viability, analyzing the number and size of the clones in the colony formation experiments.

1.2.1 PI-103 blocks *in vitro* melanoma cell proliferation in a dose-dependent manner

37-31E-F0 cell proliferation was inhibited in a PI-103 dose dependent manner. The concentration of PI-103 needed to inhibit proliferation to 50% (GI50) was above 100 nM PI-103. Proliferation was only effectively inhibited at 500 nM PI-103. The colony formation assays confirmed that treatment with 100 nM PI-103 was not enough to inhibit 37-31E-F0 viability and proliferation (Figure 11A).

37-31E-F3 cells also responded to the drugs in a dose-dependent manner but were more sensitive than the 37-31E-F0 since treatment with 50 nM or 100 nM PI-103 inhibited effectively the *in vitro* cell line proliferation. The GI50 for PI-103 was 40±2 nM PI-103, (2,5 fold lower than in 37-31E-F0). These results were in agreement with the colony formation assays where cell viability and proliferation was effectively blocked with concentrations higher than 50 nM PI-103 (Figure 11B).

The results indicated that PI-103 blocked melanoma cell proliferation more efficiently in 37-31E-F3 than in 37-31E-F0.

Figure 11. PI-103 blocks melanoma cell proliferation in a dose dependent manner.

*37-31E-F0 (**A**) and 37-31E-F3 (**B**) melanoma cell lines were treated with HGF and the indicated PI-103 concentrations in complete media. Cells were counted at the time points indicated in the graphs. In viability assays, cells were treated with HGF and the indicated drug concentrations in complete media for 7 days. Plates were stained with crystal violet. Representative pictures are shown. All experiments were done in triplicates.*

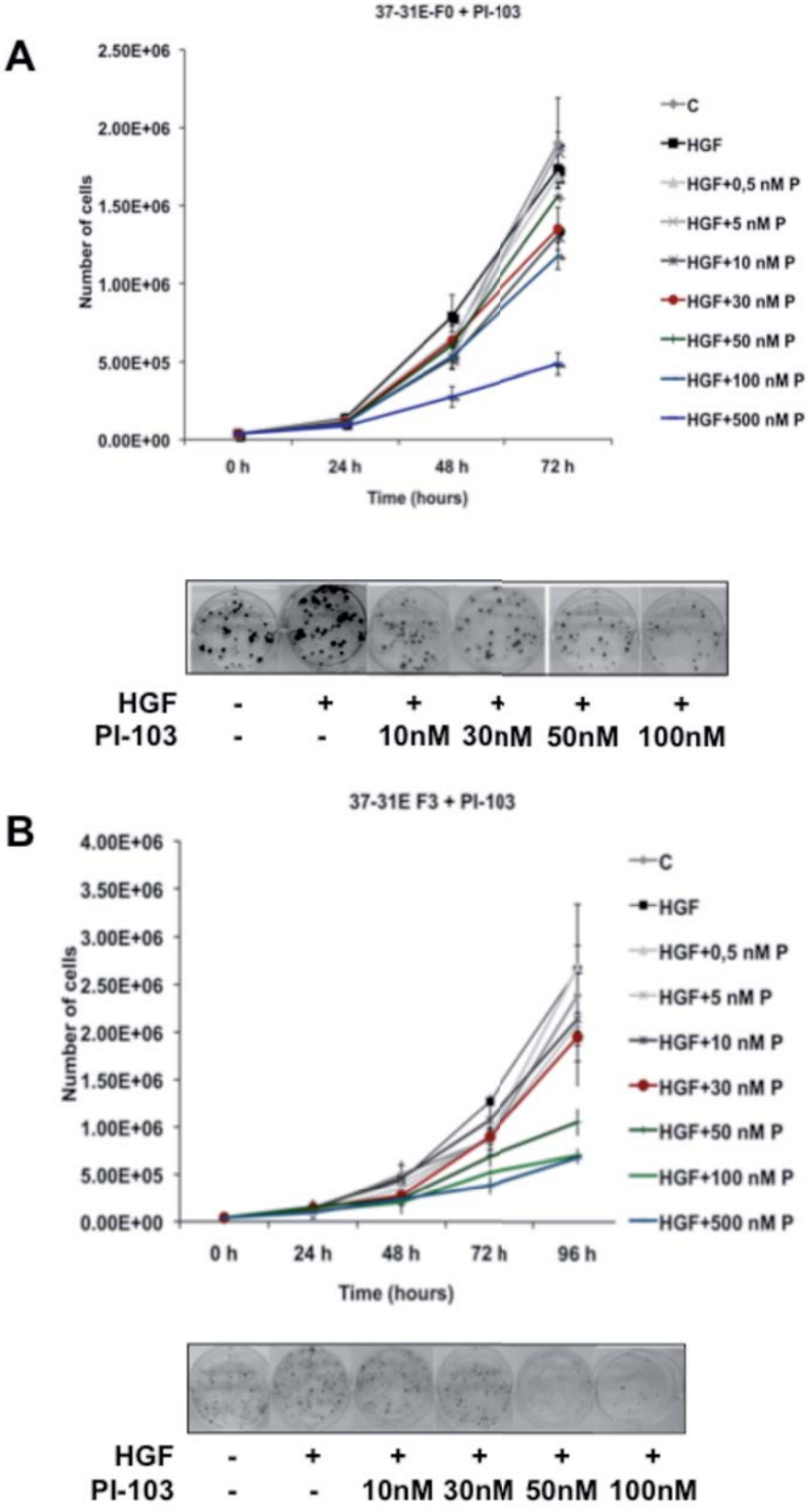
A
37-31E-F0 + PI-103
2.50E+06
2.00E+06
1.50E+06
1.00E+06
5.00E+05
0.00E+00
Number of cells
0 h
24 h
48 h
72 h
Time (hours)
C
HGF
HGF+0,5 nM P
HGF+5 nM P
HGF+10 nM P
HGF+30 nM P
HGF+50 nM P
HGF+100 nM P
HGF+500 nM P
HGF - + + + + +
PI-103 - - 10nM 30nM 50nM 100nM
B
37-31E F3 + PI-103
4.00E+06
3.50E+06
3.00E+06
2.50E+06
2.00E+06
1.50E+06
1.00E+06
5.00E+05
0.00E+00
Number of cells
0 h
24 h
48 h
72 h
96 h
Time (hours)
C
HGF
HGF+0,5 nM P
HGF+5 nM P
HGF+10 nM P
HGF+30 nM P
HGF+50 nM P
HGF+100 nM P
HGF+500 nM P
HGF - + + + + +
PI-103 - - 10nM 30nM 50nM 100nM

Figure 11

1.2.2 Sorafenib blocks *in vitro* melanoma cell proliferation in a dose-dependent manner

Sorafenib inhibited 37-31E-F0 and 37-31E-F3 melanoma cell proliferation in a dose-dependent manner. 37-313-F0 cells' proliferation was inhibited to 50% with 5±0,29 μM sorafenib whereas concentrations between 10 μM and 15 μM sorafenib were needed to obtain the same percentage of cell proliferation inhibition in 37-31E-F3 cells. Concentrations higher than 10 μM sorafenib completely abolished 37-31E-F0 proliferation and viability (Figure 12A). However, 37-31E-F3 cells proliferation and viability was completely inhibited at 30 μM sorafenib (Figure 12B).

According to these results, targeting the Ras/Erk1/2 pathway with sorafenib inhibited melanoma cell proliferation where 37-31E-F0 cells were more sensitive to sorafenib than 37-31E-F3 cells.

Figure 12. Sorafenib blocks melanoma cell proliferation and viability in a dose-dependent manner.

*37-31E-F0 (**A**) and 37-31E-F3 (**B**) melanoma cell lines' proliferation was measured by cell counting at the time points and sorafenib concentrations indicated. Clonogenic assays were performed in complete media plus HGF and the indicated concentrations of sorafenib for 7 days. Plates were stained with crystal violet. Representative pictures are shown. All experiments were done in triplicates.*

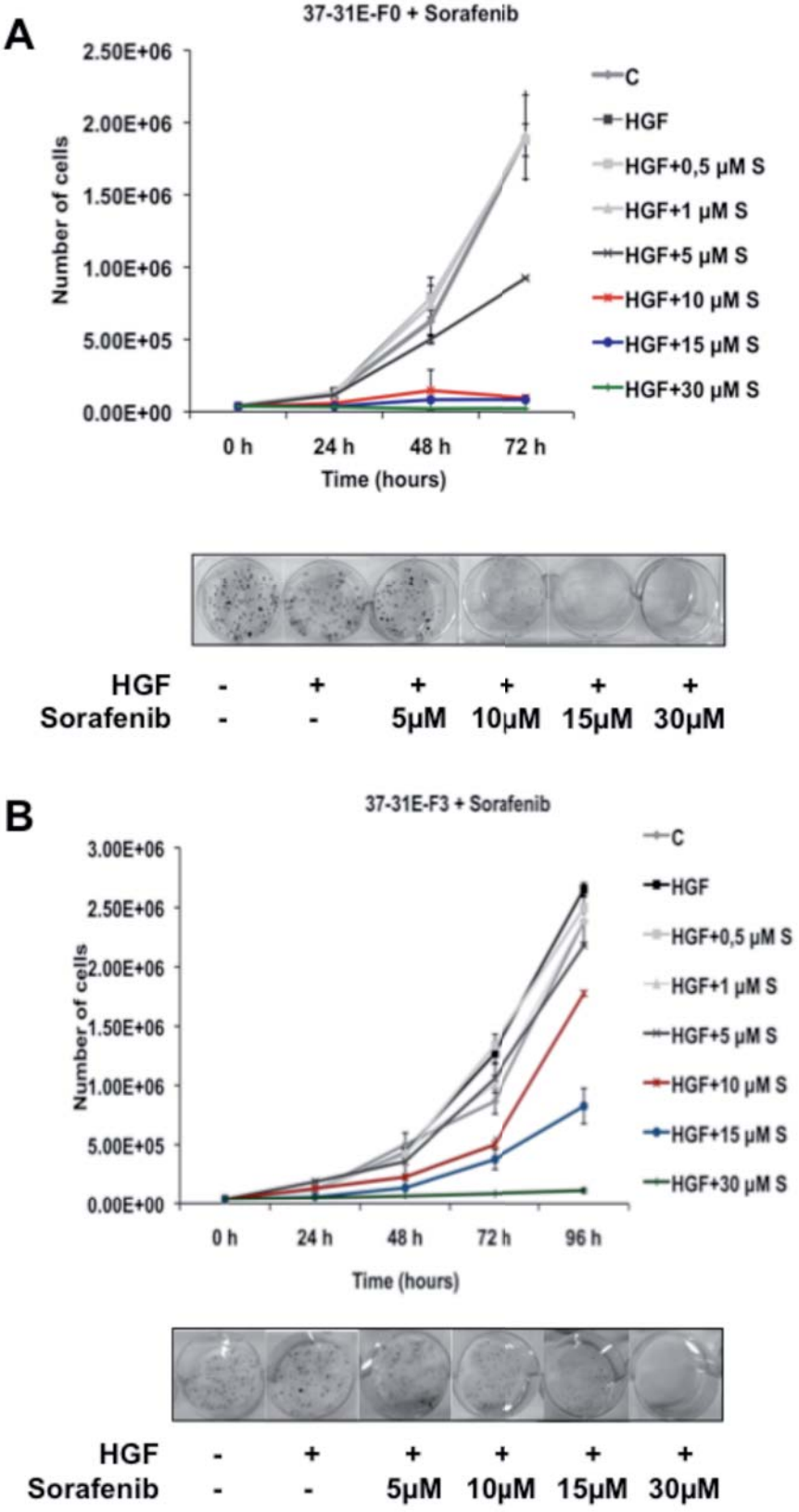
A
37-31E-F0 + Sorafenib
Number of cells
2.50E+06
2.00E+06
1.50E+06
1.00E+06
5.00E+05
0.00E+00
0 h
24 h
48 h
72 h
Time (hours)
C
HGF
HGF+0,5 µM S
HGF+1 µM S
HGF+5 µM S
HGF+10 µM S
HGF+15 µM S
HGF+30 µM S
HGF - + + + + +
Sorafenib - - 5µM 10µM 15µM 30µM
B
37-31E-F3 + Sorafenib
Number of cells
3.00E+06
2.50E+06
2.00E+06
1.50E+06
1.00E+06
5.00E+05
0.00E+00
0 h
24 h
48 h
72 h
96 h
Time (hours)
C
HGF
HGF+0,5 µM S
HGF+1 µM S
HGF+5 µM S
HGF+10 µM S
HGF+15 µM S
HGF+30 µM S
HGF - + + + + +
Sorafenib - - 5µM 10µM 15µM 30µM

Figure 12

1.3 Pathway inhibition in response to PI-103 and sorafenib as combined agents

Next, we wanted to analyze whether the combination of the drugs showed any cooperation inhibiting both pathways. To that purpose, we performed the following approaches. First, we fixed the concentration of one inhibitor according to its particular IC50 in each cell line, adding increasing concentrations of the second inhibitor for 2 hours. Then, we measured the levels of p-Erk1/2 and p-Akt 10 minutes after HGF triggering. Secondly, we performed the experiment in the reverse way.

1.3.1 PI-103 and sorafenib inhibit Pi3k and Ras/Erk1/2 pathways synergistically in 37-31E-F3

Treatment of 37-31E-F0 cells with 10 μM of sorafenib and increasing concentrations of PI-103 (5, 10 and 20 nM PI-103) did not show any cooperation inhibiting Ras/Erk1/2 pathway in response to HGF compared to 10 μM sorafenib alone. The addition of 10 μM sorafenib and 20 nM PI-103 was effective inhibiting Pi3k pathway (Figure 13A). The addition of increasing concentrations of sorafenib (5, 10 and 15 μM sorafenib) together with 20 nM PI-103 was effective inhibiting Pi3k pathway. Ras/Erk1/2 pathway was inhibited when cells were treated with 20 nM PI-103 and 5 μM sorafenib. However, no further inhibition was found when 10 μM or 15 μM sorafenib were added together with 20 nM PI-103 (Figure 13B).

The treatment of 37-31E-F3 with 10 μM sorafenib and 10 nM or 20 nM PI-103 cooperated synergistically inhibiting both pathways in response to HGF (Figure 13C). The addition of 15 μM of sorafenib with 20 nM PI-103 did not add any benefit inhibiting Pi3k and Ras/Erk1/2 pathways (Figure 13D).

These data indicated that in 37-31E-F3 cells, the combination of both drugs was synergistic inhibiting Ras/Erk1/2 and Pi3k activation in response to HGF.

Figure 13. PI-103 and sorafenib inhibit Pi3k and Ras/Erk1/2 pathways synergistically in a cell type dependent manner.

*37-31E-F0 (**A**, **B**) and 37-31-E-F3 (**C**, **D**) cells were treated with the indicated concentrations of PI-103 and sorafenib for 2 hours in serum starvation conditions. Then, cells were triggered with HGF for 10 min. Protein extracts were analyzed by western blot against the indicated antibodies. Graphs (**E**, **F**) show the quantification of p-Erk1/2 and p-Akt levels in response to the indicated treatments.*

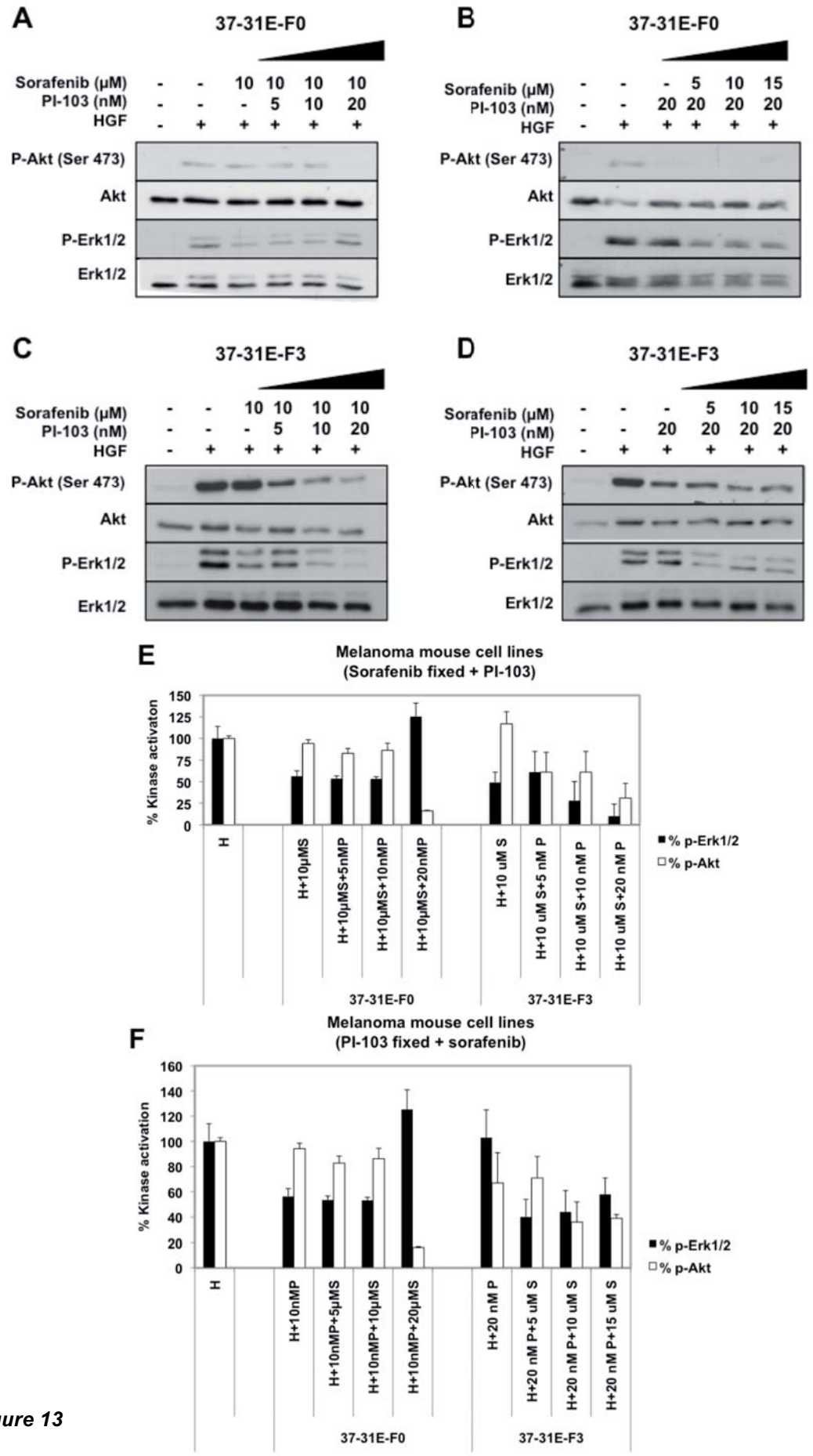
A
37-31E-F0
Sorafenib (μM) - - 10 10 10 10
PI-103 (nM) - - - 5 10 20
HGF - + + + + +
P-Akt (Ser 473)
Akt
P-Erk1/2
Erk1/2
B
37-31E-F0
Sorafenib (μM) - - - 5 10 15
PI-103 (nM) - - 20 20 20 20
HGF - + + + + +
P-Akt (Ser 473)
Akt
P-Erk1/2
Erk1/2
C
37-31E-F3
Sorafenib (μM) - - 10 10 10 10
PI-103 (nM) - - - 5 10 20
HGF - + + + + +
P-Akt (Ser 473)
Akt
P-Erk1/2
Erk1/2
D
37-31E-F3
Sorafenib (μM) - - - 5 10 15
PI-103 (nM) - - 20 20 20 20
HGF - + + + + +
P-Akt (Ser 473)
Akt
P-Erk1/2
Erk1/2
E
Melanoma mouse cell lines
(Sorafenib fixed + PI-103)
% Kinase activaton
150
125
100
75
50
25
0
H
H+10μMS
H+10μMS+5nMP
H+10μMS+10nMP
H+10μMS+20nMP
H+10 uM S
H+10 uM S+5 nM P
H+10 uM S+10 nM P
H+10 uM S+20 nM P
37-31E-F0
37-31E-F3
% p-Erk1/2
% p-Akt
F
Melanoma mouse cell lines
(PI-103 fixed + sorafenib)
% Kinase activation
160
140
120
100
80
60
40
20
0
H
H+10nMP
H+10nMP+5μMS
H+10nMP+10μMS
H+10nMP+20μMS
H+20 nM P
H+20 nM P+5 uM S
H+20 nM P+10 uM S
H+20 nM P+15 uM S
37-31E-F0
37-31E-F3
% p-Erk1/2
% p-Akt

Figure 13

1.4 Biological effect of PI-103 and sorafenib as combined agents in melanoma cell lines

1.4.1 PI-103 and sorafenib inhibit synergistically 37-31E-F3 cells proliferation

Since PI-103 and sorafenib inhibited synergistically the activation of Ras/Erk1/2 and Pi3k pathways in 37-31E-F3 cells, we decided to investigate whether the drugs were also synergistic blocking the *in vitro* cell proliferation. We performed a cell proliferation assay treating 37-31E-F3 cells with 20 nM PI-103, 5 μM sorafenib or 20 nM PI-103 plus 5 μM sorafenib.

As shown in figure 14, neither 20 nM PI-103 nor 5 μM sorafenib reduced 37-31E-F3 cell proliferation at 72 hours of treatment in complete media plus HGF. However, the combination of 5 μM sorafenib and 20 nM PI-103 inhibited synergistically 37-31E-F3 cells proliferation compared with the HGF treated cells.

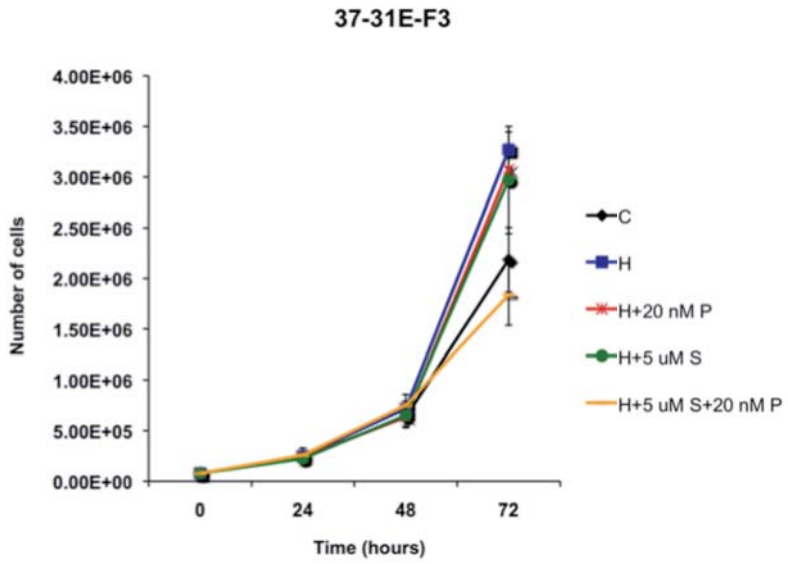

Figure 14. PI-103 and sorafenib inhibit synergistically in vitro cell proliferation of 37-31E-F3 melanoma cell line.

37-31E-F3 cells were treated with HGF and the indicated drug concentrations in complete media. Cells were counted at the different time points indicated.

2. *In vivo* effectiveness of PI-103 and sorafenib in orthotopic melanoma mouse models

2.1 37-31E-F0 and 37-31E-F3 tumorigenic capabilities

As above mentioned, 37-31E-F0 and 37-31E-F3 cell lines were obtained from neoplasic melanoma lesions arose in a melanoma mouse model that recapitulates chronologically and histopathologycally all the stages of human melanoma [26]. Thus, these cell lines are syngeneic to the FVB/N mouse. This provides us the opportunity to perform *in vivo* tumor growth experiments using an immunocompetent animal model.

37-31E-F0 and 37-31E-F3 cells were able to form tumors when injected subcutaneously in FVB/N mice although with different tumoral capabilities: while 37-31E-F0 were able to form tumors 1 month after injection, same number of 37-31E-F3 cells formed tumors only 8 days after its injection (Figure 15).

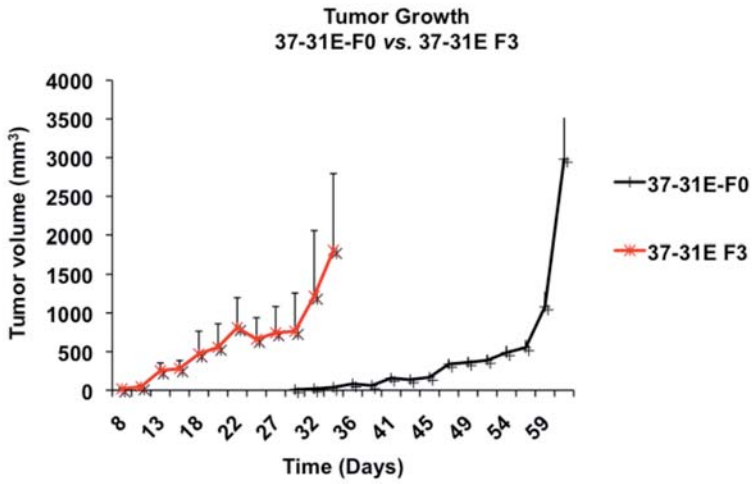

Figure 15. 37-31E-F0 and 37-31E-F3 tumorigenic capabilities.

One million of 37-31E-F0 (black line) or 37-31E-F3 (red line) were subcutaneously injected in FVB/N mice. Tumor size was monitored every two days.

2.2 PI-103 induces tumor growth in orthotopic xenograph immunocompetent mice

The above data suggested that, the addition of PI-103 and sorafenib inhibited synergistically the *in vitro* activation of Ras/Erk1/2 and Pi3k pathways and the *in vitro* cell proliferation in 37-31E-F3 cells. Based on these data, we decided to investigate whether PI-103 and sorafenib were also effective reducing tumor growth *in vivo* performing orthotopic xenographs in the immunocompetent mouse model (FVB/N mouse) using 37-31E-F3 cell line.

37-31E-F3 melanoma cell line was subcutaneously injected in FVB/N mice**.** Once the tumors reached a volume of 50 mm^3 the animals were treated daily via ip. either with DMSO (controls), 10 mg/Kg PI-103, 50 mg/Kg sorafenib or the drug's combination. We did not observe any obvious adverse effect in the general animal health as indicated by their body weights (Figure 16B). As previously described for other models [93], sorafenib treatment was effective blocking tumor growth (48±15% reduction). Unexpectedly, treatment with PI-103 promoted *in vivo* tumor growth (98±34% increase over control) and the drugs combination showed no further benefits compared to the sorafenib-treated tumors. Moreover, the tumors from the double treated mice were slightly bigger than the sorafenib ones (Figure 16A).

To further characterize these tumors we obtained fresh tumor tissue samples to analyze them by immunohistochemistry.

The immunohistochemical analysis of the paraffin-embebed tumor samples showed that all the treatments were efficient blocking their targets. According to the p-Akt, p-S6 and p-4EBP1 levels, PI-103 blocked efficiently Pi3k/mTOR pathway *in vivo*. Sorafenib was also effective *in vivo* blocking Ras/Erk1/2 pathway as indicated by the p-Erk1/2 levels. The data also showed that the drug combination was effective blocking both pathways (Figure 16C).

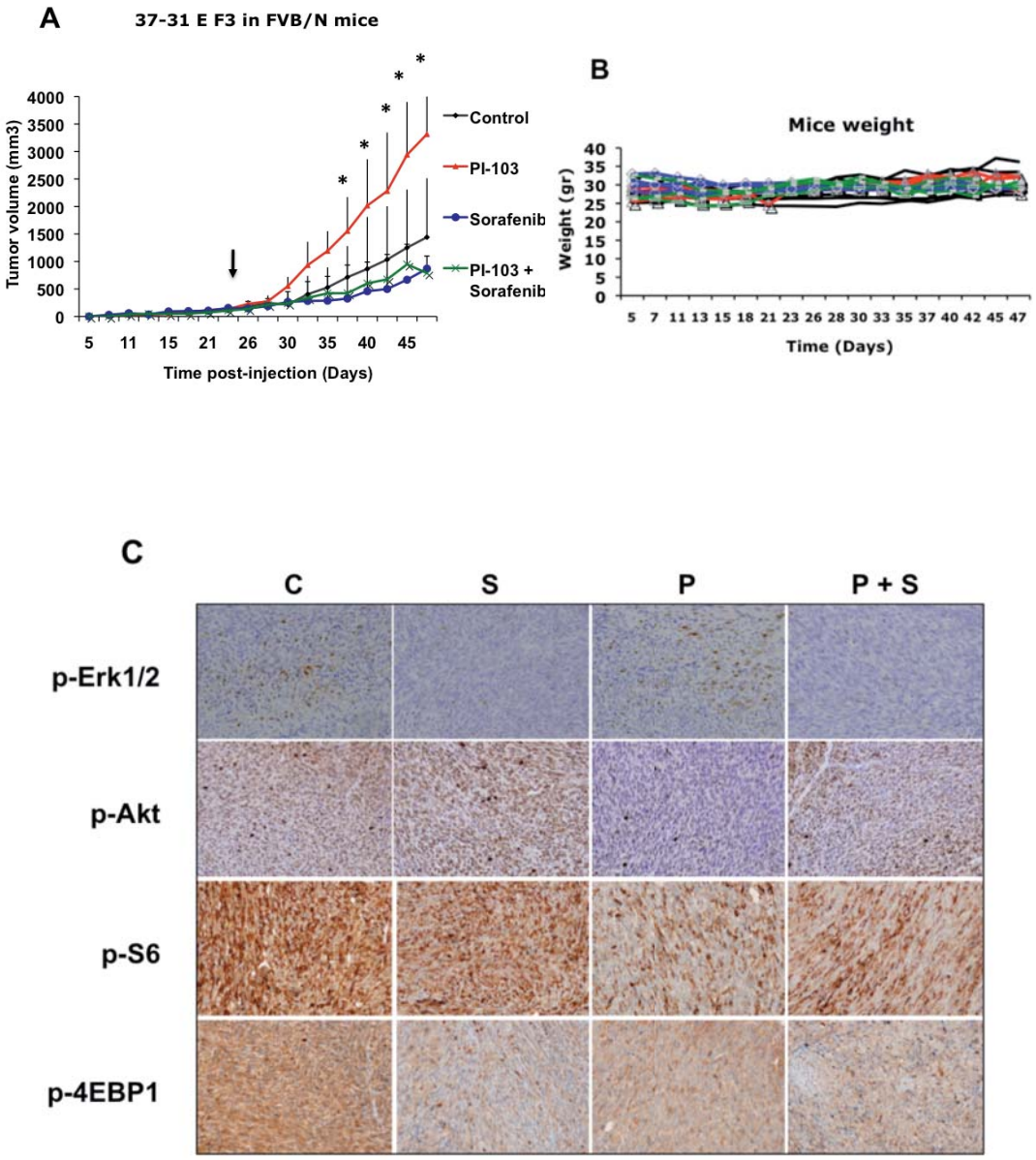

Figure 16. PI-103 promotes tumor-growth in immunocompetent mice.

A. *37-31E-F3 melanoma cells were injected subcutaneously to FVB/N immunocompetent mice. Animals were treated daily via ip with DMSO (C), 10 mg/Kg PI-103 (P), 50 mg/Kg sorafenib (S), or 10 mg/Kg PI-103 plus 50 mg/Kg sorafenib (P+S).* ***B.*** *Graphs show tumor volume and mice weight of each group during the treatment. The arrow indicates the treatment start point.* ***C.*** *Immunohistochemistry with the indicated antibodies of fresh tumor samples.*

2.3 PI-103 induced tumor growth in a drug dosage independent manner

The above data indicated that sorafenib and PI-103 were effective targeting Ras/Erk1/2 and Pi3k pathways respectively. However, PI-103-treated tumors showed an increased proliferation rate. Several publications have shown differences in the effectiveness of PI-103 inhibiting *in vivo* tumor growth in different animal models [94,99-102]. We investigated whether higher doses of PI-103 would have the desired effect. We performed the same experiment treating the animals either with DMSO (control) or 70 mg/Kg PI-103. Treated mice did not show any discomfort sign and their health was not affected by the treatment according to the weight data (data not shown). Interestingly, treatment of mice with 70 mg/kg of PI-103 also promoted *in vivo* tumor growth by 116±40% (Figure 17).

These results indicated that in our model, PI-103 induced *in vivo* tumor growth in a dose-independent manner.

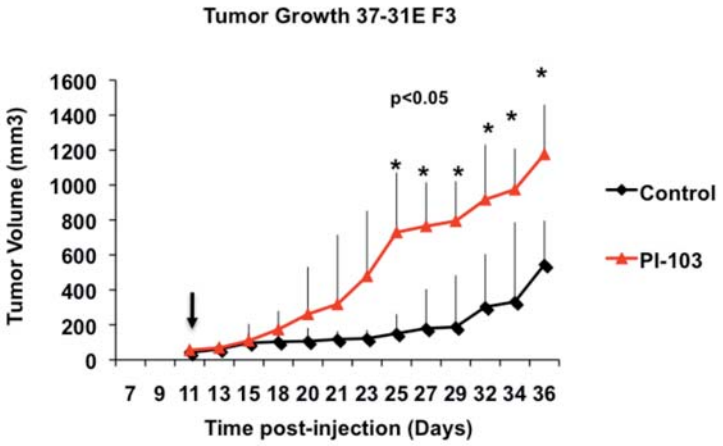

Figure 17. PI-103 induces tumor growth in a drug dosage independent manner.

37-31E-F3 cells were injected subcutaneously in FVB/N immunocompetent mice. Mice were treated daily with DMSO, 70 mg/Kg PI-103. Graphs show the tumor progression during the treatment and the arrow indicates the treatment starting point.

2.4 PI-103 induces tumor growth in a cell type-independent manner

Next, we investigated whether or not the observed effect was cell line dependent. To that end, we repeated the *in vivo* experiment by injecting 37-31E-F0 cells in FVB/N immunocompetent mice and treating them with DMSO (control) or 10 mg/Kg PI-103 daily (Figure 18A). Again, the tumors raised in PI-103-treated animals were bigger than the controls. PI-103-treated tumors showed an increase of 91±7,5% in tumor volume compared with the controls (Figure 18B).

The results suggested that the PI-103-mediated effects on *in vivo* tumor growth were cell line-independent

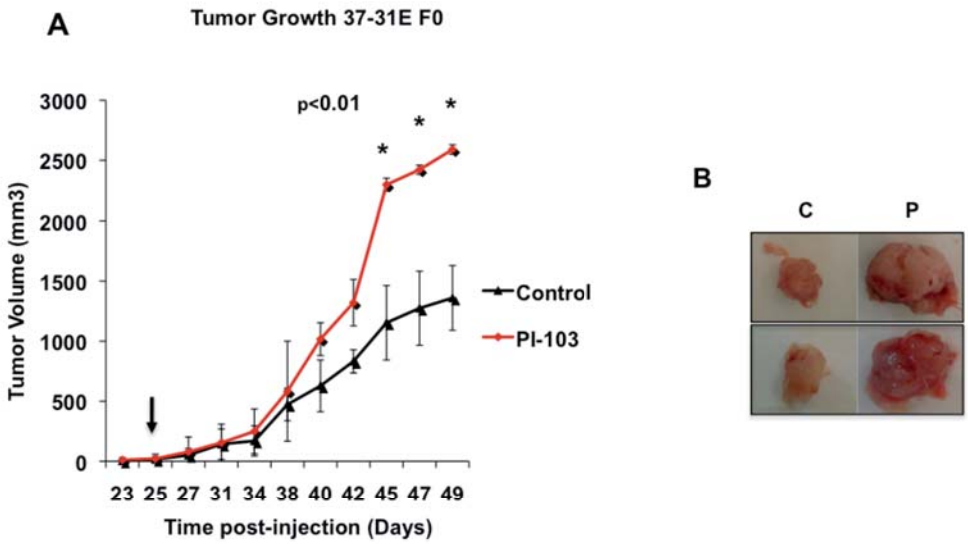

Figure 18. PI-103 induces tumor growth in a cell type independent manner.

A. *37-31E-F0 cells were subcutaneously injected in FVB/N immunocompetent mice. Mice were treated with DMSO (control) or 10 mg/Kg PI-103 daily via ip. Arrow indicates the treatment start point.* ***B.*** *Representative photographs of tumors after treatment. C: control P: PI-103-treated.*

2.5 PI-103 reduces tumor growth in immunocompromised balb c/nude mice

The above results describe an unexpected response to PI-103 treatment in an immunocompetent mouse model. Several studies have shown the effectiveness of PI-103 blocking *in vivo* tumor growth using Balb c/nude mice [94,99] These mice are immunocompromised and are unable to produce T cells. Therefore, we investigated the PI-103 effectiveness in an immunocompromised mouse model.

37-31E-F0 cells were subcutaneously injected into Balb /c nude mice. Tumors appeared evident one week after the injection, while the same cell line in immnocompetent mice took a month to develop a tumor. When the tumors reached 50 mm^3, animals were treated with DMSO (controls) or 10 mg/Kg PI-103 daily. In agreement with previous reports [94,99], PI-103 was effective reducing tumor growth in Balb/c nude mice by a 77±4% (Figures 19A and 19B), suggesting an active role of the host selecting tumor cells and/or possible drug's systemic effects.

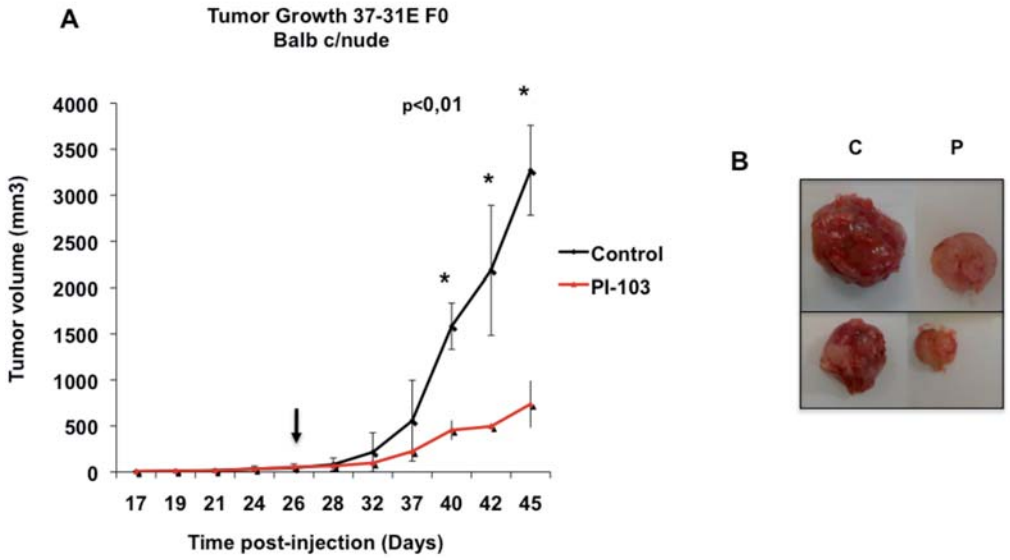

Figure 19. PI-103 reduces tumor growth in immunocompromised balb c/nude mice.

A. *Orthotopic xenograft explants with 37-31E-F0 in balb c/nude mice were performed. Mice were treated with DMSO (control) or 10 mg/Kg PI-103 daily. Graph shows tumor progression during the treatment.* ***B.*** *Representative photographs of two paired tumors after the treatment. C: control, P: PI-103 –treated.*

3. Host dependent tumor cell selection

3.1 PI-103 promotes tumor growth *in vivo* increasing cell proliferation and blocking apoptosis

Since PI-103 promoted tumor growth in a dose and cell-independent manner in immunocompetent mice, we hypothesized that PI-103-treated tumors could be either growing faster and/or having slower apoptotic rate compared to the DMSO-treated tumors. First, we investigated the status of some proliferation markers such as cyclin D1 and Ki67. As shown in figure 20A, paraffin embebed tumor tissue samples from PI-103 treated mice showed an increase in the levels of cyclin D1 staining compared with the control, sorafenib treated mice or mice treated with both drugs. These results were confirmed by western-blot using tumor protein lysates (Figure 20B). In agreement with this, PI-103 treated tumors also showed significant increased levels of Ki67 positive cells.

In addition to this, we analyzed the apoptosis rates within tumors by TUNEL assay and measuring the levels of cleaved-caspase-3. The TUNEL assay and cleaved-caspase-3 staining revealed that whereas sorafenib clearly induced apoptosis, PI-103 treated samples had the lowest apoptotic rate. Interestingly, the double treated samples had less apoptosis than tumors treated with sorafenib alone, suggesting an antiapoptotic role for PI-103 (Figure 20A).

Altogether, these results indicated that in our model, PI-103 induced cell proliferation and inhibited apoptosis.

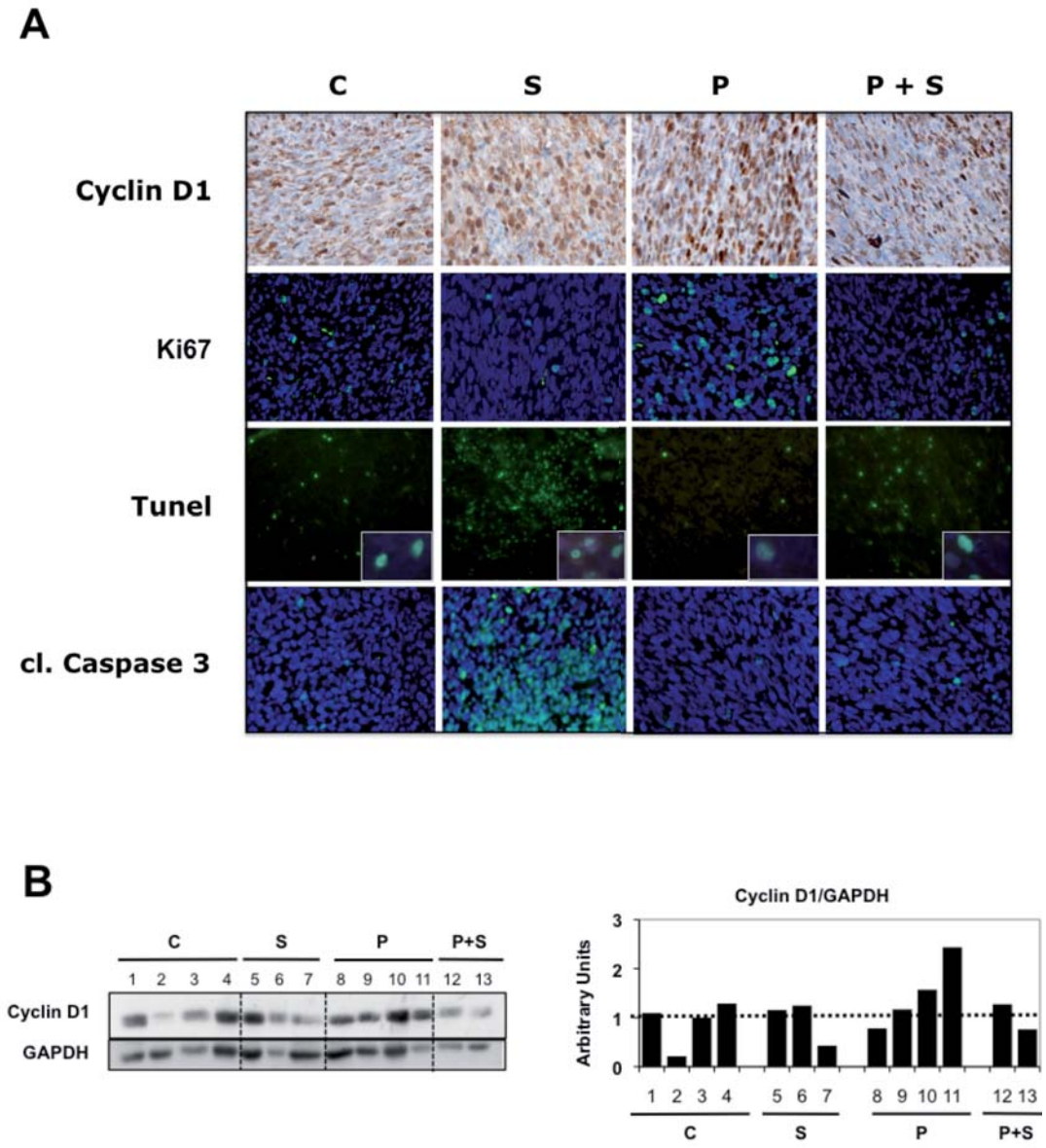

Figure 20. PI-103 increases proliferation and blocks apoptosis in vivo.

*Immunohistochemistries and immunofluorescence (**A**) and western blot (**B**) from tumor samples from mice treated with DMSO (C), PI-103 (P, 10 mg/Kg), sorafenib (S, 50 mg/kg) or PI-103 plus sorafenib (P+S, 10 mg/kg, 50 mg/Kg). Graph shows the quantification of the western blot for cyclin D1. GAPDH was used as a loading control.*

3.2 PI-103 up regulates the antiapoptotic BH3 family proteins *in vivo* and *in vitro*

The above data showed that the PI-103-treated tumors had the lowest apoptotic rate suggesting that PI-103 could be implicated in the regulation of apoptosis within the tumors.

Interestingly, the antiapoptotic BH3 family proteins have been described to be involved in resistance mechanisms to the mTOR inhibitor rapamycin [103,104]. We analyzed the levels of some antiapoptotic proteins of this family in control and PI-103 tumor-treated samples obtained from FVB/N mice and Balb c/nude mice. Interestingly, PI-103-treated samples from immunocompetent mice showed an increase of the BH3-family proteins Bcl-X and Mcl-1. On the other hand, PI-103-treated tumors from immunocompromised mice showed an opposite response (Figure 21A).

In order to get some insights in the antiapoptotic molecular mechanisms induced by PI-103, we performed some experiments in primary cell lines derived from tumors raised in immunocompetent DMSO-treated mice (37-31E-F3K61, 37-31E-F3K63) (Figure 16).

First, we analyzed the basal levels of the antiapoptotic proteins in the parental (37-31E-F0, 37-31E-F3) and tumor derived cell lines (37-31E-F3K61, 37-31E-F3K63) from control mice. The data showed that tumor derived cell lines expressed higher levels of Mcl-1 than parental cells. 37-31E-F3K63 also expressed more Bcl-2 than the rest of cell lines (Figure 21B).

Next, we investigated whether PI-103 and sorafenib were able to regulate *in vitro* the levels of these antiapoptotic proteins. To that purpose, we treated the parental and the tumor derived cell lines with increasing concentrations of PI-103 and sorafenib for 48 hours and checked the levels of the antiapoptotic proteins by western blot. Surprisingly, PI-103 treatment induced the upregulation of the levels of Mcl-1 and Bcl-2 in the two tumor derived cell lines but not in the parental cell line. However, concentrations above 15 μM of sorafenib reduced the levels of the antiapoptotic proteins in the three cell lines (Figure 21C). Moreover, these results correlated with the clonogenic assays where the tumor derived cell line 37-31E-F3K63 showed an increased survival and proliferation capabilities after treatment with 50 nM and 100 nM PI-103 compared with the parental cell line 37-31E-F3 (Figure 21D).

Figure 21. PI-103 regulates antiapoptotic BH3-family members in vivo and in vitro.

A. *Western blot with tumor samples from immunocompetent mice treated with DMSO or 10 mg/Kg PI-103 (left) and tumor samples from immunosuppressed mice treated with DMSO or 10 mg/Kg PI-103 (right). Graphs on the right show the quantification of the bands for every group. GAPDH was used as a loading control.* ***B.*** *Protein extracts from the indicated cell lines were isolated and analyzed by western blot with the indicated antibodies. 37-31E-F3, 37-31E-F3K61 and 37-31E-F3K63 cells were treated with the indicated drug concentrations in complete media for 48 hours.* ***C.*** *37-31E-F3, 37-31E-F3K61 and 37-31E-F3K63 cells were treated with the indicated drug concentrations in complete media for 48 hours. Protein extracts were resolved in acrylamide gels and blotted with the indicated antibodies* ***D.*** *37-31E-F3 and 37-31E-F3K63 cells were treated with 50 nM and 100 nM PI-103 for a week. Then, plates were fixed and stained with crystal violet. Representative photographs are showed.*

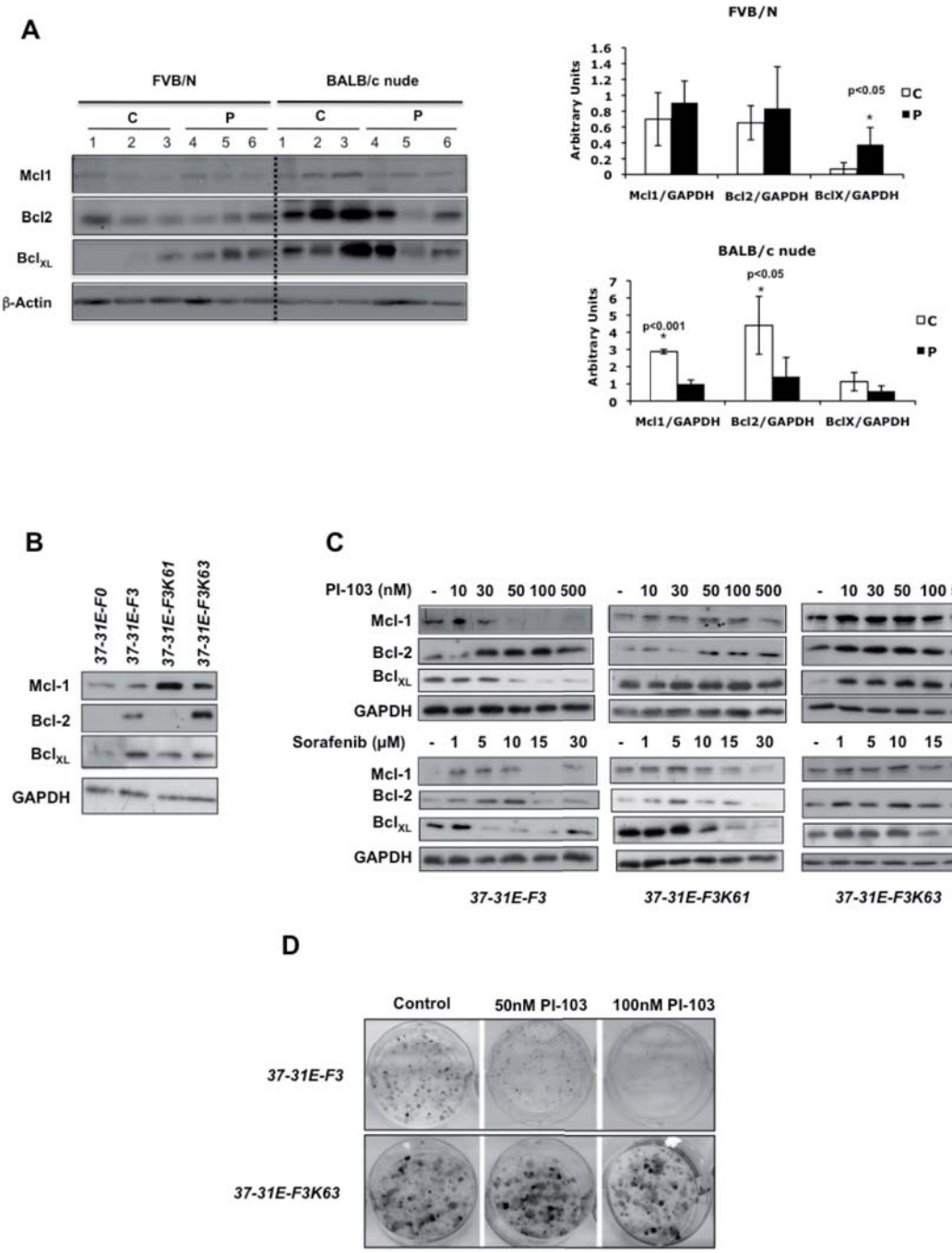
A
FVB/N
BALB/c nude
C
P
1 2 3 4 5 6 1 2 3 4 5 6
Mcl1
Bcl2
BclXL
β-Actin
FVB/N
Arbitrary Units
p<0.05
C
P
Mcl1/GAPDH
Bcl2/GAPDH
BclX/GAPDH
BALB/c nude
p<0.001
p<0.05
B
37-31E-F0
37-31E-F3
37-31E-F3K61
37-31E-F3K63
Mcl-1
Bcl-2
BclXL
GAPDH
C
PI-103 (nM) - 10 30 50 100 500
Sorafenib (μM) - 1 5 10 15 30
37-31E-F3
37-31E-F3K61
37-31E-F3K63
D
Control
50nM PI-103
100nM PI-103
37-31E-F3
37-31E-F3K63

Figure 21

3.3 PI-103 increases survival of sorafenib treated melanoma cells

The *in vivo* tumor growth data (Figure 16) showed that tumors treated with sorafenib and PI-103 were slightly bigger than tumors treated with sorafenib alone. Furthermore, PI-103 seemed to protect from sorafenib-mediated apoptosis (Figure 20).

We studied the *in vitro* survival capabilities of 37-31E-F3 cells treated with sorafenib and increasing concentrations of PI-103. As showed in figure 22A, the addition of HGF and 10 nM PI-103 did not affect the survival of the cells while treatment with 10 μM sorafenib totally abolished cell survival. Interestingly, the addition of increasing concentrations of PI-103 to 10 μM sorafenib increased melanoma cells survival in a dose-dependent manner. Furthermore, the increased survival correlated with the accumulation of the antiapoptotic proteins Mcl-1 and Bcl-2 (Figure 22B).

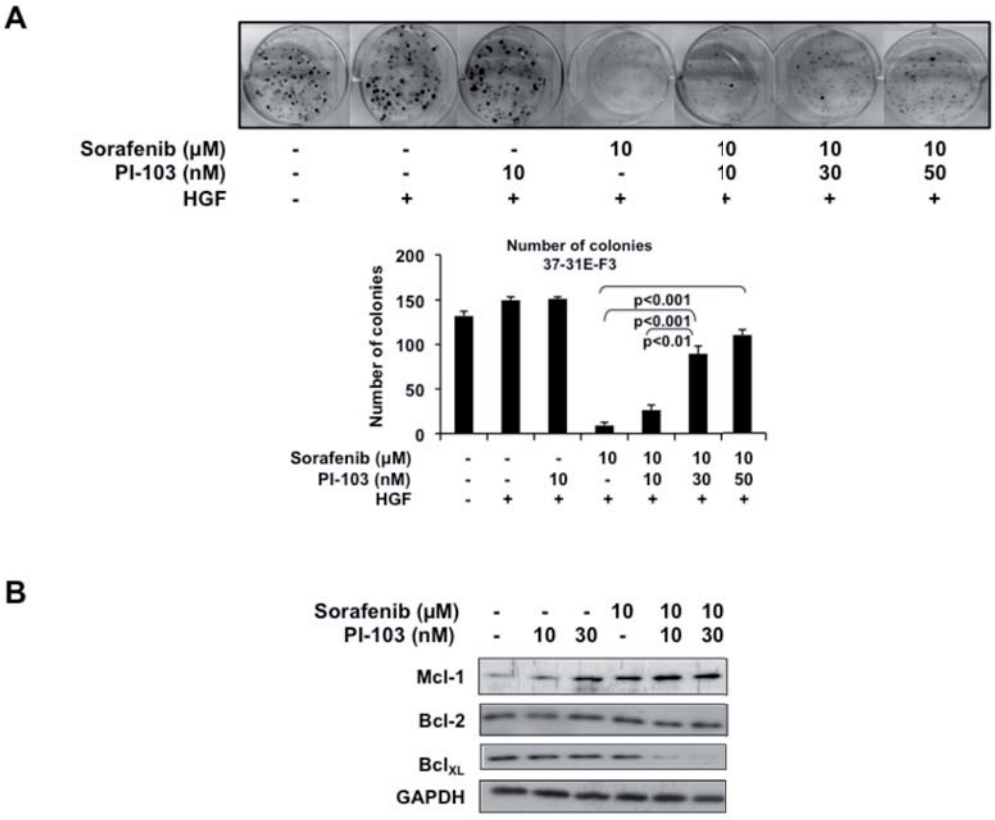

Figure 22. PI-103 increases survival of sorafenib-treated melanoma cell lines.

A. *Clonogenic assay in 37-31E-F3 treated with the indicated drug concentrations in complete media. Graph shows the quantification of the number of colonies in each condition.* ***B.*** *37-31E-F3 cells were treated as indicated for 48 h in complete media. Then, protein extracts were analyzed by Western Blot for the antiapoptotic proteins indicated.*

4. PI-103-mediated systemic effects

The efficacy of PI-103 in the two different mouse models suggested that the genetic background of the host could be important in order to obtain a successful therapy. We have shown data using two different mouse models (FVB/N and Balb c/nude mice) that differ not only in their genetic background but also in their immunological status. Balb c/nude mice are athymic and therefore unable to produce T cells. PI-103 is a dual Pi3k/mTOR inhibitor. It is widely known that mTOR inhibitors such as rapamycin are broadly used as immunosuppressant agents [73]. Thus, we investigated whether PI-103 was inducing any systemic effect interfering with the immune system.

4.1 PI-103 induces thymus atrophy in immunocompetent mice

It has been described that rapamycin promotes thymus atrophy depleting the thymocyte and splenocyte population after eight days treatment [105]. We analyzed the thymocyte and splenocyte population in mice treated for a week with PI-103, the PI3K inhibitor LY 294002 and the mTOR inhibitor rapamycin.

The results showed that PI-103 induced thymus atrophy. PI-103 treated mice showed lower numbers of thymocytes and an increased number of dead cells (20%) respect to the control mice (Figure 23A). This increase in cell death was more evident according to the 7AAD staining data, where 64% of cells were dead. As expected, the mTOR inhibitor rapamycin almost totally reduced the thymocyte population, while the PI3K inhibitor LY 294002 only induced 5% in thymocyte cell death population.

Splenocytes were partially affected by PI-103 and rapamycin treatments (15% and 20% of cell death respectively). However, no significant differences in splenocyte population were noticed in LY 294002-treated animals (Figure 23B).

To further confirm these results, we also analyzed the thymocytes and splenocytes populations from mice used in the *in vivo* tumor growth experiments treated for three weeks with PI-103. The results showed that PI-103 induced thymus atrophy reducing the thymocyte population and inducing cell death by 67,2% according to the 7AAD staining data. The splenocyte population remained unchanged (Figure 23C).

Figure 23. PI-103 induces thymus atrophy.

FVB/N mice were treated daily for a week with DMSO (C), PI-103 (P, 10 mg/Kg), LY 294002 (LY, 25 mg/Kg) or rapamycin (R, 1 mg/Kg). Then, thymocytes and splenocytes were isolated and its viability was assessed by counting in Guava-Viacount or by FACS with 7AAD staining. ***A.*** *Graphs on the left show the number of thymocytes in the thymus of each mice group. Graphs on the middle represent the percentage of non-viable thymocyte cells in each group. Graph on the left shows the percentage of dead cells according to 7AAD staining.* ***B.*** *Same as in A with the splenocytes population.* ***C.*** *Same procedure with mice that have been treated with the drugs for 3 weeks.*

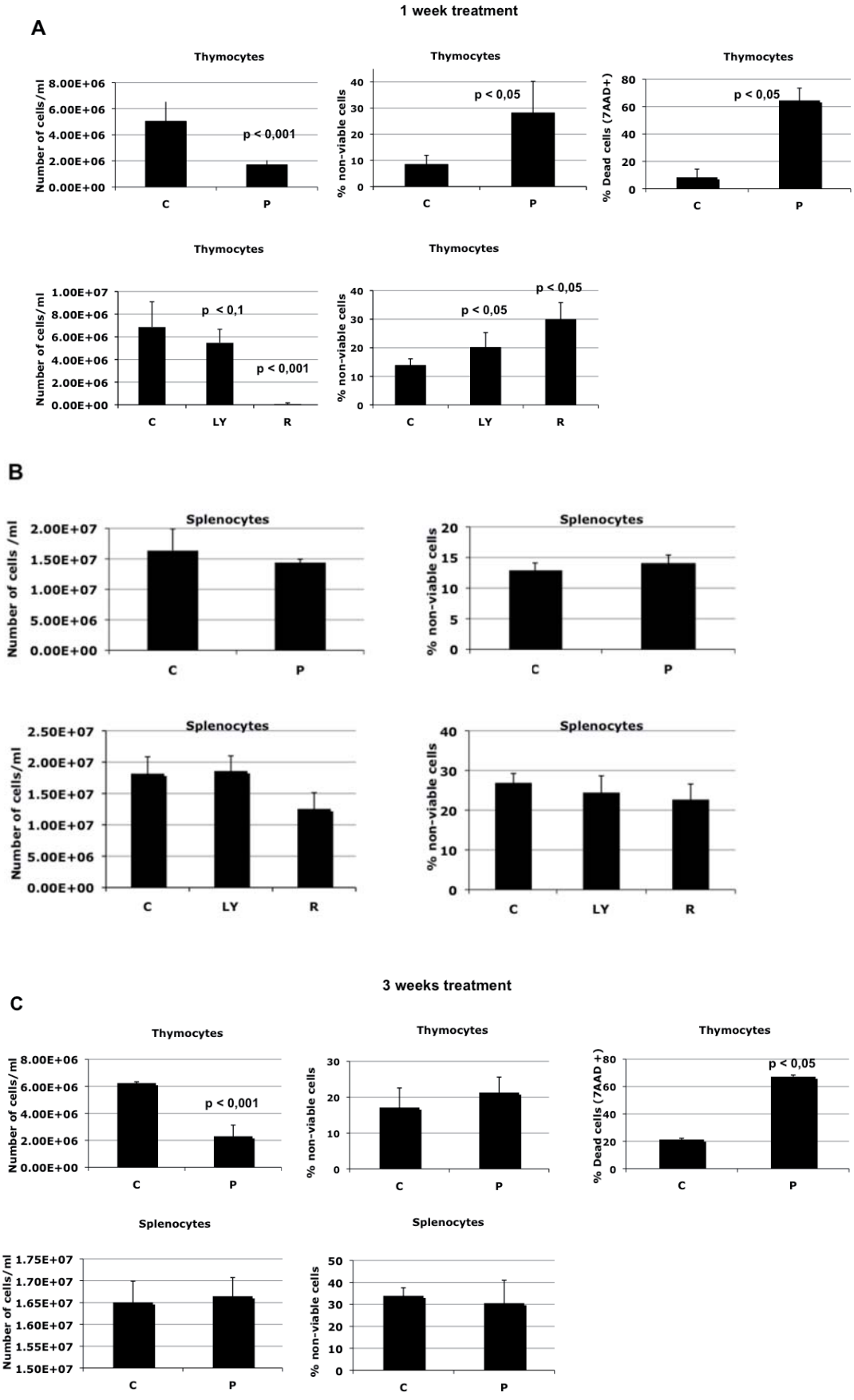
1 week treatment
A
Thymocytes
Number of cells/ml
8.00E+06
6.00E+06
4.00E+06
2.00E+06
0.00E+00
p < 0,001
C
P
Thymocytes
% non-viable cells
40
30
20
10
0
p < 0,05
C
P
Thymocytes
% Dead cells (7AAD+)
80
60
40
20
0
p < 0,05
C
P
Thymocytes
Number of cells/ml
1.00E+07
8.00E+06
6.00E+06
4.00E+06
2.00E+06
0.00E+00
p < 0,1
p < 0,001
C
LY
R
Thymocytes
% non-viable cells
40
30
20
10
0
p < 0,05
p < 0,05
C
LY
R
B
Splenocytes
Number of cells /ml
2.00E+07
1.50E+07
1.00E+07
5.00E+06
0.00E+00
C
P
Splenocytes
% non-viable cells
20
15
10
5
0
C
P
Splenocytes
Number of cells/ml
2.50E+07
2.00E+07
1.50E+07
1.00E+07
5.00E+06
0.00E+00
C
LY
R
Splenocytes
% non-viable cells
40
30
20
10
0
C
LY
R
3 weeks treatment
C
Thymocytes
Number of cells/ml
8.00E+06
6.00E+06
4.00E+06
2.00E+06
0.00E+00
p < 0,001
C
P
Thymocytes
% non-viable cells
30
20
10
0
C
P
Thymocytes
% Dead cells (7AAD +)
80
60
40
20
0
p < 0,05
C
P
Splenocytes
Number of cells/ml
1.75E+07
1.70E+07
1.65E+07
1.60E+07
1.55E+07
1.50E+07
C
P
Splenocytes
% non-viable cells
50
40
30
20
10
0
C
P

Figure 23

4.2 PI-103 increases the immunosuppressors IL-6, IL-10 within the tumors

In addition to the thymus atrophy promoted by PI-103 treatment in FVB/N mice, we investigated whether PI-103 had any effect regulating immunosuppressant cytokines. We analyzed the transcriptional levels of the immunosuppressive cytokines IL-6, IL-10 and VEGF within the tumors of the three different *in vivo* experiments. PI-103 treated tumors from two different experiments in FVB/N immunocompetent mice (10 mg/kg and 70 mg/kg) showed higher levels of IL-6 and IL-10 mRNAs compared to the tumors from control mice (Figures 24A and 24B). Interestingly, sorafenib treated tumors did not show any significant differences in the transcriptional regulation of the IL-6, IL-10 and VEGF compared with the control samples. Notably, PI-103 treated samples from tumors raised in immunocompromised balb c/nude mice showed a transcriptional downregulation of these cytokines (Figure 24C).

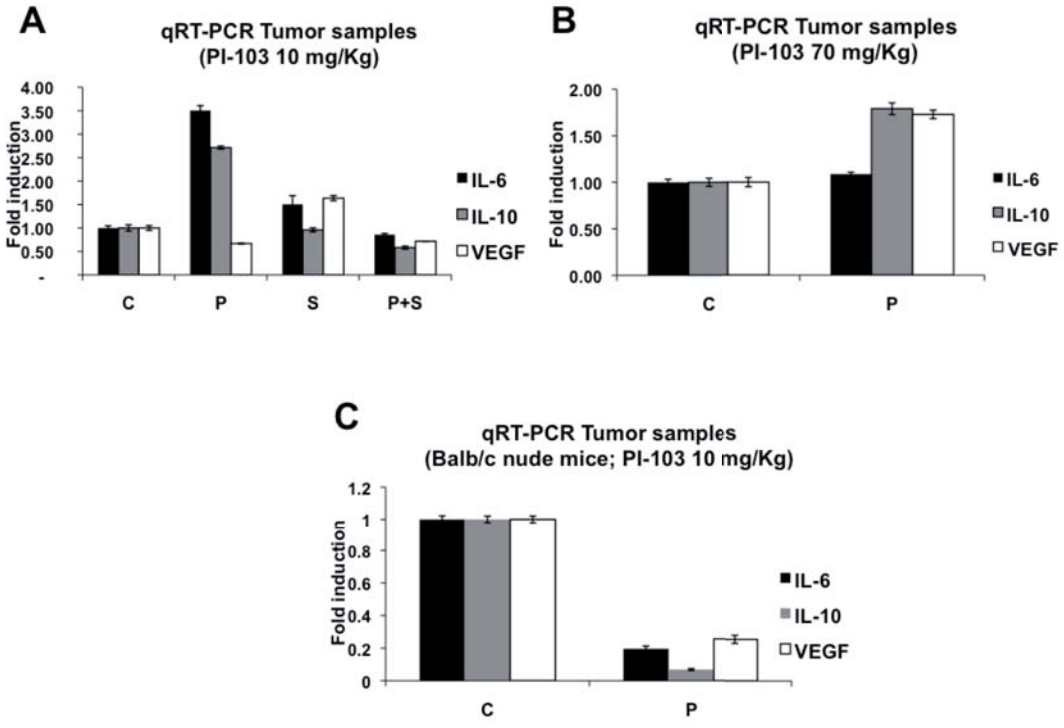

Figure 24. PI-103 induces an increase in the immunosuppressors IL-6 and IL-10 levels within the tumors.

*mRNA from tumors from experiments described in figures 16 (**A**), 17 (**B**) and 19 (**C**) were isolated and IL-6, IL-10 and VEGF levels were assessed by real-time quantitative PCR. Results were normalized with GAPDH.*

Next, we went further and investigated whether this increase in the intratumoral immunosuppressive cytokines was due to a direct effect of PI-103 on the tumoral cells.

Interestingly, the *in vitro* treatment of 37-31E-F3 melanoma cell line with PI-103 induced a slight transcriptional upregulation of IL-6 and VEGF (Figure 25A). Then, we were interested in finding the molecular event in the tumoral cell that could be responsible for the transcriptional upregulation of the immunosuppressive cytokines upon PI-103 treatment.

It has been described that the crosstalk between tumoral cells and the immune system is driven by STAT pathway, mainly by STAT3. STAT3 is a transcription factor that regulates the transcription of plenty of molecules, among them, the immunosuppressive cytokines IL-6, IL-10 and VEGF (for review [106]). Thus, we investigated the levels of p-Stat3 in our system in response to PI-103.

Interestingly, the *in vitro* treatment of 37-31E-F3 cells with PI-103 induced an increase in the levels of p-Stat3. On the other hand, the treatment of these cells with sorafenib did not promote the same response (Figure 25B). More importantly, these *in vitro* results correlated with our *in vivo* data: PI-103 treated tumor samples showed elevated levels of p-Stat3 that were not detected in the sorafenib neither in the double treated tumors (Figure 25C).

All together, these results indicated that PI-103 treatment, but not sorafenib, was able to modulate the levels of p-Stat3 *in vivo* and *in vitro*. This increased levels of p-Stat3 correlated with the upregulation of the immunosuppressive cytokines observed both *in vivo* and *in vitro.*

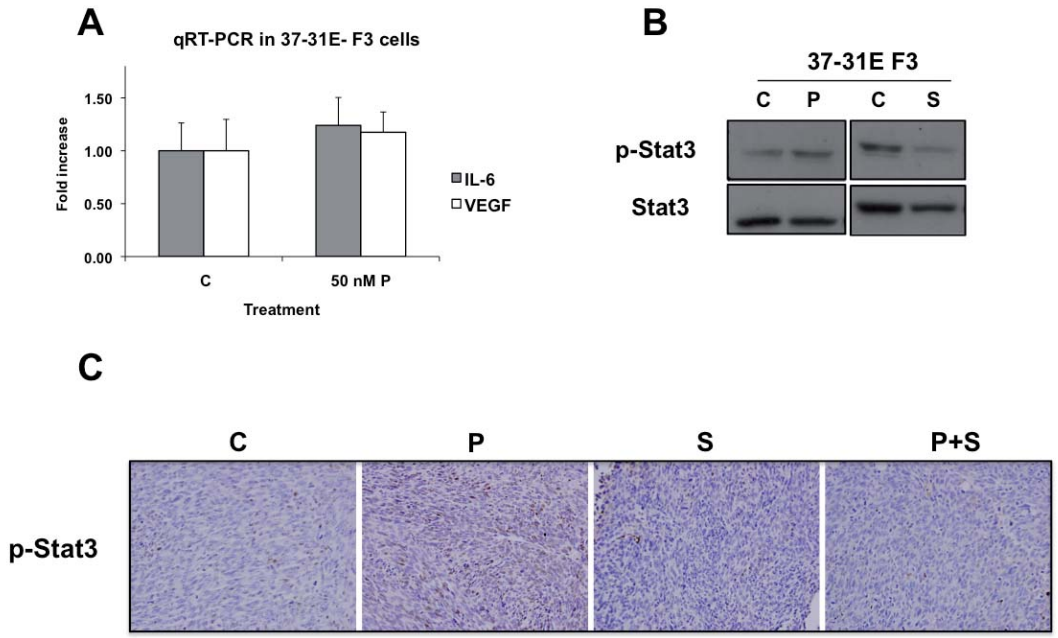

Figure 25. PI-103 modulates the levels of p-Stat3 in melanoma cell lines and tumor samples.

37-31E-F3 cells were treated with PI-103 (P, 50 nM PI-103) or sorafenib (S, 15 μM sorafenib) in complete media for 48 hours. ***A****. RNA was isolated and IL-6 and VEGF levels were analyzed by qRT-PCR.* ***B.*** *Protein extracts were probed with the indicated antibodies C. Fresh tumor samples from immunocompetent mice treated with sorafenib (S, 50 mg/kg), PI-103 (P, 10 mg/ Kg) or PI-103 plus sorafenib (P+S, 10 mg/Kg, 50 mg/Kg) were stained with p-Stat3.*

4.3 PI-103 regulate p-STAT3 levels *in vitro* in mouse and human melanoma cell lines

Since the dual PI3K/mTOR inhibitor PI-103 induced the phosphorylation of Stat3, we next wanted to investigate whether this regulation was broader in scope affecting to other PI3K/mTOR inhibitors such as BEZ-235.

To that purpose, we treated at different time points 37-31E-F0 and 37-31E-F3 cell lines with 50 nM PI-103, 50 nM BEZ-235 and 15 μM sorafenib and checked by western blot the levels of p-Stat3.

As previously showed for 37-31E-F3, the treatment with PI-103 was able to increase the levels of phosphorilated Stat3 at 24 hours in both cell lines 37-31E-F0 and 37-31E-F3 (Figure 26A). Interestingly, the treatment with BEZ-235 was also able to modulate the levels of p-Stat3 in both cell lines at the same time points (Figure 26B). Importantly, the treatment with the multikinase inhibitor sorafenib did not promote any increase in p-Stat3 in 37-31E-F0 cells. Although a slight increase was detected at 48 hours in 37-31E-F3, it was not significant compared with the basal levels (Figure 26C).

In order to check whether the modulation of STAT3 in response to the PI3K/mTOR pathway inhibition was also extensible to human cell lines, we repeated these experiments treating two primary human melanoma cell lines obtained from melanoma patients (MGPM-3 and MLNM-10) with the inhibitors.

The treatment with PI-103 clearly increased p-STAT3 at 24 hours in both cell lines (Figure 27A). However, the two cell lines used showed different sensitivities to BEZ-235. While MGPM-3 cells were resistant (data not shown) to BEZ-235 and showed elevated levels of p-STAT3 at 24 hours, MLNM-10 cells were dead at 48 hours and no increase in STAT3 phosphorylation was detected (Figure 27B). In addition to this, long-term sorafenib treatment induced cell death in both cell lines (data not shown) that correlated with a decrease in STAT3 signaling (Figure 27C).

These data showed that the inhibition of PI3K/mTOR pathway with PI-103 or BEZ-235 modulated *in vitro* the levels of p-STAT3 in mouse and human melanoma cell lines in a cell line-dependent manner. On the other hand, the inhibition of the RAF pathway with sorafenib did not promote the same response.

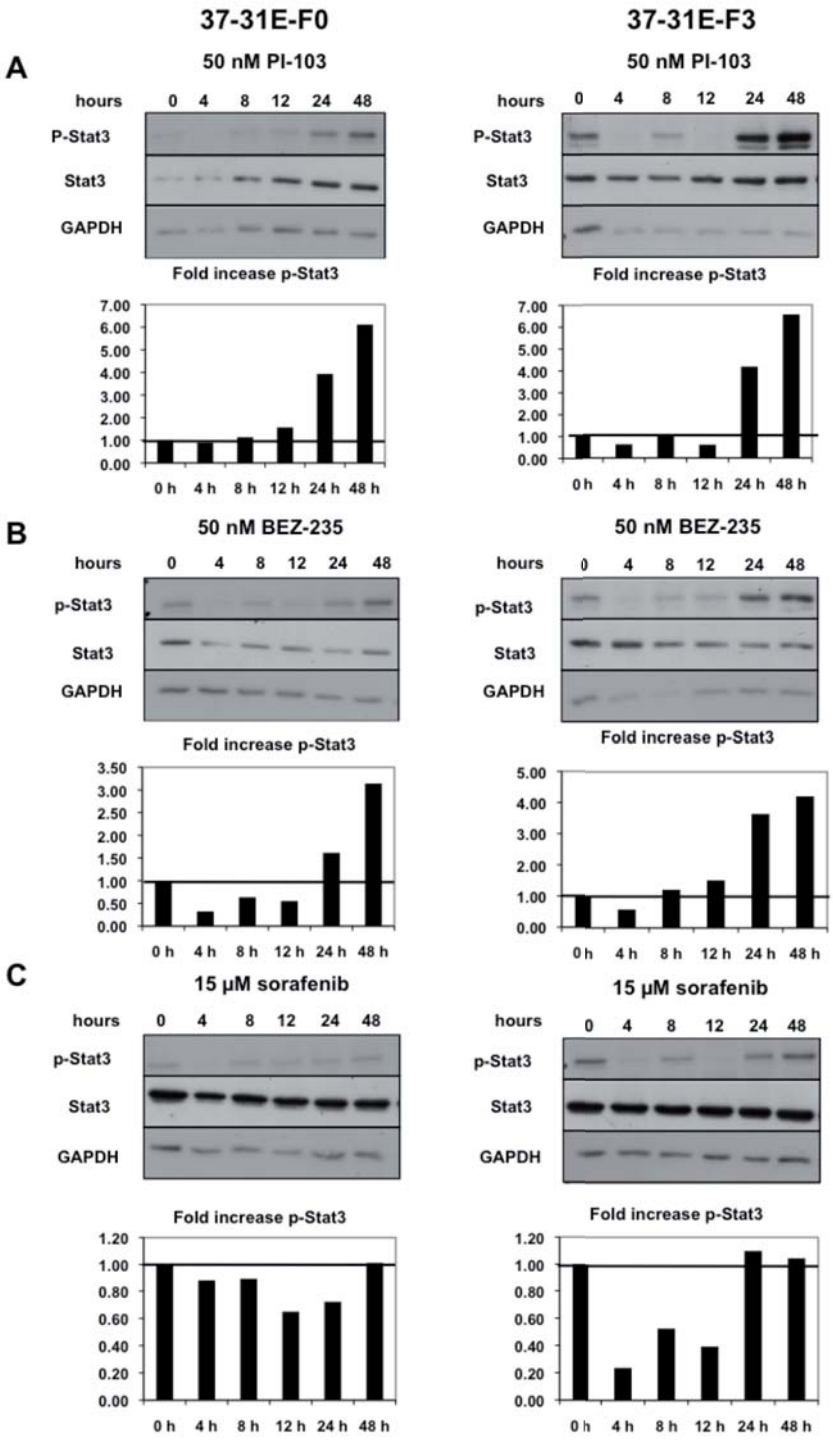

Figure 26. Two dual Pi3k/mTOR inhibitors, PI-103 and BEZ-235, induced an increase in vitro in p-Stat3 levels in mouse melanoma cell lines.

*37-31E-F0 (left) and 37-31E-F3 (right) cells were treated for the indicated time points with 50 nM PI-103 (**A**), 50 nM BEZ-235 (**B**) and 15 µM sorafenib (**C**) in complete media. Protein extracts were analyzed by western blot. Graphs show the fold increases in p-Stat3 levels. All the quantifications were normalized with GAPDH.*

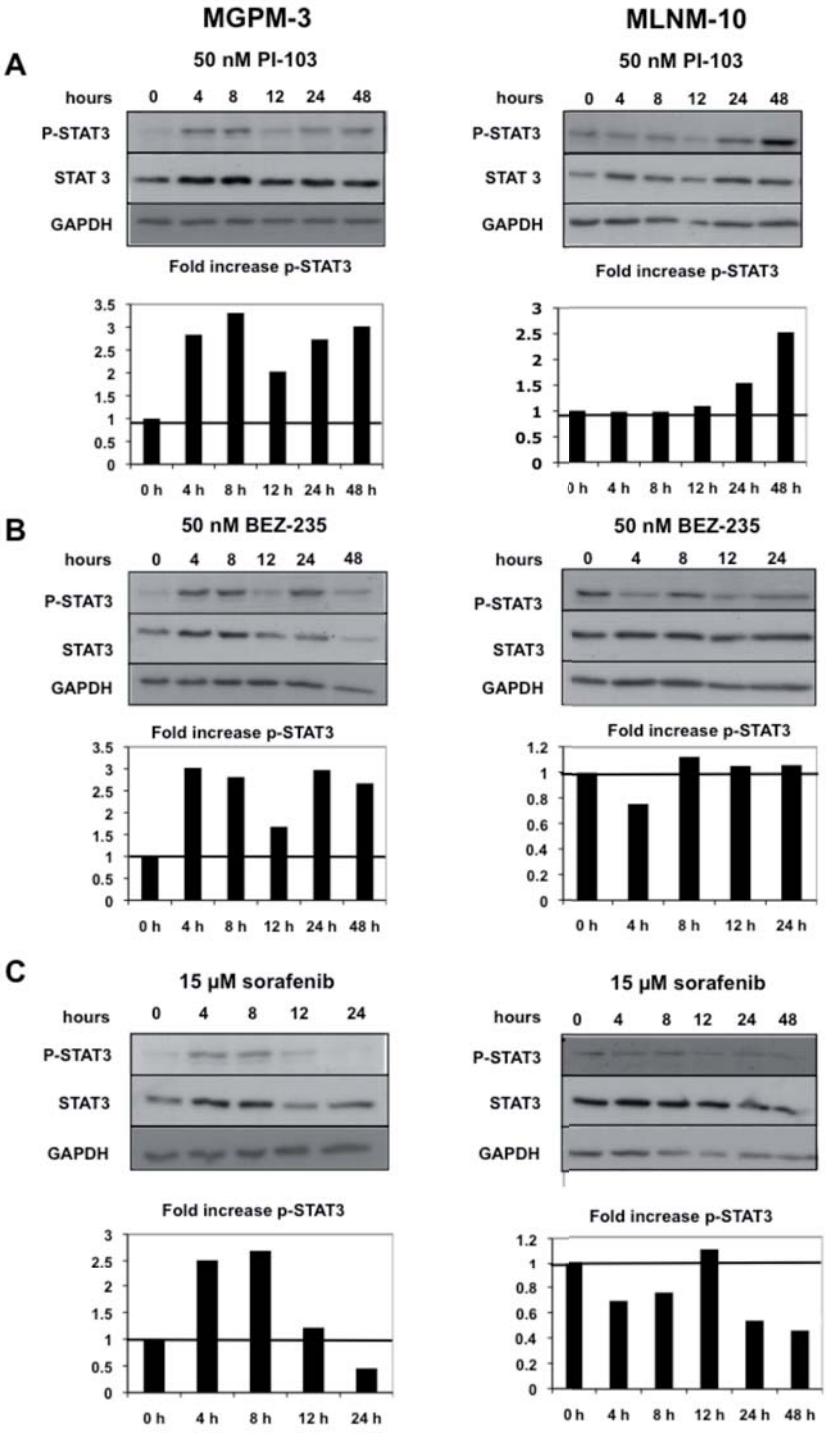

Figure 27. The PI3K/mTOR inhibitor, PI-103 induced an increase in vitro in p-STAT3 levels in human melanoma cell lines.

*MGPM-3 (left) and MLNM-10 (right) cells were treated for the indicated time points with 50 nM PI-103 (**A**), 50 nM BEZ-235 (**B**) and 15 µM sorafenib (**C**) in complete media. Protein extracts were analyzed by western blot. Graphs show the fold increases in p-STAT3 levels. All the quantifications were normalized with GAPDH.*

V. DISCUSSION

Melanoma is the most aggressive skin cancer that could be easily treated by surgery when detected at early stages. However, when it reaches its more advanced stages and metastatizes, it becomes resistant to current therapies and lethal.

During the last decades, many efforts have been made in order to better understand the molecular mechanisms involved in melanoma development and progression. It has been well established that RAS/ERK1/2 and PI3K pathway are very important in melanoma progression and maintenance. Therefore, targeting these pathways with specific compounds seems to be a promising approach to treat melanoma.

Here, we have studied the *in vivo* and i*n vitro* effectiveness of two small kinase inhibitors targeting PI3K and RAS pathways in melanoma: PI-103 (a dual PI3K/mTOR inhibitor) and sorafenib (a multikinase inhibitor that targets RAF kinases). We performed these studies using two different cell lines (37-31E-F0 and 37-31E-F3) derived from spontaneous tumors arose in the UV induced HGF transgenic melanoma mouse model.

According to our results, PI-103 inhibits *in vitro* Pi3k pathway in a dose-dependent manner. In agreement with the different sensitivity to the drug showed by the two melanoma cell lines, it has been reported that PI-103 inhibits PI3K pathway in different cancer cell lines in a cell-genotype dependent manner [95]. As previously described in other systems [55,57], in our model sorafenib also inhibited Ras/Erk1/2 pathway in a dose-dependent manner.

Although both inhibitors were effective blocking *in vitro* melanoma cell proliferation, it seems that the inhibition of Raf pathway is much more efficient inhibiting melanoma cell proliferation. PI-103 inhibits melanoma cell proliferation at very high concentrations (from 100 to 500 nM) probably targeting other kinases in addition to Pi3k and mTOR. On the other hand, 10 μM sorafenib (targeting Raf kinases more specifically) is enough to abolish melanoma cell proliferation. These data agrees with previous publications [22,36] that indicate that melanoma cell proliferation is mainly dependent on the Ras/Erk1/2 pathway.

Interestingly, the combined treatment with PI-103 and sorafenib inhibited synergistically *in vitro* Pi3k and Raf pathways in 37-31E-F3 but not in 37-31E-F0 cells. Moreover, treatment of 37-31E-F0 with 20 nM PI-103 and 10 μM sorafenib led to an increase in p-Erk1/2 levels. This result is in agreement with recent publications that identificated a feedback loop where the inhibition of mTORC1 resulted in the activation of ERK [107].

The combined targeting of PI3K/mTOR and RAS/ERK1/2 pathways has been shown to be effective blocking human melanoma cell lines *in vitro* proliferation [108]. In this matter, PI-103 and sorafenib cooperated inhibiting 37-31E-F3 *in vitro* melanoma cell proliferation.

Most part of preclinical studies are obligated to use immunocompromised mice models without taking into account the role of the immune system, tumor-cell selection and/or possible systemic effects of the drug. In this study, we tested the effectiveness of PI-103 and sorafenib in an immunocompetent mouse model taking into consideration these issues: (i) tumor cell selection in a more physiological environment and (ii) possible undesired systemic effects promoted by the treatment.

Despite the encouraging *in vitro* results obtained with 37-31E-F3 melanoma cell line, the *in vivo* tumor growth assays in immunocompetent mice gave an unexpected result. Surprisingly, daily treatment with PI-103 induced tumor growth in a dose and cell type independent manner. Sorafenib, as previously described in other models [55,93], reduced significantly the *in vivo* tumor growth and unfortunately, the combined treatment of PI-103 and sorafenib did not add any further benefit compared to the sorafenib treated tumors.

Different groups have tested the i*n vivo* antitumoral effectiveness of PI-103 using different tumor models in immunosuppressed mice. We have also observed the PI-103's effectiveness in balb c/nude mice. However, some differences in the drug effectiveness have been observed among the different cancer models depending on the treatment schedule or the genetic background. For instance, the best responses observed in an ovarian carcinoma model were those obtained when treating the animals twice per day with 100 mg/kg PI-103. Similar results were observed in a colorectal cancer xenograph model, where a unique dose of 30 mg/Kg of PI-103 was not effective reducing tumor growth. However, the same model treated twice daily with 30 mg/Kg of PI-103 reduced tumor growth [95]. Additionally, it has been also described that PI-103 was effective in a glioblastoma model only when combined with radiation whereas the daily treatment with 10 mg/Kg PI-103 alone did not affect the tumor growth compared to the control mice [109]. Other groups [94,100] used cell lines which were particularly dependent on the PI3K pathway since they carried activating mutations on the pathway. Thus, tumors raised in those models were particularly sensitive to PI3K/mTOR inhibition.

Recently, it has been described that several dual PI3K/mTOR inhibitors were advantageous to attenuate melanoma growth in a B16BL6 immunocompetent melanoma model [110]. Despite the tumor growth reduction that they observed in this

model upon treatment with PI-103, they also showed that PI-103 was the less effective PI3K/mTOR inhibitor tested: PI-103 was the only dual PI3K/mTOR inhibitor that did not induce necrosis, it did not reduce lymph node metastasis and it was not able to reduce angiogenesis.

The low *in vivo* effectiveness of PI-103 could be attributed to the low solubility of PI-103 and its poor pharmacokinetics. PI-103 has been described to have a high metabolic rate when incubated with human and mouse microsomes. In addition, PI-103 has been observed to have a high clearance rate: after the ip injection of 2,5 mg/kg PI-103, the concentrations in plasma, liver, spleen or kidney fall down only 1 hour after. However, following ip administration of 50 mg/Kg PI-103, the PI-103 levels in plasma are sustained for longer than 12 hours [95]. Nevertheless, in our system the pharmacokinetics showed by PI-103 was sufficient to block the phosphorylation of the downstream Pi3k/mTOR effectors Akt, S6 and 4EBP1 within tumor samples.

Our results do not show any cooperation between PI-103 and sorafenib reducing tumor growth in comparison to the sorafenib treated tumors. Recent studies suggest that the effectiveness of the combined therapy targeting RAS and PI3K pathways simultaneously might be restricted to melanomas harboring activating mutations in these pathways. For instance, sorafenib in combination with the mTOR inhibitor rapamycin suppressed invasive melanoma growth in organotypic culture of human $BRAF^{V600E}$ melanoma cells [91]. In addition to this, different spontaneous melanoma mouse models harboring hiperactivation of the Pi3k and Raf pathways have been used to assess successfully the effectiveness of drugs targeting these pathways. These include the DMBA-induced TPRas mouse melanoma model [82] and the Tyr::CreER; $BRaf^{CA}$ /+$xPTen^{lox/lox}$ melanoma mouse model [81].

Bedgoni et al. tested the PI3K inhibitor LY 294002 and the MEK inhibitor U0212 in spontaneous melanomas raised in the TPRas mouse model after topical DMBA administration. These spontaneous melanomas are totally dependent on the Ras pathway, which signals to both, the Raf and Pi3k pathways. Thus, these DMBA-induced melanomas are supposed to be much more sensitive to the double inhibition than our tumors, that according to the low basal levels of p-Erk1/2 and p-Akt, do not harbor mutations in these pathways. Moreover, the response to the drug combination in the TPRas mouse model was not totally effective, since 21,6% of treated tumors progressed.

The study from Dankort et al. showed that transgenic mice expressing $BRaf^{V600E}$ failed to develop melanoma. In the same way, the Pten silencing was not enough to form melanoma tumors. Interestingly, mice that combined the expression of $BRaf^{V600E}$

and the Pten silencing developed melanomas, confirming the importance of Pi3k and Raf pathways in melanoma development. Additionally, these data indicated that these melanomas were highly dependent on Pi3k and Raf pathways. Moreover, it has been established that melanomas bearing the $BRAF^{V600E}$ mutation are particularly sensitive to MEK inhibition [65]. Thus, it is not surprising that the combined treatment with the MEK inhibitor PD-325901 and the mTOR inhibitor rapamycin was effective reducing tumor growth in this melanoma mouse model. Nevertheless, the enhanced cooperation between PD-325901 and rapamycin only accounted for a 20% reduction compared to the PD-325901 treated.

In our study the different tumor latency observed between immunocompetent and immunocompromised mice, revealed that cells were differentially selected through the two models. Interestingly, the different basal levels of the BH3-family of antiapoptotic proteins between the tumors from balb c/nude and FVB mice support the different selection through the host. Moreover, these tumors had opposite responses to PI-103 in the regulation of the antiapoptotic proteins that correlated with the observed tumor development (Figure 28). Indeed, melanomas are described to have a low basal level of apoptosis and they are *in vitro* resistant to apoptosis inducing drugs [48].

Importantly, Mcl-1 and Bcl-2 are two members of the BH3 family of antiapoptotic proteins that have been related to be involved in rapamycin-resistance mechanisms [103,104]. Furthermore, it has been described that these proteins could be induced by rapamycin treatment [111,112]. Interestingly, the *in vitro* treatment with PI-103 of cell lines derived from control tumors arose in the FVB mice induced the upregulation of these antiapoptotic proteins. Thus, it can be assumed that PI-103, as rapamycin, directly regulates the levels of the antiapoptotic proteins *in vivo* and *in vitro* and supports the diminished apoptotic rate observed in the tumors. On the other hand, in agreement with previous studies [57], sorafenib reduced the expression of these proteins in the tumor-derived cell lines that correlates with the observed *in vivo* apoptosis.

In addition to this, in our system the double treated tumors were slightly bigger than the sorafenib-treated ones. Interestingly, in these tumors PI-103 blocked the sorafenib-induced apoptosis inducing the *in vitro* accumulation of Mcl-1 and Bcl-2 proteins and increasing survival upon PI-103 treatment in sorafenib-treated melanoma cells. These data reinforce the regulation of apoptosis observed by PI-103 treatment and supports the tumoral size observed after treatment.

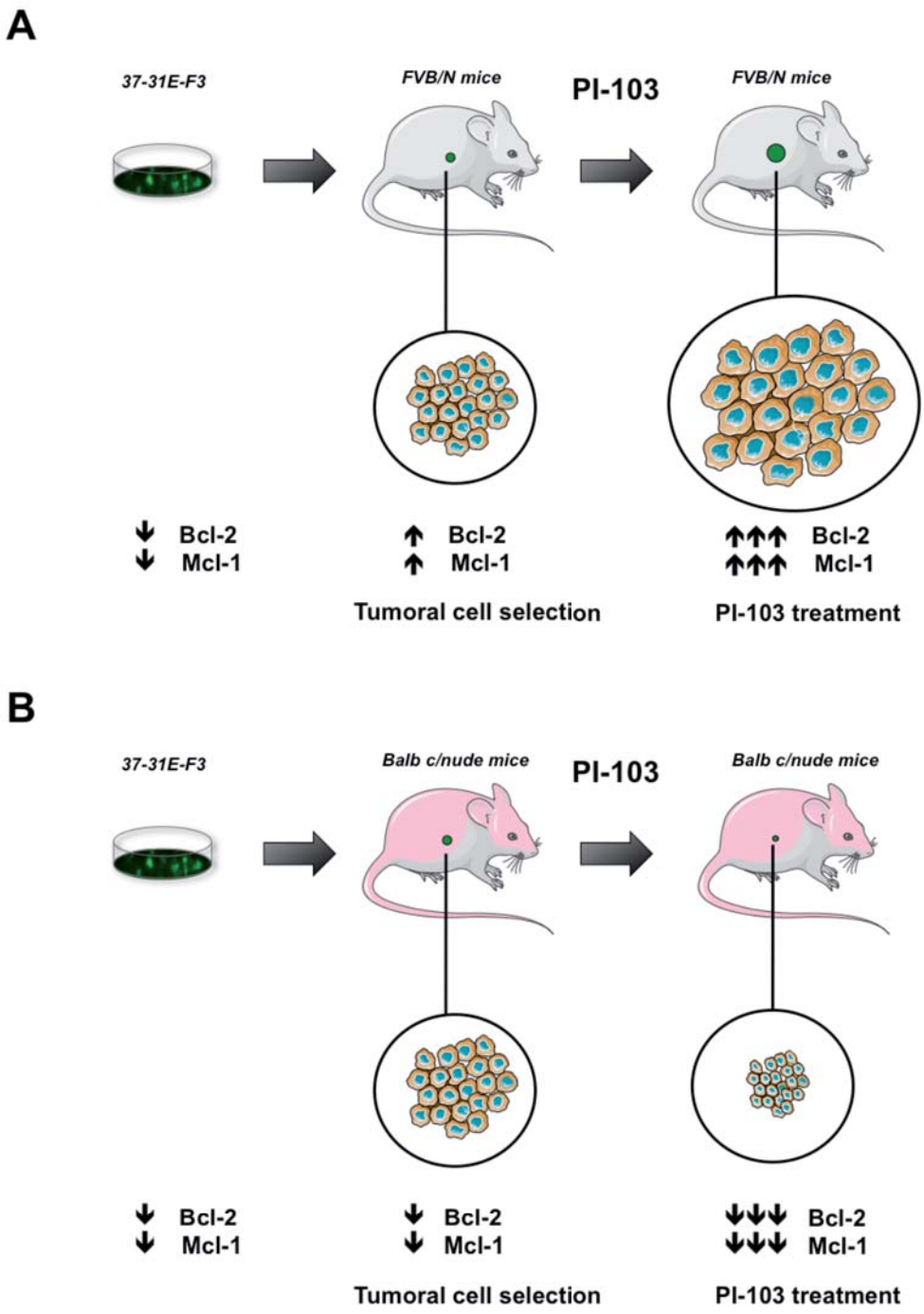

Figure 28. Host-mediated selection and PI-103 treatment in FVB/N and balb c/nude orthotopic melanoma mouse models.

A. *Tumoral cells selected by the immune system in FVB/N mice express higher levels of the antiapoptoic proteins Bcl-2 and Mcl-1 than the parental cells. In addition, PI-103 treatment increases the levels of these proteins within the tumors resulting in an enhanced tumor growth effect.* ***B.*** *PI-103 induces tumor regression in balb c/nude by downregulating the levels of the antiapoptotic proteins Bcl-2 and Mcl-1.*

Besides the tumoral cell selection through the host, we have identified a systemic effect produced by PI-103 in the immunocompetent mice. It is well established that the mTOR inhibitor rapamycin is an immunosuppressant agent [72,73,105]. In addition, it has been reported that PI-103 blocks the proliferation of T cells [99], enhances the IgE production and reduces type 2 cytokine release *in vivo* [113,]. Thus, we considered the possibility that maybe PI-103, as a dual PI3K/mTOR inhibitor, was producing a systemic effect in FVB/N mice. Notably, our data suggest that PI-103 induces immunosuppression in FVB/N mice by inducing thymus atrophy. Unfortunately, the study from Marone et al. using PI-103 in a B16BL6 immunocompetent mouse model do not show any data regarding thymocytes and thymus atrophy. However, they show no variations on cell numbers in spleen and bone marrow from PI-103 treated mice [110]. In agreement with this, we neither observed any variation in the splecnocyte population from PI-103 treated mice.

Importantly, the immunosuppressive effect of PI-103 has also been reported recently by others [114]. In this study, the authors show that in C57BL/6J mice, therapeutical concentrations of PI-103 decreases the total number of B and T cells in the spleen and affects the spleen structure by displacing the marginal zone.

In addition to the thymus atrophy, PI-103 treatment induced the upregulation of the immunosuppressant cytokines IL-6, IL-10 and VEGF and modulated the levels of p-Stat3 *in vivo* within tumor samples from immunocompetent mice and *in vitro* in tumoral cells.

STAT pathway has been described to be hyperactivated in a big variety of tumors [115]. Interestingly, it has been shown that the activation of the pathway is directly related to melanoma progression. Thus, human metastatic samples have higher levels of p-STAT3 than nevi [116]. STAT3 is a transcription factor that can be activated by different pathways, including the cytokine signaling through JAK or different RTK such as c-MET [106]. STAT3 plays a critical role in tumorigenesis, since it regulates cell proliferation, angiogenesis or apoptosis among other important processes for cell homeostasis [106]. Interestingly, one of the roles of STAT3 involves the regulation of the immune evasion [106]. Immune evasion is one of the malignant phenotypes that allow malignant cells to survive in the host. STAT3 signaling is implicated in the inhibition of molecules involved in the immune activation against tumor cells and the expression of some immunosuppressive factors, including IL-6, IL-10 and VEGF. These immunosuppressive cytokines activate STAT3 in different immune cells (thymocytes, natural killer (NK), macrophages…) producing an immunosuppressive response that favors the tumor growth (for review [106]). According to our data, we speculate that the

modulation of p-Stat3 levels in response to PI-103 could be mediating the upregulation of IL-6, IL-10 and VEGF observed in our tumors. Furthermore, this cytokines could promote autocrine loops sustaining the levels of p-Stat3. This immunosuppressive response would contribute to the enhanced tumor growth observed in the PI-103 treated mice (Figure 29).

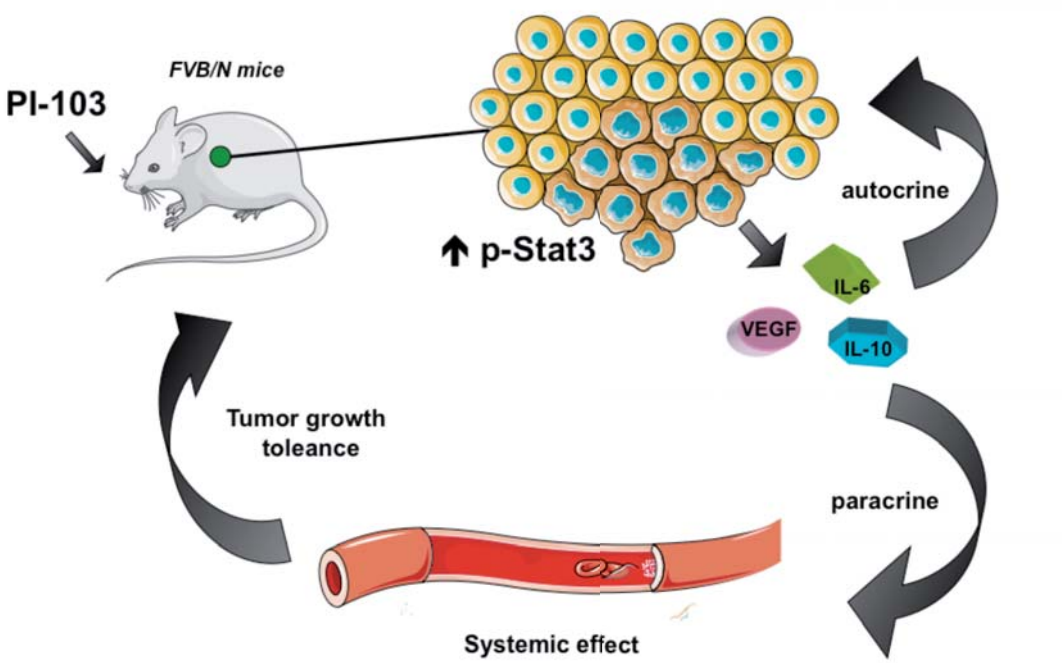

Figure 29. Proposed mechanism for the systemic effect induced by PI-103.

The treatment with PI-103 induces p-Stat3 in the tumoral cells, that upregulates the levels of VEGF, IL-6 and IL-10 within the tumors. Those cytokines would be partially responsible for the immunosuppressive effect that promotes tumor-growth tolerance.

In addition to the immunosuppressive effect, it was particularly interesting that STAT3 participates in the regulation of the mechanisms related to apoptosis evasion in human melanoma. STAT3 negatively regulates the expression of TRAIL, protecting cells from TRAIL induced apoptosis [117] and it is involved in the regulation of the antiapoptotic proteins Mcl-1 and Bcl-X_L [118]. Interestingly, our data indicated that PI-103, but not sorafenib, modulates the levels of Mcl-1 and Bcl-2 *in vivo* and *in vitro*, which correlates with the high levels of p-Stat3.

Additionally, our preliminary data suggest that the modulation of STAT3 phosphorylation not only is extensible to other dual PI3K/mTOR inhibitors (BEZ-235) but also to human melanoma cell lines. This data suggest that STAT pathway could be involved in resistance mechanisms to dual PI3K/mTOR inhibitors in melanoma.

The crosstalk between the inhibition of PI3K and the modulation of p-STAT3 levels is still not well characterized. However, there are data supporting our findings. STAT3 together with c-jun have been described to cooperate inhibiting FAS-induced apoptosis in a PI3K dependent manner. Thus, the pharmacological blockage of PI3K leads to an increase of the transcriptional activities of STAT3 and c-Jun resulting in an antiapoptotic effect [119]. Altogether, we believe that the upregulation of p-Stat3 upon PI-103 treatment might be acting *in vivo* at two different levels: controlling immunosuppression in the host and inducing antiapoptotic proteins in tumor cells.

To conclude, in this study we have observed that PI-103 and sorafenib inhibit effectively Pi3k and Ras/Erk1/2 pathways *in vitro* in mouse melanoma cells. In addition, we have observed that both drugs cooperated blocking *in vitro* Pi3k and Ras/Erk1/2 pathways and cell proliferation in a cell type-dependent manner. The *in vivo* experiments in immunocompetent mice showed that while sorafenib was effective reducing tumor growth, PI-103 induced tumor growth in a cell type and dose independent manner and the combination did not cooperate reducing tumor growth. The use of an immunocompetent mouse model allowed us to take into account the tumoral cell selection through the host and systemic effects derived by the treatments. Interestingly, in our system PI-103 treatment upregulated the expression of BH3-family of antiapoptotic proteins and induced immunosuppression probably through the modulation of p-Stat3 levels. These effects contribute to the enhanced growth effect observed in the PI-103 treated mice. All together, our results claim the importance of using an appropriate mouse model in preclinical studies in order to discard undesired effects induced by drugs.

Future directions

Personal therapies according to the genetic background of the tumor might be a step-forward in cancer treatment. Our results show that the genetic background of the host is important in order to get an effective therapeutic response without a systemic effect. Moreover, melanomas are very resistant to chemotherapeutical induced-apoptosis. They use different molecular mechanisms to evade apoptosis (for review [120]). Thus, further studies should be addressed in order to understand better these drug-resistance mechanisms and find out the way to overcome it.

In this study we have detected an enhanced tumor growth response to PI-103 in an immunocompetent mice model. Finding the molecular pathways involved in this unexpected effect can help to get new insights about resistance mechanisms to PI3K/mTOR inhibitors. In fact, we propose that Stat3 signaling could be participating in the enhanced tumor growth and immunosuppressive effect that we have observed after PI-103 treatment in our mouse melanoma model. In addition, the upregulation of Stat3 upon Pi3k/mTOR targeting can be related to other dual PI3K/mTOR inhibitors that are currently in clinical trials, such as BEZ-235. More interestingly, both inhibitors are also able to increase p-STAT3 levels in human melanoma cell lines discarding a specie-dependent effect. All together, these results suggest that STAT pathway might be involved in resistance mechanisms to dual PI3K/mTOR inhibitors in tumors. In agreement, it has been recently described that STAT3 participates in resistance mechanisms to other chemotherapeutical agents in human cancer cell lines [121]. Moreover, it has been shown that targeting STAT3 in melanoma decreases melanoma cell lines proliferation, increases caspase-3 induced apoptosis and reduces tumor growth in mice [122].

In a near future, it would be interesting to assess the p-STAT3 levels in human melanoma patients treated or not with dual PI3K/mTOR inhibitors to see whether there is a correlation or not with tumor regression, treatment resistance and recurrence. Moreover, further studies could be driven in order to find out the molecular mechanism by which the dual PI3K/mTOR inhibitors induce this STAT3 activation. Thus, new suitable targets for melanoma treatment would come out.

VI. CONCLUSIONS

The conclusions of this work are as follow:

1. The dual PI3K/mTOR inhibitor PI-103 and the multikinase inhibitor sorafenib are effective as single agents and in combination blocking Pi3k and Raf signaling pathways and *in vitro* cell proliferation of melanoma cells.

2. PI-103 causes different tumor treatment responses depending on the immunological status of the animal model.

3. Tumoral cells are differentially selected in a host-dependent manner.

4. PI-103 upregulates the expression of the antiapoptotic BH3 family of proteins promoting apoptosis resistance while sorafenib induces the downregulation of antiapoptotic proteins and induces apoptosis.

5. PI-103 induces immunosuppression inducing thymus atrophy and increasing the levels of the immunosupressors IL-6 and IL-10 within the tumors.

6. In PI-103-treated tumor samples, we observed a correlation between elevated p-Stat3 levels and an increased levels of antiapoptotic proteins and immunosupressors.

7. Dual PI3K/mTOR inhibitors induced the phosphorylation of STAT3 suggesting that STAT3 pathway might play a role in resistance mechanism to PI3K/mTOR inhibitors.

8. Our data make an argument to using more physiological mouse models in preclinical studies in order to discard systemic effects.

VII. SUMMARY IN SPANISH

VII. RESUMEN DE LA TESIS DOCTORAL

RESUMEN DE LA TESIS DOCTORAL*

INTRODUCCIÓN

1. Introducción a la biología del melanoma

El melanoma es un tipo de cáncer que afecta a los melanocitos. Los melanocitos son unas células derivadas de la cresta neural que se localizan en la capa basal de la epidermis. Éstos secretan melanina en respuesta a la radiación ultravioleta, protegiendo así a las células circundantes, los queratinocitos, del daño inducido por ultravioleta.

La proliferación incontrolada de melanocitos da lugar a un tipo de cáncer de piel denominado **melanoma maligno**. El melanoma maligno es el cáncer de piel más agresivo que existe ya que representa el 75% de los casos de muerte por cáncer de piel y tiene una tasa de supervivencia de unos cinco años. A pesar de ser el cáncer de piel menos frecuente, su incidencia en las últimas décadas ha aumentado más rápido que la de cualquier otro tipo de cáncer.

1.1 Factores de riesgo

Los factores de riesgo para desarrollar melanoma pueden ser ambientales o genéticos, pero la interacción entre ambos puede ser importante para el desarrollo de la enfermedad.

Entre los factores ambientales destaca la exposición a radiación ultravioleta, la cuál está epidemiológicamente relacionada con el riesgo a desarrollar melanoma. Además, experimentos en modelos animales de melanoma inducidos por ultravioleta sugieren que la radiación UV-B es la responsable del desarrollo del melanoma [2]. Se sabe que la radiación ultravioleta puede favorecer el desarrollo del melanoma porque causa daños genéticos en la piel, altera el sistema inmune cutáneo, y aumenta la producción de factores de crecimiento y de moléculas que dañan el DNA (ROS).

El hecho que un 5% de los casos de melanoma maligno ocurra en familias con uno o dos parientes cercanos afectados, sugirió que podía existir un componente

* *En este apartado se presenta una versión resumida en castellano de la versión original en ingles. Con el fin de no repetir las figuras y tablas, se referencian las figuras y tablas correspondientes en la versión en inglés. Para facilitar la lectura, se presenta un índice de las figuras y tablas en el inicio de la tesis.*

genético en el riesgo a padecer melanoma. Gracias a la disponibilidad de muestras de estas familias propensas a padecer melanoma, se han identificado genes cuya pérdida o mutación pueden indicar una alta susceptibilidad a padecer melanoma [3]. Por ejemplo, un tercio de los pacientes de melanoma presentan mutaciones inactivadoras o depleciones en CDKN2A. CDKN2A está implicado en la regulación del ciclo celular mediante la expresión de dos proteínas supresoras de ciclo celular. También se han detectado mutaciones activadoras en la quinasa reguladora de ciclo celular CDK4 o diferentes variantes genéticas del MC1R, el receptor de melanocortinina-1, que dan lugar a la síntesis de pigmentos no protectivos de la radiación ultravioleta.

2. Progresión del melanoma

El proceso de transformación de los melanocitos a melanoma sigue un modelo de progresión secuencial [5,6] (Figura 2).

En el primer estadio se forman **nevus melanocíticos**, que son proliferaciones benignas de melanocitos con una capacidad limitada de proliferación. Los nevus pueden permanecer senescentes durante décadas y raramente progresan a melanoma.

El siguiente estadio se conoce como **fase de crecimiento radial** (RGP) e incluye el crecimiento incontrolado de melanocitos de forma localizada en la epidermis sin invadir la dermis. Los melanomas detectados en esta fase pueden ser tratados eficientemente por cirugía.

El estadio más avanzado de la enfermedad incluye la **fase de crecimiento vertical** (VGP)**,** en la cuál los melanocitos son capaces de invadir la dermis, proliferar en esta nueva localización y metastizar a través del torrente sanguíneo a otros órganos del cuerpo dando lugar a la fase más avanzada de la enfermedad o **melanoma metastático**. El melanoma metastático es la forma más agresiva y no tiene tratamiento efectivo.

3. Mecanismos moleculares implicados en la progresión del melanoma

El avance en las técnicas moleculares han permitido identificar los mecanismos moleculares implicados en el desarrollo de la enfermedad. Las principales alteraciones moleculares en melanoma han sido identificadas en moléculas involucradas en la regulación del ciclo celular y en vías de transducción de señales. Las vías de

señalización implicadas en el desarrollo del melanoma son la vía de RAS/ERK1/2 y la vía de PI3K.

3.1 Receptores Tirsosin-quinasa

Tanto la vía de RAS/ERK1/2 como la vía de las PI3K pueden activarse por la unión de un factor de crecimiento a un receptor tirosina quinasa. Los receptores tirosina quinasa están frecuentemente mutados en muchos tipos de cáncer, incluido el melanoma. Entre ellos, destaca **c-MET**. C-MET es el receptor del factor de crecimiento de hepatocitos (HGF) y está mutado en muchos tipos de cáncer. En melanoma, se ha visto que la expresión de c-MET correlaciona directamente con la progresión de la enfermedad. Así, la expresión de c-MET es más elevada en muestras metastáticas que en nevus melanocíticos [19,20].

HGF es una citoquina multifuncional secretada por células mesenquimales que funciona como agente mitogénico, motogénico y morfogénico en células epiteliales. HGF activa la proliferación de los melanocitos a través de c-MET. Se ha descrito que tanto c-MET como HGF se expresan en altos niveles en células de melanoma, permitiendo así la estimulación autocrina del receptor. Además, HGF regula la motilidad, la adhesión celular y la invasión celular [22-24]. De forma interesante, existe un modelo murino de melanoma maligno transgénico para HGF que presenta una hiperpigmentación de la piel [25]. Además, éste modelo desarrolla melanoma maligno cutáneo en respuesta a radiación ultravioleta y recapitula histológicamente y cronológicamente todas las fases del melanoma humano [26].

3.2 Vía de RAS/ERK1/2

El estudio de muestras humanas de melanoma ha desvelado que la vía de las RAS/ERK1/2 tiene un papel importante en el desarrollo del melanoma. El 90% de los melanomas presenta elevados niveles de fosforilación en ERK y se ha visto que la activación constitutiva de la vía está relacionada con la progresión del melanoma [17,27,28].

Los estudios de muestras humanas de melanoma revelaron que entre un 15-30% de los casos presentan mutaciones activadoras en NRAS [32,33] y un 60% de los casos presenta mutaciones activadoras en BRAF. La mutación más frecuente en BRAF es la sustitución de una ácido glutámico por una valina en la posición 600 ($BRAF^{V600E}$) [34].

3.3 Vía de PI3K

Los estudios de muestras humanas de melanoma también revelaron que la vía de las PI3K participa activamente en el desarrollo y progresión del melanoma. El 43-60% de los casos de melanoma presenta una sobreexpresión de AKT3 y el 30% presentan depleciones en PTEN, la fosfatasa que regula negativamente la vía [40,42]. Además, se han encontrado mutaciones puntuales en PI3K y PTEN en una pequeño número de casos [44-47].

4. Dianas terapéuticas en melanoma maligno

El 80% de los casos de melanoma pueden ser tratados por cirugía cuando se detectan en un estadio temprano de desarrollo. Sin embargo, los melanomas detectados en un estadio avanzado son altamente resistentes a las terapias actúales.

La identificación de las vías de señalización implicadas en el desarrollo y progresión del melanoma ha revelado una gran cantidad de dianas susceptibles de ser inhibidas mediante nuevos compuestos específicos. El uso de estos inhibidores se basa en la teoría que la supervivencia de las células malignas es más dependiente de estas vías que las células normales. Así, las células malignas que presentan estas vías hiperactivadas serán mucho más sensibles a la inhibición que las células normales. En los últimos años, se han probado muchas drogas específicas solas y en combinación en estudios preclínicos y clínicos.

4.1 Dianas terapéuticas en la vía de RAS/ERK1/2 en melanoma maligno

El hecho que el 60% de los melanomas presenten la mutación $BRAF^{V600E}$ [34] y el 40% presenten mutaciones activadoras en NRAS [32,33] sugirió que la vía de RAS/ERK1/2 era una buena candidata a diana terapéutica en melanoma. La inhibición de la vía de RAS/ERK1/2 podría detener la progresión tumoral disminuyendo el crecimiento tumoral o promoviendo muerte celular.

Numerosos trabajos han apoyado esta idea mostrando que la proliferación de líneas celulares de melanoma, particularmente las mutadas en $BRAF^{V600E}$, es dependiente de la vía de RAS/ERK1/2 [49 50]. Otros han mostrado que la supresión de BRAF inhibe la transformación de los melanocitos e induce apoptosis [49]. Además, se

ha descrito el papel fundamental de $BRaf^{V600E}$ en el crecimiento tumoral en modelos animales [51].

Todos estos datos apoyan el desarrollo de nuevos compuestos farmacéuticos contra los miembros de esta vía.

4.1.1 Inhibidores

Ver figura 5.

Inhibidores de RAF

El primer inhibidor de la vía de RAS/ERK1/2 que entró en ensayos clínicos fue BAY 43-9006 (sorafenib). Sorafenib es un inhibidor multiquinasa que inhibe tanto la forma wild type de BRAF como la forma mutada $BRAF^{V600E}$, además de otras quinasas como C-RAF, VEGFR-2 y 3, PDGFR y c-KIT [55].

Se ha descrito que en líneas celulares de melanoma, sorafenib inhibe la actividad quinasa de $BRAF^{V600E}$ e induce apoptosis. Además, sorafenib reduce el crecimiento tumoral en modelos xenograph de melanoma [56,57].

A pesar de los resultados prometedores en ensayos preclínicos, el tratamiento de pacientes de melanoma avanzado con sorafenib no ha sido efectivo [58]. No obstante, se han observado ciertas respuestas parciales al tratamiento de pacientes de melanoma avanzado con combinaciones de sorafenib con otros agentes quimioterapeuticos [60-63].

Sin embargo, los últimos datos obtenidos con un nuevo inhibidor específico de $BRAF^{V600E}$ llamado PLX4720 (Plexicon) son alentadores. Éstos muestran que PLX4720, además de ser efectivo en líneas celulares de melanoma portadoras de la mutación $BRAF^{V600}$, parece ser efectivo en ensayos clínicos de fase I en pacientes de melanoma portadores de la mutación (datos aún no publicados). Actualmente se están planificando ensayos de fase II y III con este inhibidor.

4.2 Dianas terapéuticas en la vía de PI3K en melanoma maligno

La vía de las PI3K tiene también una gran relevancia en melanoma. Se han detectado elevados niveles de p-AKT en muestras humanas y se ha descrito que las principales alteraciones genéticas de la vía incluyen la pérdida de PTEN y la sobreexpresión de AKT3.

Además, el silenciamiento de AKT3 o la sobreexpresión de PTEN en líneas celulares de melanoma reduce el crecimiento de melanoma *in vivo* promoviendo apoptosis [40,68]. Estos datos sugieren que la vía de las PI3K es otra buena candidata a inhibir en melanoma y se han desarrollado numerosos inhibidores específicos de quinasas implicadas en la vía.

4.2.1 Inhibidores

Ver figura 6.

Inhibidores de PI3K

Dos de los primeros inhibidores de PI3K fueron LY294002 (Ely Lilly) y wortmannin. Ambos se han utilizado en muchos estudios preclínicos proporcionando muchos datos sobre la biología del melanoma, pero debido a sus pobres características farmacocinéticas no se han utilizado en ensayos clínicos.

Actualmente, existen otros inhibidores de PI3K con mejores características farmacocinéticas que se están utilizando en ensayos clínicos de fase I-II. Algunos de ellos son BKM120 (Novartis), XL147 (Exelixis) o GDC0941 (Genentech).

Inhibidores de mTOR

El inhibidor de mTOR más conocido es la rapamicina (Sirolimus, Rapamune Wyeth) pero éste ha resultado ser un potente inmunosupresor [72,73]. No obstante, se han desarrollado fármacos análogos a la rapamicina con mejores características farmacológicas, como RAD001 (Everolimus, Novartis) o CCI-778 (Tensirolimus, Wyeth). Éstos fármacos han sido aprobados para el tratamiento de pacientes avanzados de carcinoma renal. Sin embargo, su uso en pacientes de otro tipo de tumores, incluido el melanoma, no ha resultado efectivo [74].

Inhibidores duales de PI3K/mTOR

Se ha descrito un feedback loop en el cuál la inhibición de mTOR produce la activación de AKT [75,76]. Por este motivo, se pensó que la inhibición de este feedback mediante inhibidores duales de PI3K y mTOR podrían ser más efectivos que los inhibidores de mTOR. La mayor parte de inhibidores duales de PI3K/mTOR han resultado ser efectivos en estudios preclínicos y se encuentran en ensayos clínicos de

fase I en pacientes con tumores sólidos avanzados. Algunos de estos inhibidores son BEZ235 (Novartis), XL765 (Exelixis) y SF1126 (Semafor).

4.3 Tratamientos combinados

Algunos estudios genómicos en melanoma han revelado que las mutaciones en PI3K o depleciones en PTEN pueden coexistir con mutaciones en NRAS o BRAF [35]. Estos datos, junto con estudios recientes en un modelo de ratón [81], indican que las vías de Pi3k y Raf cooperan en el desarrollo del melanoma. Por ésto, se pensó que el tratamiento combinado con drogas que inhiben ambas vías podría ser beneficioso en melanoma. De hecho, algunos estudios preclínicos en modelos de melanoma muestran la eficacia de la inhibición de ambas vías [81,82]. Así, el tratamiento simultáneo con inhibidores específicos de estas vías podría ser efectivo en melanoma.

5. Modelos animales

Los modelos animales se usan frecuentemente en investigación para caracterizar la función de un gen particular en la progresión de una enfermedad o para probar nuevos compuestos farmacéuticos en un contexto fisiológico. El modelo animal más común en investigación es el ratón. Gracias a la reciente secuenciación del genoma del ratón, resulta fácil manipularlo genéticamente y así obtener modelos animales transgénicos que recapitulen los tumores humanos.

La disponibilidad de un buen modelo animal de melanoma es clave para poder estudiar la biología del melanoma así como para testar nuevos compuestos farmacéuticos. Sin embargo, es difícil conseguir un buen modelo de ratón de melanoma ya que la piel de los ratones es muy distinta a la de los humanos. En humanos, los melanocitos residen en la capa basal de la epidermis, mientras que en ratones se localizan en los folículos pilosos, dermis y muy raramente en la capa basal.

Se pueden distinguir dos tipos diferentes de modelos animales en melanoma: los no transgénicos y los transgénicos.

5.1 Modelos de melanoma no transgénicos

Dado que la mayor parte de la comunidad científica trabaja con células humanas, el modelo animal más utilizado son ratones inmunodeprimidos para así evitar el rechazo a la inyección de células exógenas causada por el sistema inmune.

Existen diferentes modelos de ratones con distintos grados de inmunosupresión, como los ratones balb c/nude o los NOD/SCID.

Por otro lado, también se trabaja con líneas celulares aisladas de melanomas espontáneos obtenidos en modelos murinos de melanoma. Éstas líneas celulares son singénicas con el ratón y pueden ser inyectadas en ratones inmunocompetentes. De esta forma, se obtiene un escenario mucho más fisiológico para realizar ensayos preclínicos que en ratones inmunodeprimidos.

5.2 Modelos transgénicos de melanoma

Gracias al avance en las tecnologías de ingeniería genética se han podido realizar distintos ratones transgénicos para estudiar la melanomagénesis o probar nuevas drogas.

Entre ellos, destaca el modelo de melanoma inducido por ultravioleta en ratones transgénicos para HGF. HGF es una citoquina multifuncional que regula la motilidad, proliferación e invasión celular además de activar simultáneamente las vías de Ras/Erk1/2 y Pi3k a través del receptor c-met. C-met es un receptor tirosin quinasa cuya expresión correlaciona directamente con la progresión del melanoma.

El ratón transgénico para HGF sobreexpresa esta citoquina en muchos órganos [25]. La pecularied ad de estos ratones transgéncios para HGF es que sus melanocitos se localizan en la dermis, epidermis y en la capa basal, asemejándose así a la piel humana [87]. Éstos ratones son capaces de desarrollar melanomas a los 21 meses de edad. Sin embargo, una dosis única de radiación ultravioleta en neonatos transgénicos para HGF de 3,5 días de edad es suficiente para desarrollar melanoma con una alta penetrancia. Además, estos melanomas recapitulan cronológicamente e histopatológicamente todas las fases del melanoma humano, incluido el metastático [26].

Así, el modelo de melanoma inducido por radiación ultravioleta en ratones transgénicos para HGF supone una herramienta idónea para estudiar el desarrollo del melanoma y probar nuevas terapias.

OBJETIVOS

Se ha descrito que la vía de las PI3K y RAS/ERK1/2 podrían ser dos buenas candidatas en la terapia dirigida en melanoma [82,91]. La disponibilidad del modelo murino de melanoma transgénico para HGF y de células de melanomas singénicas con este modelo representan una gran oportunidad para probar la efectividad de terapias dirigidas en un modelo animal de melanoma relevante.

En este estudio investigamos la efectividad de dos inhibidores de quinasa que inhiben estás vías: PI-103, un inhibidor dual de PI3K/mTOR, y sorafenib, un inhibidor de RAF.

Los principales objetivos de esta tesis son:

1. Probar la eficacia de PI-103 y sorafenib *in vitro* individualmente y en combinación en líneas celulares de melanoma aisladas de tumores espontáneos obtenidos en el modelo de melanoma inducido por ultravioleta.

2. Probar la eficacia de PI-103 y sorafenib *in vivo* individualmente y en combinación en modelos ortotópicos de melanoma en ratones inmunocompetentes.

RESULTADOS Y DISCUSIÓN

El melanoma es el tipo de cáncer de piel más agresivo no habiendo una terapia efectiva cuando alcanza su fase metástatica. Existen datos experimentales que revelan que la vía de PI3K y RAS son de suma importancia en el desarrollo y mantenimiento del melanoma siendo por ello dos buenas candidatas para ser inhibidas mediante compuestos específicos.

En este estudio hemos investigado la efectividad de dos inhibidores de quinasa (PI-103 y sorafenib) *in vivo* e *in vitro* en dos líneas celulares de melanoma (37-31E-F0 y 37-31E-F3) obtenidas de melanomas espontáneos de un modelo de melanoma inducido por radiación ultravioleta en ratones transgénicos para HGF.

PI-103 es un inhibidor dual de PI3K/mTOR que inhibe específicamente la subunidad p110α de PI3K [96]. Éste inhibidor es mucho más potente y específico que el inhibidor de PI3K LY 294002 (Tabla 5).

Sorafenib es un inhibidor multiquinasa que inhibe BRAF, $BRAF^{V600E}$, CRAF, PDGFR, C-KIT y VGFR (Tabla 6).

Ensayos *in vitro*

Nuestros resultados muestran que PI-103 inhibe la vía de Pi3k de forma dosis-dependiente en las líneas celulares 37-31E-F0 y 37-31E-F3. Además, observamos cierta diferencia entre ambas líneas celulares en la sensibilidad a la droga (Figura 9). Éstos datos correlacionan con estudios que muestran que PI-103 inhibe la vía de PI3K de forma dependiente de dosis y del background genético de la célula [95].

Sorafenib también inhibe de forma dosis-dependiente la vía de las Raf/Erk1/2 en nuestras líneas celulares (Figura 10) tal y cómo ya se había descrito previamente [55,57].

Además, ambas drogas inhiben de forma dependiente de dosis la proliferación celular *in vitro* de las dos líneas celulares (Figuras 11 y 12) No obstante, en éste aspecto parece ser que la inhibición de la vía de Raf mediante sorafenib es más efectiva que la inhibición de la vía de Pi3k.

Algunos estudios muestras que la inhibición simultánea de las vías de PI3K y RAF en líneas celulares de melanoma humanas es más efectiva que los tratamientos individuales [108]. Nuestros datos sugieren que la combinación de PI-103 y sorafenib inhiben de forma sinérgica las vías de las Raf/Erk1/2 y Pi3k en la línea celular 37-31E-F3 (Figura 13). Además, ambas drogas cooperan inhibiendo la proliferación celular de

ésta línea celular en comparación con los tratamientos con cada droga individualmente (Figura 14).

Tratamientos *in vivo*

El uso de un modelo animal de melanoma apropiado puede ser relevante en ensayos preclínicos. La mayoría de ensayos preclínicos utilizan ratones inmunodeprimidos sin tener en cuenta el papel que ejerce el sistema inmune en la selección de células tumorales o los posibles efectos sistémicos que pueda producir la droga. En este estudio, hemos probado la efectividad de PI-103 y sorafenib en un modelo de ratón inmunocompetente que tiene en consideración ambos aspectos.

Dado que las células 37-31E-F3 resultaron ser particularmente sensibles al tratamiento combinado con PI-103 y sorafenib, realizamos un experimento *in vivo* inyectando por vía subcutánea esta línea celular en ratones inmunocompetentes FVB/N. Tras el tratamiento, se observó que sorprendentemente, el tratamiento diario con PI-103 promovía crecimiento tumoral en comparación con los controles. El tratamiento con sorafenib redujo el volumen tumoral tal y cómo se había descrito en otros modelos animales [55,93] y el tratamiento con la combinación de las dos drogas no supuso ninguna reducción significante en comparación con los tratados con sorafenib (Figura 16).

Posteriormente, comprobamos mediante otros ensayos *in vivo* que éste efecto de crecimiento tumoral inducido por PI-103 era independiente de dosis y de tipo celular (Figuras 17 y 18).

Éstos resultados *in vivo* contradecían a estudios anteriores efectuados con esta droga [94,99,100]. Cabe destacar que, en todos estos estudios se usaron ratones inmunodeprimidos balb c/nude como modelo animal; mientras que nosotros utilizábamos ratones con un sistema inmune completo**.** Por éste motivo, repetimos el experimento *in vivo* inyectando nuestra línea celular murina en ratones balb c/nude. Nuestros resultados, al igual que aquellos descritos previamente [94,99,100], mostraban la efectividad de PI-103 reduciendo el volumen tumoral en éste modelo animal (Figura 19).

A pesar de que en todos estos estudios utilizaban el mismo modelo animal, también se observaron ciertas diferencias en cuánto a la efectividad de la droga entre los distintos modelos de cáncer dependiendo de la dosis y de la frecuencia administrada. Así, en los modelos dónde el tratamiento resultaba ser más efectivo se requerían dos administraciones diarias a dosis muy elevadas [95]. Además, en un modelo de glioblastoma, el tratamiento con PI-103 sólo era efectivo reduciendo el

tamaño tumoral cuando se combinaba con radiación, mientras que la droga por sí sola era totalmente inefectiva [109]. Por otro lado, en todos estos estudios utilizaban líneas celulares que presentaban mutaciones activadoras de la vía y por tanto, eran dependientes de la vía de PI3K [94,100]. En cambio, la línea celular 37-31E-F3 no parece ser particularmente dependiente de la vía de las Pi3k según los niveles basales de p-Akt que presentan y nuestros ensayos de proliferación *in vitro* en respuesta a PI-103.

Recientemente, se ha descrito que varios inhibidores duales de Pi3k/mTOR, incluido el PI-103, resultaron ser efectivos reduciendo el crecimiento tumoral en un modelo de melanoma B16BL6 inmunocompetente [110]. Sin embargo, éste estudio también muestra que PI-103 resultó ser el inhibidor menos efectivo: PI-103 fue el único inhibidor que no inducía necrosis, no reducía las metástasis en nódulos linfáticos ni tampoco reducía la angiogenesis.

La baja efectividad *in vivo* de PI-103 se puede atribuir a su baja solubilidad y su pobre farmacocinética [95]. Sin embargo, la farmacocinética de PI-103 en nuestro sistema fue suficiente para inhibir las dianas correspondientes, según muestran los niveles de p-Akt, p-S6 y p-4EBP1 en los tejidos tumorales (Figura 20).

El tratamiento de los ratones FVB/N con la combinación de PI-103 y sorafenib no mostró ningún beneficio en la reducción del volumen tumoral en comparación con el de los tratados con sorafenib. Estudios recientes sugieren que la efectividad de la terapia combinada inhibiendo las vías de PI3K y RAS/ERK-2 puede estar limitada a melanomas portadores de mutaciones activadoras en estas vías [91]. Además, se ha probado la eficacia de la inhibición de estas vías mediante compuestos específicos en modelos murinos de melanoma, como el ratón transgénico TPRas inducido por DMBA [82] o el Tyr::CreER; $BRaf^{CA}$ /+x$Pten^{lox/lox}$ [81]. Los melanomas obtenidos en ambos casos son totalmente dependientes de la vía de Ras/Erk1/2 o Ras/Erk1/2 y Pi3k respectivamente. Por lo tanto, no resulta sorprendente la efectividad del tratamiento reduciendo el volumen tumoral. En cambio, según los bajos niveles de p-Akt o p-Erk1/2, nuestros tumores no parecen ser particularmente dependientes de estas vías.

El distinto tiempo de latencia de las células tumorales en los dos modelos de ratón utilizados, sugería que las células estaban siendo seleccionadas diferencialmente a través del huésped. Las células 37-31E-F0 tardaban 4 semanas en formar tumores en los ratones FVB/N mientras que sólo era necesario 1 semana para formar tumores en ratones balb c/nude. Esta distinta selección se traducía con una distinta expresión basal de las proteínas antiapoptóticas entre los tumores de los dos modelos (Figura 21A). Además, el tratamiento con PI-103 producía la sobreexpresión de las proteínas antiapoptoticas Mcl-1, Bcl-2 y Bcl_{XL} *in vivo* correlacionando con el

volumen tumoral observado tras el tratamiento. Curiosamente, se ha descrito que la expresión de Mcl-1 y Bcl-2 está relacionada con mecanismos de resistencia a inhibidores duales de PI3K/mTOR [103,104]. Además, se ha descrito que la expresión de estas proteínas puede ser inducida por el tratamiento con rapamicina [111,112].

Para caracterizar mejor este posible efecto antiapoptotico inducido por PI-103, aislamos líneas celulares a partir de los tumores de ratones control de nuestros experimentos. Estas líneas celulares seleccionadas a través del ratón (37-31E-F3K61, 37-31E-F3K63) expresaban niveles basales más elevados de estas proteínas antiapoptoticas que las líneas parentales (37-31E-F0, 37-31E-F3) (Figura 21B). Además, el tratamiento *in vitro* de las líneas celulares derivadas de tumores con concentraciones crecientes de PI-103 inducía la sobreexpresión de las proteínas antiapoptoticas. Esta acumulación de proteínas antiapoptóticas se correspondía con un aumento en la viabilidad de estas células en presencia de PI-103 (Figura 21 C y D). Sin embargo, éste efecto no se observaba en los tratamientos con sorafenib ni en las células parentales 37-31E-F3. Los resultados de estos experimentos correlacionaban perfectamente con los niveles de apoptosis detectados en los tumores: sorafenib reducía los niveles de las proteínas antiapoptóticas e inducía apoptosis tal y cómo había sido descrito previamente [57] mientras que PI-103 producía el efecto contrario (Figura 20A).

El diferente efecto biológico producido por el inhibidor PI-103 en dos modelos diferentes de ratón, sugirió que la droga podía estar produciendo un efecto a nivel sistémico en el ratón. Además de tener un fondo genético diferente, los ratones FVB/N se diferencian de los balb c/nude por tener un sistema inmunológico completo. Por otro lado, está claramente descrito que la rapamicina, un inhibidor de mTOR, es un inmunosupresor que produce atrofia en el timo disminuyendo así la población de timocitos [72,73,105]. Por esta razón, nos preguntamos si PI-103, como inhibidor dual de PI3K/mTOR podía estar afectando el sistema inmune de los ratones FVB/N, de forma que favoreciera así el crecimiento tumoral. Los resultados mostraron que al igual que la rapamicina, PI-103 reducía de forma significativa la población de timocitos en el timo de los ratones. En cambio, la población de esplecnocitos no se veía afectada por la droga (Figura 23). El estudio de Marone et al. no muestra datos sobre la población de timocitos en el timo de sus ratones inmunocompetentes B16BL6 tratados con PI-103. Por otro lado, al igual que nuestros resultados, estos ratones no mostraron diferencias en la población de esplecnocitos [110].

El efecto *in vivo* inmunosupresor de PI-103 también ha sido recientemente caracterizado por otro grupo [114]. En este estudio, los autores muestran que el

tratamiento con PI-103 en ratones C75BL/6J reduce el número total de células B y T en el bazo.

Con fin de caracterizar mejor éste efecto inmunosupresor, comprobamos los niveles transcripcionales intratumorales de las citoquinas inmunosupresoras IL-6, IL-10 y VEGF en los tumores de nuestros experimentos. Los resultados mostraron que los niveles de estas citoquinas estaban sobreregulados en las muestras de ratones FVB/N tratados con PI-103 de dos experimentos diferentes. En cambio, no observamos esta regulación en los tumores de ratones tratados con sorafenib o con la combinación de las dos drogas. De forma relevante, los tumores de ratones balb c/nude tratados con PI-103 mostraban una reducción considerable de los niveles de éstas citoquinas (Figura 24).

La sobreregulación de estas citoquinas podría ser originada por un efecto de la droga en huésped o en las células tumorales. Curiosamente, el tratamiento *in vitro* de las células 37-31E-F3 con PI-103 producía la sobreexpresión transcripcional de las citoquinas (Figura 25A) sugiriendo que era un efecto que el PI-103 producía en las células tumorales. Entonces, nos interesamos por encontrar el mecanismo molecular mediante el cuál PI-103 regulaba los niveles de estas citoquinas. Curiosamente, se ha descrito que STAT3 es un factor de transcripción implicado en varios procesos importantes para la tumorogénesis, como la proliferación celular, la inhibición de la apoptosis o la evasión del sistema inmune. La evasión del sistema inmune es un mecanismo que permite a las células malignas sobrevivir en el huésped. Además, la vía de STAT está hiperactivada en una gran variedad de tumores [115] y su activación está directamente relacionada con la progresión del melanoma [116]. STAT3 representa un punto de convergencia de muchas vías de señalización molecular, incluyendo receptores tirosina quinasa y está implicado en la regulación transcripcional de las citoquinas inmunosupresoras IL-6, IL-10 y VEGF [106].

Curiosamente, el tratamiento *in vitro* de las células de melanoma con PI-103 inducía un aumento de los niveles de fosforilación de Stat3 (Figura 25B). Además, las muestras de tumores de ratones inmunocompetentes tratados con PI-103 mostraban altos niveles de p-Stat3 en comparación con los controles o los tratados con sorafenib o la combinación de las dos drogas (Figura 25C). Estos datos sugieren que la modulación de la fosforilación de Stat3 por PI-103 podría ser la responsable del efecto inmunosupresor de la droga. Este efecto inmunosupresor podría contribuir a favorecer el crecimiento tumoral observado en los ratones tratados con PI-103 (Figura 29).

Por otro lado, STAT3 también participa en mecanismos de evasión de la apoptosis en melanoma humano. Se ha descrito que además de estar implicado en la

protección celular de la apoptosis inducida por TRAIL [117], STAT3 participa en la regulación de las proteínas antiapoptóticas Mcl-1 y Bcl-X_L [118]. Nuestros datos muestran que PI-103, pero no sorafenib, induce la sobre expresión de Mcl-1 y Bcl-2 y correlaciona con un altos niveles de p-Stat3.

El mecanismo mediante el cuál la inhibición de PI3K/mTOR modula la fosforilación de STAT3 no está todavía bien caracterizado. Sin embargo, hay estudios que muestran que la inhibición de PI3K provoca el aumento de la actividad transcripcional de STAT3 resultando en un efecto antiapoptotico [119]. Además, nuestros datos preliminares muestran que otros inhibidores duales de PI3K/mTOR como BEZ-235 también modulan los niveles de fosforilación de STAT3 tanto en líneas celulares de ratón como en humanas (Figuras 26 y 27).

En conclusión, nuestro trabajo muestra que PI-103 y sorafenib son efectivos inhibiendo las vías de Pi3k y Ras/Erk1/2 respectivamente en líneas murinas de melanoma. Además, ambas drogas inhiben sinergísticamente *in vitro* las vías de Pi3k y Ras/Erk1/2 y la proliferación celular de forma dependiente de línea celular. Los ensayos *in vivo* en xenographs ortotópicos en ratones inmunocompetentes revelan que mientras sorafenib reducía el volumen tumoral, PI-103 promovía el crecimiento tumoral y el tratamiento combinado de sorafenib y PI-103 no cooperaba reduciendo el volumen tumoral. El uso de un modelo de ratón inmunocompetente nos permitió tener en consideración tanto la selección de las células tumorales a través del sistema inmune como la posibilidad de detectar posibles efectos sistémicos en el ratón derivados del tratamiento. Curiosamente, en nuestro sistema, el tratamiento con PI-103 producía una sobreregulación de la expresión de las proteínas antiapoptóticas de la familia BH3 *in vivo* e *in vitro*. Además, el tratamiento con PI-103 producía una inmunosupresión *in vivo* probablemente a través de p-Stat3.

CONCLUSIONES

Las conclusiones derivadas de esta tesis son las siguientes:

1. El inhibidor dual de PI3K/mTOR y el inhibidor multiquinasa sorafenib son efectivos individualmente y en combinación inhibiendo *in vitro* las vías de Pi3k y Raf y la proliferación en líneas celulares de melanoma.

2. El tratamiento *in vivo* con PI-103 produce diferentes respuestas tumorales dependiendo del modelo animal utilizado.

3. Las células tumorales son seleccionadas diferencialmente de forma dependiente de huésped.

4. PI-103 regula la expresión de las proteínas antiapoptoticas de la familia BH3 *in viv*o y en líneas celulares primarias aisladas de tumores de ratones control. Sorafenib reduce la expresión de éstas proteínas produciendo una mayor apoptosis.

5. PI-103 produce inmunosupresión induciendo la atrofia del timo e induciendo la sobreexpresión de inmunosupresores intratumorales.

6. En las muestras de ratones tratadas con PI-103 los niveles de p-Stat3 correlacionan con niveles elevados de proteínas antiapoptóticas y citoquinas inmunosupresoras.

7. La regulación de p-Stat3 por la inhibición de PI3K/mTOR es extensible a líneas celulares humanas y otros inhibidores duales de PI3K/mTOR, sugiriendo que STAT3 podría jugar un papel en los mecanismos de resistencia a inhibidores de PI3K/mTOR.

8. Nuestros datos proponen el uso de modelos animales más fisiológicos en los estudios preclínicos para poder detectar efectos sistémicos.

VIII. REFERENCES

1. BIBLIOGRAPHY

1. Hanahan, D. & Weinberg, R.A. The hallmarks of cancer. *Cell* **100**, 57-70 (2000).
2. De Fabo, E.C., Noonan, F.P., Fears, T. & Merlino, G. Ultraviolet B but not ultraviolet A radiation initiates melanoma. *Cancer Res* **64**, 6372-6 (2004).
3. Chin, L., Merlino, G. & DePinho, R.A. Malignant melanoma: modern black plague and genetic black box. *Genes Dev* **12**, 3467-81 (1998).
4. Miyauchi, H. & Horio, T. Ultraviolet B-induced local immunosuppression of contact hypersensitivity is modulated by ultraviolet irradiation and hapten application. *J Invest Dermatol* **104**, 364-9 (1995).
5. Chudnovsky, Y., Khavari, P.A. & Adams, A.E. Melanoma genetics and the development of rational therapeutics. *J Clin Invest* **115**, 813-24 (2005).
6. Miller, A.J. & Mihm, M.C., Jr. Melanoma. *N Engl J Med* **355**, 51-65 (2006).
7. Braig, M. & Schmitt, C.A. Oncogene-induced senescence: putting the brakes on tumor development. *Cancer Res* **66**, 2881-4 (2006).
8. Moodie, S.A., Willumsen, B.M., Weber, M.J. & Wolfman, A. Complexes of Ras.GTP with Raf-1 and mitogen-activated protein kinase kinase. *Science* **260**, 1658-61 (1993).
9. Warne, P.H., Viciana, P.R. & Downward, J. Direct interaction of Ras and the amino-terminal region of Raf-1 in vitro. *Nature* **364**, 352-5 (1993).
10. Sjolander, A., Yamamoto, K., Huber, B.E. & Lapetina, E.G. Association of p21ras with phosphatidylinositol 3-kinase. *Proc Natl Acad Sci U S A* **88**, 7908-12 (1991).
11. Alessi, D.R. et al. Characterization of a 3-phosphoinositide-dependent protein kinase which phosphorylates and activates protein kinase Balpha. *Curr Biol* **7**, 261-9 (1997).
12. Stephens, L. et al. Protein kinase B kinases that mediate phosphatidylinositol 3,4,5-trisphosphate-dependent activation of protein kinase B. *Science* **279**, 710-4 (1998).
13. Toker, A. & Newton, A.C. Akt/protein kinase B is regulated by autophosphorylation at the hypothetical PDK-2 site. *J Biol Chem* **275**, 8271-4 (2000).
14. Feng, J., Park, J., Cron, P., Hess, D. & Hemmings, B.A. Identification of a PKB/Akt hydrophobic motif Ser-473 kinase as DNA-dependent protein kinase. *J Biol Chem* **279**, 41189-96 (2004).

15. Delcommenne, M. et al. Phosphoinositide-3-OH kinase-dependent regulation of glycogen synthase kinase 3 and protein kinase B/AKT by the integrin-linked kinase. *Proc Natl Acad Sci U S A* **95**, 11211-6 (1998).
16. Sarbassov, D.D., Guertin, D.A., Ali, S.M. & Sabatini, D.M. Phosphorylation and regulation of Akt/PKB by the rictor-mTOR complex. *Science* **307**, 1098-101 (2005).
17. Satyamoorthy, K. et al. Constitutive mitogen-activated protein kinase activation in melanoma is mediated by both BRAF mutations and autocrine growth factor stimulation. *Cancer Res* **63**, 756-9 (2003).
18. Prickett, T.D. et al. Analysis of the tyrosine kinome in melanoma reveals recurrent mutations in ERBB4. *Nat Genet* **41**, 1127-32 (2009).
19. Natali, P.G. et al. Expression of the c-Met/HGF receptor in human melanocytic neoplasms: demonstration of the relationship to malignant melanoma tumour progression. *Br J Cancer* **68**, 746-50 (1993).
20. Elia, G. et al. Mechanisms regulating c-met overexpression in liver-metastatic B16-LS9 melanoma cells. *J Cell Biochem* **81**, 477-87 (2001).
21. Beuret, L. et al. Up-regulation of MET expression by alpha-melanocyte-stimulating hormone and MITF allows hepatocyte growth factor to protect melanocytes and melanoma cells from apoptosis. *J Biol Chem* **282**, 14140-7 (2007).
22. Recio, J.A. & Merlino, G. Hepatocyte growth factor/scatter factor activates proliferation in melanoma cells through p38 MAPK, ATF-2 and cyclin D1. *Oncogene* **21**, 1000-8 (2002).
23. Li, G. et al. Downregulation of E-cadherin and Desmoglein 1 by autocrine hepatocyte growth factor during melanoma development. *Oncogene* **20**, 8125-35 (2001).
24. Hamasuna, R. et al. Regulation of matrix metalloproteinase-2 (MMP-2) by hepatocyte growth factor/scatter factor (HGF/SF) in human glioma cells: HGF/SF enhances MMP-2 expression and activation accompanying up-regulation of membrane type-1 MMP. *Int J Cancer* **82**, 274-81 (1999).
25. Takayama, H., La Rochelle, W.J., Anver, M., Bockman, D.E. & Merlino, G. Scatter factor/hepatocyte growth factor as a regulator of skeletal muscle and neural crest development. *Proc Natl Acad Sci U S A* **93**, 5866-71 (1996).
26. Noonan, F.P. et al. Neonatal sunburn and melanoma in mice. *Nature* **413**, 271-2 (2001).
27. Cohen, C. et al. Mitogen-actived protein kinase activation is an early event in melanoma progression. *Clin Cancer Res* **8**, 3728-33 (2002).

28. Zhuang, L. et al. Activation of the extracellular signal regulated kinase (ERK) pathway in human melanoma. *J Clin Pathol* **58**, 1163-9 (2005).
29. Zhang, X.D., Borrow, J.M., Zhang, X.Y., Nguyen, T. & Hersey, P. Activation of ERK1/2 protects melanoma cells from TRAIL-induced apoptosis by inhibiting Smac/DIABLO release from mitochondria. *Oncogene* **22**, 2869-81 (2003).
30. Esteve-Puig, R., Canals, F., Colome, N., Merlino, G. & Recio, J.A. Uncoupling of the LKB1-AMPKalpha energy sensor pathway by growth factors and oncogenic BRAF. *PLoS One* **4**, e4771 (2009).
31. Wang, Y.F. et al. Apoptosis induction in human melanoma cells by inhibition of MEK is caspase-independent and mediated by the Bcl-2 family members PUMA, Bim, and Mcl-1. *Clin Cancer Res* **13**, 4934-42 (2007).
32. Omholt, K., Platz, A., Kanter, L., Ringborg, U. & Hansson, J. NRAS and BRAF mutations arise early during melanoma pathogenesis and are preserved throughout tumor progression. *Clin Cancer Res* **9**, 6483-8 (2003).
33. Herlyn, M. & Satyamoorthy, K. Activated ras. Yet another player in melanoma? *Am J Pathol* **149**, 739-44 (1996).
34. Davies, H. et al. Mutations of the BRAF gene in human cancer. *Nature* **417**, 949-54 (2002).
35. Tsao, H., Goel, V., Wu, H., Yang, G. & Haluska, F.G. Genetic interaction between NRAS and BRAF mutations and PTEN/MMAC1 inactivation in melanoma. *J Invest Dermatol* **122**, 337-41 (2004).
36. Chin, L. et al. Essential role for oncogenic Ras in tumour maintenance. *Nature* **400**, 468-72 (1999).
37. Emuss, V., Garnett, M., Mason, C. & Marais, R. Mutations of C-RAF are rare in human cancer because C-RAF has a low basal kinase activity compared with B-RAF. *Cancer Res* **65**, 9719-26 (2005).
38. Goel, V.K., Lazar, A.J., Warneke, C.L., Redston, M.S. & Haluska, F.G. Examination of mutations in BRAF, NRAS, and PTEN in primary cutaneous melanoma. *J Invest Dermatol* **126**, 154-60 (2006).
39. Dhawan, P., Singh, A.B., Ellis, D.L. & Richmond, A. Constitutive activation of Akt/protein kinase B in melanoma leads to up-regulation of nuclear factor-kappaB and tumor progression. *Cancer Res* **62**, 7335-42 (2002).
40. Stahl, J.M. et al. Deregulated Akt3 activity promotes development of malignant melanoma. *Cancer Res* **64**, 7002-10 (2004).
41. Dai, D.L., Martinka, M. & Li, G. Prognostic significance of activated Akt expression in melanoma: a clinicopathologic study of 292 cases. *J Clin Oncol* **23**, 1473-82 (2005).

42. Tsao, H., Mihm, M.C., Jr. & Sheehan, C. PTEN expression in normal skin, acquired melanocytic nevi, and cutaneous melanoma. *J Am Acad Dermatol* **49**, 865-72 (2003).
43. Guldberg, P. et al. Disruption of the MMAC1/PTEN gene by deletion or mutation is a frequent event in malignant melanoma. *Cancer Res* **57**, 3660-3 (1997).
44. Teng, D.H. et al. MMAC1/PTEN mutations in primary tumor specimens and tumor cell lines. *Cancer Res* **57**, 5221-5 (1997).
45. Tsao, H., Zhang, X., Benoit, E. & Haluska, F.G. Identification of PTEN/MMAC1 alterations in uncultured melanomas and melanoma cell lines. *Oncogene* **16**, 3397-402 (1998).
46. Birck, A., Ahrenkiel, V., Zeuthen, J., Hou-Jensen, K. & Guldberg, P. Mutation and allelic loss of the PTEN/MMAC1 gene in primary and metastatic melanoma biopsies. *J Invest Dermatol* **114**, 277-80 (2000).
47. Omholt, K., Krockel, D., Ringborg, U. & Hansson, J. Mutations of PIK3CA are rare in cutaneous melanoma. *Melanoma Res* **16**, 197-200 (2006).
48. Soengas, M.S. & Lowe, S.W. Apoptosis and melanoma chemoresistance. *Oncogene* **22**, 3138-51 (2003).
49. Hingorani, S.R., Jacobetz, M.A., Robertson, G.P., Herlyn, M. & Tuveson, D.A. Suppression of BRAF(V599E) in human melanoma abrogates transformation. *Cancer Res* **63**, 5198-202 (2003).
50. Wellbrock, C. et al. V599EB-RAF is an oncogene in melanocytes. *Cancer Res* **64**, 2338-42 (2004).
51. Hoeflich, K.P., Jaiswal, B., Davis, D.P. & Seshagiri, S. Inducible BRAF suppression models for melanoma tumorigenesis. *Methods Enzymol* **439**, 25-38 (2008).
52. Eskandarpour, M. et al. Suppression of oncogenic NRAS by RNA interference induces apoptosis of human melanoma cells. *Int J Cancer* **115**, 65-73 (2005).
53. End, D.W. et al. Characterization of the antitumor effects of the selective farnesyl protein transferase inhibitor R115777 in vivo and in vitro. *Cancer Res* **61**, 131-7 (2001).
54. Smalley, K.S. & Eisen, T.G. Farnesyl transferase inhibitor SCH66336 is cytostatic, pro-apoptotic and enhances chemosensitivity to cisplatin in melanoma cells. *Int J Cancer* **105**, 165-75 (2003).
55. Wilhelm, S.M. et al. BAY 43-9006 exhibits broad spectrum oral antitumor activity and targets the RAF/MEK/ERK pathway and receptor tyrosine kinases involved in tumor progression and angiogenesis. *Cancer Res* **64**, 7099-109 (2004).

56. Karasarides, M. et al. B-RAF is a therapeutic target in melanoma. *Oncogene* **23**, 6292-8 (2004).
57. Panka, D.J., Wang, W., Atkins, M.B. & Mier, J.W. The Raf inhibitor BAY 43-9006 (Sorafenib) induces caspase-independent apoptosis in melanoma cells. *Cancer Res* **66**, 1611-9 (2006).
58. Eisen, T. et al. Sorafenib in advanced melanoma: a Phase II randomised discontinuation trial analysis. *Br J Cancer* **95**, 581-6 (2006).
59. Ratain, M.J. et al. Phase II placebo-controlled randomized discontinuation trial of sorafenib in patients with metastatic renal cell carcinoma. *J Clin Oncol* **24**, 2505-12 (2006).
60. Flaherty, K.T. et al. A phase I trial of the oral, multikinase inhibitor sorafenib in combination with carboplatin and paclitaxel. *Clin Cancer Res* **14**, 4836-42 (2008).
61. Hauschild, A. et al. Results of a phase III, randomized, placebo-controlled study of sorafenib in combination with carboplatin and paclitaxel as second-line treatment in patients with unresectable stage III or stage IV melanoma. *J Clin Oncol* **27**, 2823-30 (2009).
62. McDermott, D.F. et al. Double-blind randomized phase II study of the combination of sorafenib and dacarbazine in patients with advanced melanoma: a report from the 11715 Study Group. *J Clin Oncol* **26**, 2178-85 (2008).
63. Amaravadi, R.K. et al. Phase II Trial of Temozolomide and Sorafenib in Advanced Melanoma Patients with or without Brain Metastases. *Clin Cancer Res* (2009).
64. Tsai, J. et al. Discovery of a selective inhibitor of oncogenic B-Raf kinase with potent antimelanoma activity. *Proc Natl Acad Sci U S A* **105**, 3041-6 (2008).
65. Solit, D.B. et al. BRAF mutation predicts sensitivity to MEK inhibition. *Nature* **439**, 358-62 (2006).
66. Hersey, P. et al. Small molecules and targeted therapies in distant metastatic disease. *Ann Oncol* **20 Suppl 6**, vi35-40 (2009).
67. Emery, C.M. et al. MEK1 mutations confer resistance to MEK and B-RAF inhibition. *Proc Natl Acad Sci U S A* **106**, 20411-6 (2009).
68. Stahl, J.M. et al. Loss of PTEN promotes tumor development in malignant melanoma. *Cancer Res* **63**, 2881-90 (2003).
69. Madhunapantula, S.V. & Robertson, G.P. The PTEN-AKT3 signaling cascade as a therapeutic target in melanoma. *Pigment Cell Melanoma Res* **22**, 400-19 (2009).

70. Liu, P., Cheng, H., Roberts, T.M. & Zhao, J.J. Targeting the phosphoinositide 3-kinase pathway in cancer. *Nat Rev Drug Discov* **8**, 627-44 (2009).
71. LoPiccolo, J., Blumenthal, G.M., Bernstein, W.B. & Dennis, P.A. Targeting the PI3K/Akt/mTOR pathway: effective combinations and clinical considerations. *Drug Resist Updat* **11**, 32-50 (2008).
72. Heitman, J., Movva, N.R. & Hall, M.N. Targets for cell cycle arrest by the immunosuppressant rapamycin in yeast. *Science* **253**, 905-9 (1991).
73. Tian, L., Lu, L., Yuan, Z., Lamb, J.R. & Tam, P.K. Acceleration of apoptosis in CD4+CD8+ thymocytes by rapamycin accompanied by increased CD4+CD25+ T cells in the periphery. *Transplantation* **77**, 183-9 (2004).
74. Faivre, S., Kroemer, G. & Raymond, E. Current development of mTOR inhibitors as anticancer agents. *Nat Rev Drug Discov* **5**, 671-88 (2006).
75. O'Reilly, K.E. et al. mTOR inhibition induces upstream receptor tyrosine kinase signaling and activates Akt. *Cancer Res* **66**, 1500-8 (2006).
76. Wan, X., Harkavy, B., Shen, N., Grohar, P. & Helman, L.J. Rapamycin induces feedback activation of Akt signaling through an IGF-1R-dependent mechanism. *Oncogene* **26**, 1932-40 (2007).
77. Hodi, F.S. et al. Major response to imatinib mesylate in KIT-mutated melanoma. *J Clin Oncol* **26**, 2046-51 (2008).
78. Schmitt, C.A., Rosenthal, C.T. & Lowe, S.W. Genetic analysis of chemoresistance in primary murine lymphomas. *Nat Med* **6**, 1029-35 (2000).
79. Jansen, B. et al. bcl-2 antisense therapy chemosensitizes human melanoma in SCID mice. *Nat Med* **4**, 232-4 (1998).
80. Bedikian, A.Y. et al. Bcl-2 antisense (oblimersen sodium) plus dacarbazine in patients with advanced melanoma: the Oblimersen Melanoma Study Group. *J Clin Oncol* **24**, 4738-45 (2006).
81. Dankort, D. et al. Braf(V600E) cooperates with Pten loss to induce metastatic melanoma. *Nat Genet* **41**, 544-52 (2009).
82. Bedogni, B. et al. Inhibition of phosphatidylinositol-3-kinase and mitogen-activated protein kinase kinase 1/2 prevents melanoma development and promotes melanoma regression in the transgenic TPRas mouse model. *Mol Cancer Ther* **5**, 3071-7 (2006).
83. Larue, L. & Beermann, F. Cutaneous melanoma in genetically modified animals. *Pigment Cell Res* **20**, 485-97 (2007).
84. Tietze, M.K. & Chin, L. Murine models of malignant melanoma. *Mol Med Today* **6**, 408-10 (2000).

85. Lesko, E. & Majka, M. The biological role of HGF-MET axis in tumor growth and development of metastasis. *Front Biosci* **13**, 1271-80 (2008).
86. Benvenuti, S. & Comoglio, P.M. The MET receptor tyrosine kinase in invasion and metastasis. *J Cell Physiol* **213**, 316-25 (2007).
87. Otsuka, T. et al. c-Met autocrine activation induces development of malignant melanoma and acquisition of the metastatic phenotype. *Cancer Res* **58**, 5157-67 (1998).
88. Noonan, F.P., Otsuka, T., Bang, S., Anver, M.R. & Merlino, G. Accelerated ultraviolet radiation-induced carcinogenesis in hepatocyte growth factor/scatter factor transgenic mice. *Cancer Res* **60**, 3738-43 (2000).
89. Autier, P. & Dore, J.F. Influence of sun exposures during childhood and during adulthood on melanoma risk. EPIMEL and EORTC Melanoma Cooperative Group. European Organisation for Research and Treatment of Cancer. *Int J Cancer* **77**, 533-7 (1998).
90. Whiteman, D.C., Whiteman, C.A. & Green, A.C. Childhood sun exposure as a risk factor for melanoma: a systematic review of epidemiologic studies. *Cancer Causes Control* **12**, 69-82 (2001).
91. Lasithiotakis, K.G. et al. Combined inhibition of MAPK and mTOR signaling inhibits growth, induces cell death, and abrogates invasive growth of melanoma cells. *J Invest Dermatol* **128**, 2013-23 (2008).
92. Voorhoeve, P.M. & Agami, R. The tumor-suppressive functions of the human INK4A locus. *Cancer Cell* **4**, 311-9 (2003).
93. Sharma, A. et al. Mutant V599EB-Raf regulates growth and vascular development of malignant melanoma tumors. *Cancer Res* **65**, 2412-21 (2005).
94. Fan, Q.W. et al. A dual phosphoinositide-3-kinase alpha/mTOR inhibitor cooperates with blockade of epidermal growth factor receptor in PTEN-mutant glioma. *Cancer Res* **67**, 7960-5 (2007).
95. Raynaud, F.I. et al. Pharmacologic characterization of a potent inhibitor of class I phosphatidylinositide 3-kinases. *Cancer Res* **67**, 5840-50 (2007).
96. Knight, Z.A. et al. A pharmacological map of the PI3-K family defines a role for p110alpha in insulin signaling. *Cell* **125**, 733-47 (2006).
97. Ali, K. et al. Isoform-specific functions of phosphoinositide 3-kinases: p110 delta but not p110 gamma promotes optimal allergic responses in vivo. *J Immunol* **180**, 2538-44 (2008).
98. Wilhelm, S. et al. Discovery and development of sorafenib: a multikinase inhibitor for treating cancer. *Nat Rev Drug Discov* **5**, 835-44 (2006).

99. Kharas, M.G. et al. Ablation of PI3K blocks BCR-ABL leukemogenesis in mice, and a dual PI3K/mTOR inhibitor prevents expansion of human BCR-ABL+ leukemia cells. *J Clin Invest* **118**, 3038-50 (2008).
100. Chaisuparat, R. et al. Dual inhibition of PI3Kalpha and mTOR as an alternative treatment for Kaposi's sarcoma. *Cancer Res* **68**, 8361-8 (2008).
101. Park, S. et al. PI-103, a dual inhibitor of Class IA phosphatidylinositide 3-kinase and mTOR, has antileukemic activity in AML. *Leukemia* **22**, 1698-706 (2008).
102. Schwab, J. et al. Combination of PI3K/mTOR inhibition demonstrates efficacy in human chordoma. *Anticancer Res* **29**, 1867-71 (2009).
103. Wendel, H.G. & Lowe, S.W. Reversing drug resistance in vivo. *Cell Cycle* **3**, 847-9 (2004).
104. Slavik, J.M., Lim, D.G., Burakoff, S.J. & Hafler, D.A. Rapamycin-resistant proliferation of CD8+ T cells correlates with p27kip1 down-regulation and bcl-xL induction, and is prevented by an inhibitor of phosphoinositide 3-kinase activity. *J Biol Chem* **279**, 910-9 (2004).
105. Svirshchevskaya, E.V. et al. Rapamycin delays growth of Wnt-1 tumors in spite of suppression of host immunity. *BMC Cancer* **8**, 176 (2008).
106. Yu, H., Kortylewski, M. & Pardoll, D. Crosstalk between cancer and immune cells: role of STAT3 in the tumour microenvironment. *Nat Rev Immunol* **7**, 41-51 (2007).
107. Carracedo, A. et al. Inhibition of mTORC1 leads to MAPK pathway activation through a PI3K-dependent feedback loop in human cancer. *J Clin Invest* **118**, 3065-74 (2008).
108. Molhoek, K.R., Brautigan, D.L. & Slingluff, C.L., Jr. Synergistic inhibition of human melanoma proliferation by combination treatment with B-Raf inhibitor BAY43-9006 and mTOR inhibitor Rapamycin. *J Transl Med* **3**, 39 (2005).
109. Chen, J.S. et al. Characterization of structurally distinct, isoform-selective phosphoinositide 3'-kinase inhibitors in combination with radiation in the treatment of glioblastoma. *Mol Cancer Ther* **7**, 841-50 (2008).
110. Marone, R. et al. Targeting melanoma with dual phosphoinositide 3-kinase/mammalian target of rapamycin inhibitors. *Mol Cancer Res* **7**, 601-13 (2009).
111. Wei, G. et al. Gene expression-based chemical genomics identifies rapamycin as a modulator of MCL1 and glucocorticoid resistance. *Cancer Cell* **10**, 331-42 (2006).
112. Calastretti, A. et al. Rapamycin increases the cellular concentration of the BCL-2 protein and exerts an anti-apoptotic effect. *Eur J Cancer* **37**, 2121-8 (2001).

113. Zhang, T.T. et al. Genetic or pharmaceutical blockade of p110delta phosphoinositide 3-kinase enhances IgE production. *J Allergy Clin Immunol* **122**, 811-819 e2 (2008).
114. Janes, M.R. et al. Effective and selective targeting of leukemia cells using a TORC1/2 kinase inhibitor. *Nat Med* **16**, 205-13.
115. Yu, H. & Jove, R. The STATs of cancer--new molecular targets come of age. *Nat Rev Cancer* **4**, 97-105 (2004).
116. Messina, J.L. et al. Activated stat-3 in melanoma. *Cancer Control* **15**, 196-201 (2008).
117. Niu, G. et al. Overexpression of a dominant-negative signal transducer and activator of transcription 3 variant in tumor cells leads to production of soluble factors that induce apoptosis and cell cycle arrest. *Cancer Res* **61**, 3276-80 (2001).
118. Niu, G. et al. Roles of activated Src and Stat3 signaling in melanoma tumor cell growth. *Oncogene* **21**, 7001-10 (2002).
119. Ivanov, V.N., Krasilnikov, M. & Ronai, Z. Regulation of Fas expression by STAT3 and c-Jun is mediated by phosphatidylinositol 3-kinase-AKT signaling. *J Biol Chem* **277**, 4932-44 (2002).
120. Ivanov, V.N., Bhoumik, A. & Ronai, Z. Death receptors and melanoma resistance to apoptosis. *Oncogene* **22**, 3152-61 (2003).
121. Zhou, J., Ong, C.N., Hur, G.M. & Shen, H.M. Inhibition of the JAK-STAT3 pathway by andrographolide enhances chemosensitivity of cancer cells to doxorubicin. *Biochem Pharmacol* (2009).
122. Yang, L. et al. Uniquely modified RNA oligonucleotides targeting STAT3 suppress melanoma growth both in vitro and in vivo. *Cancer Biol Ther* **8**, 2065-72 (2009).

2. WEBSITES

World Health Organization http://www.who.int/en/

Servier Medical Art http://www.servier.com/smart/imagebank.aspx?id=729

3. GRANT SPONSOR

This work has been done with the support of "Departament d'Universitats, Recerca i Societat de la Informació de la Generalitat de Catalunya i del Fons Social Europeu".

IX. ANNEX 1

PUBLICATIONS

López-Fauqued M., Gil R., Grueso J., Hernández J., Pujol A., Moliné T., Recio J.A. The dual PI3K/mTOR inhibitor (PI-103) promotes immunosuppression, in vivo tumor growth and increases survival of Sorafenib treated melanoma cells. Int J Cancer. 2010 Apr 1;126(7):1549-61